The Astrophysical Journal Supplement Series, 239:17 (48pp), 2018 December https://doi.org/10.3847/1538-4365/aae5d2

2018 Census of Interstellar, Circumstellar, Extragalactic, Protoplanetary Disk, and Exoplanetary Molecules

Brett A. McGuire[1,2,3]
[1] National Radio Astronomy Observatory, Charlottesville, VA 22903, USA
[2] Harvard-Smithsonian Center for Astrophysics, Cambridge, MA 02138, USA
Received 2018 May 27; revised 2018 September 20; accepted 2018 September 20; published 2018 November 26

Abstract

To date, 204 individual molecular species, comprised of 16 different elements, have been detected in the interstellar and circumstellar medium by astronomical observations. These molecules range in size from 2 atoms to 70, and have been detected across the electromagnetic spectrum from centimeter wavelengths to the ultraviolet. This census presents a summary of the first detection of each molecular species, including the observational facility, wavelength range, transitions, and enabling laboratory spectroscopic work, as well as listing tentative and disputed detections. Tables of molecules detected in interstellar ices, external galaxies, protoplanetary disks, and exoplanetary atmospheres are provided. A number of visual representations of these aggregate data are presented and briefly discussed in context.

Key words: astrochemistry – ISM: molecules

Supporting material: tar.gz file

1. Introduction

Since the detection of methylidyne (CH), the first molecule identified in the interstellar medium (ISM; Swings & Rosenfeld 1937; Dunham 1937; McKellar 1940), observations of molecules have played crucial roles in a wide range of applications, from broadening our understanding of interstellar chemical evolution (Herbst & van Dishoeck 2009) and the formation of planets (Öberg et al. 2011), to providing exceptional astrophysical probes of physical conditions and processes (Friesen et al. 2013). Beginning in the early 1960s, the advent of radio astronomy enabled a boom in the detection of new molecules, a trend that has continued at a nearly linear rate ever since.

Yet, despite the remarkably steady (and perhaps even accelerating) pace of new molecular detections, the number of as yet unidentified spectral features attributable to molecules is staggering. Indeed, these mysteries extend across the electromagnetic spectrum. In the radio, high-sensitivity, broadband spectral line surveys continue to reveal hundreds of features not assignable to transitions of molecules in spectroscopic databases (Cernicharo et al. 2013a), although there is evidence that a non-trivial number of these features may be due to transitions of vibrationally excited or rare isotopic species that have not been completely cataloged (Fortman et al. 2012).

At shorter wavelengths, the unidentified infrared emission bands (UIRs)—sharp, distinct emission features ubiquitous in ultraviolet (UV)-irradiated regions in our galaxy, as well as seen in dozens of external galaxies—continue to elude conclusive molecular identification. A substantial body of literature now seems to favor the assignment of these emission features to polyclic aromatic hydrocarbons (PAHs; Tielens 2008), or at the very least sp^2-hybridized aromatic carbon structures. The possibility that these features arise from mixed aromatic/aliphatic organic nanoparticles has also been raised (Kwok & Zhang 2013). Regardless, it remains that no individual molecule has been definitely identified from UIR features.

An older mystery is the diffuse interstellar bands (DIBs), first discovered by Mary Lea Heger in 1922 (McCall & Griffin 2012). Despite nearly a century of observation and laboratory work, these sharp features seen from the IR to the UV remain nearly completely unassigned. Campbell et al. (2015) recently reported the first attribution of a molecular carrier to a DIB that has not been disputed in the literature, that of C_{60}^+. Yet, hundreds of DIBs remain to be identified.

In the following sections, known, tentatively detected, and disputed interstellar, circumstellar, extragalactic, and exoplanetary molecules are cataloged and presented. The major lists in this paper are as follows (names are in-document hyperlinks in most PDF viewers):

1. List of known interstellar and circumstellar molecules
   (a) List of tentative detections.
   (b) List of disputed detections.
2. List of molecules detected in external galaxies.
3. List of molecules detected in interstellar ices.
4. List of molecules detected in protoplanetary disks.

The primary list is that of the known interstellar and circumstellar molecules, and for each species in this list, a best-effort attempt was made to locate the first reported detection or detections of the species in the literature. The detection source or sources and instrument are given, and for some species a short description of any particularly noteworthy attributes is given as well. When available, a reference to the enabling laboratory spectroscopy work cited in the detection paper is provided. In the cases where the detection paper uses frequencies without apparent attribution to the laboratory spectroscopy, the most recent effort in the literature that would reasonably have been available at the time of publication of the detection is provided on a best-effort basis.

[3] B.A.M. is a Hubble Fellow of the National Radio Astronomy Observatory.

Table 1
Commonly Used Facility Abbreviations

Abbreviation	Description
ALMA	Atacama Large Millimeter/submillimeter Array
APEX	Atacama Pathfinder Experiment
ARO	Arizona Radio Observatory
ATCA	Australian Telescope Compact Array
BIMA	Berkeley-Illinois-Maryland Array
CSO	Caltech Submillimeter Observatory
FCRAO	Five College Radio Astronomy Observatory
FUSE	*Far Ultraviolet Spectroscopic Explorer*
GBT	Green Bank Telescope
IRAM	Institut de Radioastronomie Millimétrique
IRTF	Infrared Radio Telescope Facility
ISO	*Infrared Space Observatory*
KPNO	Kitt Peak National Observatory
MWO	Millimeter-wave Observatory
NRAO	National Radio Astronomy Observatory
OVRO	Owens Valley Radio Observatory
PdBI	Plateau de Bure Interferometer
SEST	Swedish-ESO Submillimeter Telescope
SMA	Sub-millimeter Array
SMT	Sub-millimeter Telescope
SOFIA	*Stratospheric Observatory for Infrared Astronomy*
UKIRT	United Kingdom Infrared Telescope

The classification of a molecule as detected, tentatively detected, or disputed was made as agnostically as possible. Molecules are listed as detected if a literature source has claimed that detection, did not self-identify that detection as tentative, and no subsequent literature could be found that disputes that claim. Tentative detections are listed only if the source has claimed the detection as such. Detections are considered disputed until a literature source has claimed that dispute has been resolved.

Subsets of the lists presented in this work are available both online and in numerous publications. Three exceptional web-based resources are of particular note with respect to the list of interstellar and circumstellar detections: the Cologne Database for Molecular Spectroscopy's *List of Molecules in Space* (H.S.P. Müller),[4] The Astrochymist's *A Bibliography of Astromolecules* (D. Woon),[5] and the list of M. Araki.[6] At the time of publication, these resources provide the most frequently updated lists of known interstellar and circumstellar species. This publication is intended as a complement, rather than a supplement, to these resources.

This document is intended to be updated on an annual or semi-annual basis.[7] A Python 3 script containing the full bibliographical and metadata information for all figures, tables, and molecules discussed here is available as supplementary information. The latest version of the script, updated more frequently than this document, can always be found at https://github.com/bmcguir2/astromolecule_census. A brief description of the script and some of its function are provided in Appendix B.

A list of commonly used abbreviations for facilities is given in Table 1. Tables 2 and 3 summarize the current list of known interstellar and circumstellar molecules. The column headers and individual molecule entries are active in-document hyperlinks in most PDF viewers. In Section 10, an aggregate analysis of the data is presented. These figures are available as high-quality supplemental data files in PDF and PNG formats.

[4] https://www.astro.uni-koeln.de/cdms/molecules
[5] http://www.astrochymist.org/astrochymist_ism.html
[6] http://www.rs.kagu.tus.ac.jp/tsukilab/research_seikanlist.html
[7] Suggested updates, corrections, and comments can be directed to bmcguire@nrao.edu.

2. Detection Techniques

As will be seen in the following pages, the vast majority of new molecule detections (∼80%) have been made using radio astronomy techniques in the centimer, millimeter, and submillimeter wavelength ranges. This article, and indeed this section, is therefore inherently biased toward radio astronomy. To understand this bias, it is helpful to review the techniques, and their limitations, used to detect molecules across various wavelength ranges. In the end, it comes down to the energy required, and that which is available, to populate molecular energy levels for undergoing transitions at various wavelengths. This in turn dictates the environments and sightlines in which detections can be accomplished.

2.1. Radio Astronomy

Here, radioastronomical observations are roughly defined as those stretching from centimeter to far-infrared (100's of μm) wavelengths, or below ∼2 THz (in frequency). The primary molecular signal arising in these regions is that of the rotational motion of molecules. For a linear molecule (symmetric and asymmetric tops follow similar, if more complex patterns), the rotational energy levels J are given, to first order, by Equation (1):

$$E_J = BJ(J+1), \tag{1}$$

where B is the rotational constant of the molecule. B is inversely proportional to the moment of inertia of the molecule (I):

$$B = \frac{h^2}{8\pi^2 I}, \tag{2}$$

where I is related to the reduced mass of the molecule (μ) and the radial extent of the mass (r):

$$I = \mu r^2. \tag{3}$$

Thus, lighter, smaller molecules will have large values of B (e.g., B[NH] = 490 GHz; Klaus et al. 1997) and heavier, larger molecules will have very small values of B (e.g., B[HC_9N] = 0.29 GHz; McCarthy et al. 2000). The frequencies of rotational transitions are given by the difference in energy levels (Equation (1)). Small molecules with large values of B, and correspondingly widely spaced energy levels, will have transitions at higher frequencies. Larger molecules, with smaller values of B, have closely spaced energy levels with transitions at lower frequencies.

Assuming NH and HC_9N are reasonable examples of the range of sizes of typical interstellar molecules, the ground-state rotational transitions ($J = 1 \rightarrow 0$) therefore fall between ∼1 THz (NH) and ∼500 MHz (HC_9N). As a result, observations of the pure rotational transitions of molecules are most often (nearly exclusively) conducted with radio astronomy facilities.

Table 2
List of Detected Interstellar Molecules with Two to Seven Atoms, Categorized by Number of Atoms, and Vertically Ordered by Detection Year

2 Atoms		3 Atoms		4 Atoms	5 Atoms	6 Atoms	7 Atoms
CH	CP	H_2O	N_2O	NH_3	HC_3N	CH_3OH	CH_3CHO
CN	NH	HCO^+	MgCN	H_2CO	HCOOH	CH_3CN	CH_3CCH
CH^+	SiN	HCN	$H3^+$	HNCO	CH_2NH	NH_2CHO	CH_3NH_2
OH	SO^+	OCS	SiCN	H_2CS	NH_2CN	CH_3SH	CH_2CHCN
CO	CO^+	HNC	AlNC	C_2H_2	H_2CCO	C_2H_4	HC_5N
H_2	HF	H_2S	SiNC	C_3N	C_4H	C_5H	C_6H
SiO	N_2	N_2H^+	HCP	HNCS	SiH_4	CH_3NC	c-C_2H_4O
CS	CF^+	C_2H	CCP	$HOCO^+$	c-C_3H_2	HC_2CHO	CH_2CHOH
SO	PO	SO_2	AlOH	C_3O	CH_2CN	H_2C_6	C_6H^-
SiS	O_2	HCO	H_2O^+	l-C_3H	C_5	C_5S	CH_3NCO
NS	AlO	HNO	H_2Cl^+	$HCNH^+$	SiC_4	HC_3NH^+	HC_5O
C_2	CN^-	HCS^+	KCN	H_3O^+	H_2CCC	C_5N	
NO	OH^+	HOC^+	FeCN	C_3S	CH_4	HC_4H	
HCl	SH^+	SiC_2	HO_2	c-C_3H	HCCNC	HC_4N	
NaCl	HCl^+	C_2S	TiO_2	HC_2N	HNCCC	c-H_2C_3O	
AlCl	SH	C_3	CCN	H_2CN	H_2COH^+	CH_2CNH	
KCl	TiO	CO_2	SiCSi	SiC_3	C_4H^-	C_5N^-	
AlF	ArH^+	CH_2	S_2H	CH_3	CNCHO	HNCHCN	
PN	NS^+	C_2O	HCS	C_3N^-	HNCNH	SiH_3CN	
SiC		MgNC	HSC	PH_3	CH_3O		
		NH_2	NCO	HCNO	NH_3D^+		
		NaCN		HOCN	H_2NCO^+		
				HSCN	$NCCNH^+$		
				HOOH	CH_3Cl		
				l-C_3H^+			
				HMgNC			
				HCCO			
				CNCN			

Note. Column headers and molecule formulas are in-document hyperlinks in most PDF viewers.

The absolute energies of these rotational levels also dictate the manner and environments in which they may be observed. The equivalent kT energy of most rotational levels of interstellar species is typically $<$1000 K. In sufficiently dense environments, the distribution of energy between these levels is governed by collisions with other gas particles, a condition commonly referred to as local thermodynamic equilibrium (LTE), and is thus proportional (or equal) to the kinetic temperature of the gas. For warm regions such as hot cores, sufficient energy is available to produce a population distribution (excitation temperature, T_{ex}) well above the background radiation field, permitting the observation of emission from molecules undergoing rotational transitions (see, e.g., Belloche et al. 2013). Even in very cold regions, like TMC-1 (T_{ex} = 5–10 K), sufficient energy is still present to populate the lowest few rotational energy levels, and emission can still be seen (see, e.g., Kaifu et al. 2004). Conversely, when T_{ex} is below the background radiation field temperature (typically black/graybody dust emission), molecules can be observed in absorption against this continuum (see, e.g., SH; Neufeld et al. 2012). Thus, a major advantage of radio observations is the ability to observe molecules in virtually any source, either in emission (due to the low energy needed to populate rotational levels) or in absorption against background continuum.

The major weakness of this technique is that it is blind to completely symmetric molecules (and largely blind to those that are highly symmetric). The strength of a rotational transition is proportional to the square of the permanent electric dipole moment of the molecule, and thus highly symmetric molecules often possess either very weak or no allowed pure rotational transitions (e.g., CH_4). Furthermore, as the molecules increase in size and complexity, the number of accessible energy levels increases substantially, and thus the partitioning of population among these levels results in the number of molecules emitting/absorbing at a given frequency being decreased dramatically. Finally, molecules trapped in the condensed phase cannot undergo free rotation, making their detection by rotational spectroscopy in the radio impossible.

2.2. Infrared Astronomy

Pure rotational transitions of molecules in the radio occur within a single vibrational state of a molecule. This is often, but not exclusively, the ground vibrational state (see, e.g., Goldsmith et al. 1983). Transitions can also occur between vibrational states, the energies of which normally fall between hundreds and many thousands of cm^{-1} (see, e.g., CO_2 Stull et al. 1962), and the resulting wavelengths of light between a few and a few hundred μm (i.e., the near-infrared to far-infrared). Because these energy levels are substantially higher than those of pure rotational transitions, observations of emission from vibrational transitions usually require exceptionally warm regions or a radiative pumping mechanism to populate the levels. A common example of this effect is the aforementioned UIR features, which are often attributed to the infrared vibrational transitions of PAHs that have been pumped by an external, enhanced UV radiation field (Tielens 2008).

Absent these extraordinary excitation conditions, however, observation of vibrational transitions of molecules in the IR requires a background radiation source for the molecules to be seen against in absorption. This places a number of limitations

Table 3
List of Detected Interstellar Molecules with Eight or More Atoms, Categorized by Number of Atoms, and Vertically Ordered by Detection Year

8 Atoms	9 Atoms	10 Atoms	11 Atoms	12 Atoms	13 Atoms	Fullerenes
$HCOOCH_3$	CH_3OCH_3	$(CH_3)_2CO$	HC_9N	C_6H_6	c-C_6H_5CN	C_{60}
CH_3C_3N	CH_3CH_2OH	$HO(CH_2)_2OH$	CH_3C_6H	n-C_3H_7CN		C_{60}^+
C_7H	CH_3CH_2CN	CH_2CH_2CHO	CH_3CH_2OCHO	i-C_3H_7CN		C_{70}
CH_3COOH	HC_7N	CH_3C_5N	CH_3COOCH_3			
H_2C_6	CH_3C_4H	CH_3CHCH_2O				
CH_2OHCHO	C_8H	CH_3OCH_2OH				
HC_6H	CH_3CONH_2					
CH_2CHCHO	C_8H^-					
CH_2CCHCN	CH_2CHCH_3					
NH_2CH_2CN	CH_3CH_2SH					
CH_3CHNH	HC_7O					
CH_3SiH_3						

Note. Column headers and molecule formulas are in-document hyperlinks in most PDF viewers.

on the breadth of environments that can be probed with IR astronomy, as these sightlines must not only fortuitously contain a background source, but also be optically thin enough to allow for the transmission of that light through the absorbing medium. Even given these limitations, IR astronomy has been an extraordinarily useful tool for molecular astrophysics, particularly in the identification of molecules that are highly symmetric and lack strong or non-zero permanent dipole moments.

Beyond the identification of new species, however, a substantial benefit of IR astronomy is the ability to observe molecules condensed into interstellar ices. While condensed-phase molecules cannot undergo free rotation, their vibrational transitions remain accessible. These are largely seen in absorption, as the energy required to excite a transition into emission is likely to simply cause the molecule to desorb into the gas phase. As well, the vibrational motions are not unaffected by the condensed-phase environment. Both the physical structure of the solid and the molecular content of the surrounding material can alter the frequencies and line shapes of vibrational modes in small and large ways (see, e.g., Cooke et al. 2016). That said, these changes are often readily observable and quantifiable in the laboratory, and as a result, IR astronomy has provided a unique window into the molecular content of condensed-phase materials in the ISM.

2.3. Visible and Ultraviolet Astronomy

The least well-represented wavelength ranges are the visible and ultraviolet. Transitions arising in these regions typically involve population transfer between electronic levels of molecules and atoms (see, e.g., N_2; Lofthus & Krupenie 1977). As with vibrational transitions in the infrared, no permanent dipole moment is required, enabling the detection of species otherwise blind to radio astronomy. The energy requirements for driving electronic transitions into emission are great enough that they are typically seen only in stellar atmospheres and other extremely energetic environments (see, e.g., emission from atomic Fe in Eta Carinae; Aller 1966). In these conditions, many molecules will simply dissociate into their constituent atoms.

Thus, like the infrared, the most likely avenue of molecular detection in the visible and UV is through absorption spectroscopy against a background source. This imposes similar restrictions to the infrared, but with the added challenge of the comparatively higher opacity of interstellar clouds at these wavelengths. As a result, the few detections in these ranges have all been in diffuse, line of sight (LOS) clouds to bright background continuum sources.

2.4. Summary

In summary, the detections presented below will be heavily biased toward radio astronomy. The primary molecular signal arising in the radio is that of transitions between rotational energy levels. The energetics of the environments in which most molecules are found is very well matched to that required to populate these rotational energy levels, as opposed to the vibrational and especially electronic levels dominating the IR and UV/Vis regimes. The resulting ability to observe in both emission and absorption, over a wide range of environments, substantially increases the opportunities for detection.

3. Known Interstellar Molecules

This section covers those species with published detections that have not been disputed. This list includes tentative detections and disputed detections that were later confirmed. Molecules are ordered first by number of atoms, then by year detected. A common name is provided after the molecular formula for most species. Note that for simplicity, due to differences in beam sizes, pointing centers, and nomenclature through time, detections toward sub-regions within the Sgr B2 and Orion sources have not been differentiated here. The exception to this is the Orion Bar photon-dominated/photodissociation region (PDR).

Two-atom Molecules

3.1. CH (Methylidyne)

Swings & Rosenfeld (1937) suggested that an observed line at $\lambda = 4300$ Å by Dunham (1937) using the Mount Wilson Observatory in diffuse gas toward a number of supergiant B stars might have been due to the $^2\Delta \leftarrow {}^2\Pi$ transition of CH, reported in the laboratory by Jevons (1932). McKellar (1940) later identified several additional transitions in observational data. The first radio identification was reported by Rydbeck et al. (1973) at 3335 MHz with the Onsala telescope toward more than a dozen sources using estimated fundamental rotational transition frequencies from Shklovskii (1953), Goss (1966), and Baird & Bredohl (1971). The first direct

measurement of the CH rotational spectrum was reported by Brazier & Brown (1983).

3.2. CN (Cyano Radical)

Lines of CN were first reported using the Mount Wilson Observatory around $\lambda = 3875$ Å by McKellar (1940) and Adams (1941) based on the laboratory work of Jenkins & Wooldridge (1938). Later, Jefferts et al. (1970) reported the first detection of rotational emission from CN by observation of the $J = 1-0$ transition at 113.5 GHz in Orion and W51 using the NRAO 36 ft telescope. Identification was made prior to laboratory observation of the rotational transitions of CN, and was based on rotational constants derived from electronic transitions measured by Poletto & Rigutti (1965) and dipole moments measured by Thomson & Dalby (1968). The laboratory rotational spectra were first measured seven years later by Dixon & Woods (1977).

3.3. CH^+ (Methylidyne Cation)

Swings & Rosenfeld (1937) suggested that a set of three lines at $\lambda = 4233$, 3958, and 3745 Å seen with the Mount Wilson Observatory in diffuse gas belonged to a diatomic cation. Douglas & Herzberg (1941) confirmed the assignment to CH^+ by laboratory observation of these lines in the $^1\Pi \leftarrow {}^1\Sigma$ transition. The first observation of rotational transitions of CH^+ was reported by Cernicharo et al. (1997) toward NGC 7027 using *ISO*, and was based on rotational constants derived from rovibronic transitions measured by Carrington & Ramsay (1982).

3.4. OH (Hydroxyl Radical)

Weinreb et al. (1963) reported the first detection of OH through observation of its ground state, $^2\Pi_{3/2}$, $J = 3/2$, Λ-doubled, $F = 2 \rightarrow 2$ and $F = 1 \rightarrow 1$ hyperfine transitions at 1666 MHz toward Cas A using the Millstone Hill Observatory. The frequencies were measured in the laboratory by Ehrenstein et al. (1959).

3.5. CO (Carbon Monoxide)

Wilson et al. (1970) reported the observation of the $J = 1 \rightarrow 0$ transition of CO toward Orion using the NRAO 36 ft telescope at a (velocity-shifted) frequency of 115267.2 MHz, based on a rest frequency of 115271.2 MHz from Cord et al. (1968).

3.6. H_2 (Molecular Hydrogen)

Molecular hydrogen was reported by Carruthers & Carruthers (1970) toward ξ Per using a spectrograph on an Aerobee-150 rocket launched from White Sands Missile Range. The $B^1\Sigma_u \leftarrow X^1\Sigma_g$ Lyman series in the range of 1000–1400 Å was observed and identified by direct comparison to a absorption cell observed with the same instrument used for the rocket observations.

3.7. SiO (Silicon Monoxide)

The $J = 3 \rightarrow 2$ transition of SiO at 130246 MHz was observed by Wilson et al. (1971) toward Sgr B2 using the NRAO 36 ft telescope. The transition frequency was calculated based on the laboratory work of Raymonda (1970) and Törring (1968). SiO was the first confirmed silicon-containing species in the ISM.

3.8. CS (Carbon Monosulfide)

Penzias et al. (1971) reported the detection of the $J = 3 \rightarrow 2$ transition of CS at 146969 MHz toward Orion, W51, IRC +10216, and DR21 using the NRAO 36 ft telescope. The laboratory microwave spectrum was first reported by Mockler & Bird (1955). CS was the first confirmed sulfur-containing species in the ISM.

3.9. SO (Sulfur Monoxide)

An unidentified line in NRAO 36 ft observations of Orion was assigned to the $J_K = 3_2 \rightarrow 2_1$ transition of SO by Gottlieb & Ball (1973) based on laboratory data from Winnewisser et al. (1964). The authors subsequently observed SO emission toward numerous other sources, as well as identifying the $4_3 \rightarrow 3_2$ transition using the 16 ft telescope at McDonald Observatory. SO was the first molecule detected in space in a $^3\Sigma$ ground electronic state via radio astronomy.

3.10. SiS (Silicon Monosulfide)

Morris et al. (1975) reported the detection of the $J = 6 \rightarrow 5$ and $5 \rightarrow 4$ transitions of SiS at 108924.6 MHz and 90771.85 MHz, respectively, based on the laboratory work of Hoeft (1965). The observations were conducted toward IRC +10216 using the NRAO 36 ft telescope.

3.11. NS (Nitrogen Sulfide)

Gottlieb et al. (1975) and Kuiper et al. (1975) simultaneously and independently reported the detection of NS. Gottlieb et al. (1975) observed the $J = 5/2 \rightarrow 3/2$ transition in the $^2\Pi_{1/2}$ electronic state at 115154 MHz (Amano et al. 1969) toward Sgr B2 using the 16 ft antenna at the University of Texas Millimeter Wave Observatory over three periods in 1973–1974, and confirmed the detection using the NRAO 36 ft telescope in May 1975. Kuiper et al. (1975) observed the same transitions toward Sgr B2 using the NRAO 36 ft telescope in February 1975.

3.12. C_2 (Dicarbon)

The detection of C_2 was reported by Souza & Lutz (1977) toward Cygnus OB2 No. 12 using the Smithsonian Institution's Mount Hopkins Observatory. The detected lines at 10140 Å were measured in the laboratory by Phillips (1948).

3.13. NO (Nitric Oxide)

Liszt & Turner (1978) reported the identification of NO in the ISM toward Sgr B2 using the NRAO 36 ft telescope. The detection was based on the laboratory analysis of the hyperfine splitting in the $^2\Pi_{1/2}$ $J = 3/2 \rightarrow 1/2$ transition near 150.1 GHz as reported in Gallagher & Johnson (1956).

3.14. HCl (Hydrogen Chloride)

Interstellar $H^{35}Cl$ was reported by Blake et al. (1985), who used the Kuiper Airborne Observatory to observe the $J = 1 \rightarrow 0$ transition at 625918.8 MHz toward Orion. The laboratory transition frequencies were reported in De Lucia et al. (1971).

3.15. NaCl (Sodium Chloride)

The detection of NaCl was reported by Cernicharo et al. (1987a) toward IRC+10216 using IRAM 30 m observations of six transitions between 91 and 169 GHz, as well as the $J = 8 \rightarrow 7$ transition of $Na^{37}Cl$ at 101961.9 MHz. The laboratory frequencies were obtained from Lovas & Tiemann (1974).

3.16. AlCl (Aluminum Chloride)

The detection of AlCl was reported by Cernicharo et al. (1987a) toward IRC+10216 using IRAM 30 m observations of four transitions between 87 and 160 GHz, as well as the $J = 10 \rightarrow 9$ and $11 \rightarrow 10$ transitions of $Al^{37}Cl$ at 142322.5 MHz and 156546.8 MHz, respectively. The laboratory frequencies were obtained from Lovas & Tiemann (1974).

3.17. KCl (Potassium Chloride)

The detection of KCl was reported by Cernicharo et al. (1987a) toward IRC+10216 using IRAM 30 m observations of six transitions between 100 and 161 GHz. The laboratory frequencies were obtained from Lovas & Tiemann (1974).

3.18. AlF (Aluminum Fluoride)

Cernicharo et al. (1987a) claimed a tentative detection of AlF toward IRC+10216 using IRAM 30 m observations of three transitions between 99 and 165 GHz. The laboratory frequencies were obtained from Lovas & Tiemann (1974). The detection was confirmed by Ziurys et al. (1994b) using CSO observations of IRC+10216. Three additional lines, the $J = 7 \rightarrow 6$, $8 \rightarrow 7$, and $10 \rightarrow 9$ were observed at 230793, 263749, and 329642 MHz, respectively, based on laboratory data from Wyse et al. (1970).

3.19. PN (Phosphorous Mononitride)

Sutton et al. (1985) first suggested that a feature observed in their line survey data using the OVRO 10.4 m telescope toward Orion at 234936 MHz could be attributed to the $J = 5 \rightarrow 4$ transition of PN, using the laboratory data reported in Wyse et al. (1972). Turner & Bally (1987) and Ziurys (1987) later simultaneously confirmed the detection of PN. Turner & Bally (1987) observed the $2 \rightarrow 1$, $3 \rightarrow 2$, and $5 \rightarrow 4$ transitions at 93980, 140968, and 234936 MHz, respectively, toward Orion, W51, and Sgr B2 using the NRAO 12 m telescope. Ziurys (1987) observed the $2 \rightarrow 1$, $3 \rightarrow 2$, and $5 \rightarrow 4$ transitions toward Orion using the FCRAO 14 m telescope, and the $6 \rightarrow 5$ using the NRAO 12 m telescope. The $2 \rightarrow 1$ transition was also observed toward Sgr B2 and W51. PN was the first phosphorous-containing molecule detected in the ISM.

3.20. SiC (Silicon Carbide)

Cernicharo et al. (1989) reported the detection of the SiC radical in IRC+10216 using the IRAM 30 m telescope. Fine structure and Λ-doubled lines were detected in the $J = 2 \rightarrow 1$, $4 \rightarrow 3$, and $6 \rightarrow 5$ transitions in the $^3\Pi$ electronic ground state near 81, 162, and 236 GHz, respectively, based on laboratory data presented in the same manuscript. The authors make note of unidentified lines suggestive of the SiC radical in earlier data toward IRC+10216 beginning in 1976, both in their own observations and in those of I. Dubois (unpublished) using the NRAO 36 ft telescope.

3.21. CP (Carbon Monophosphide)

Saito et al. (1989) measured the rotational spectrum of CP in the laboratory and conducted an astronomical search for the $N = 1 \rightarrow 0$ and $2 \rightarrow 1$ transitions at 48 and 96 GHz, respectively, using the Nobeyama 45 m telescope across several sources, resulting in non-detections. Guélin et al. (1990) subsequently reported the successful detection of the $2 \rightarrow 1$ and $5 \rightarrow 4$ (239 GHz) transitions toward IRC+10216 using the IRAM 30 m telescope.

3.22. NH (Imidogen Radical)

Meyer & Roth (1991) reported the detection of the $A^3\Pi - X^3\Sigma$ (0,0) $R_1(0)$ line of NH in absorption toward ξ Per and HD 27778 at 3358 Å using the KPNO 4 m telescope. The laboratory rest frequencies were obtained from Dixon (1959). The earliest reported detection of rotational transitions of NH appears to be that of Cernicharo et al. (2000), who observed the $N_J = 2_3 \rightarrow 1_2$ transition at 974 GHz toward Sgr B2 with *ISO*. Although no laboratory reference is given, the frequencies used were presumably those of Klaus et al. (1997).

3.23. SiN (Silicon Nitride)

Turner (1992b) reported the detection of the $N = 2 \rightarrow 1$ and $6 \rightarrow 5$ transitions of SiN at 87 and 262 GHz, respectively, toward IRC+10216 using the NRAO 12 m telescope. The $2 \rightarrow 1$ transition was measured by Saito et al. (1983), and the frequency for the $6 \rightarrow 5$ was calculated from the constants given therein.

3.24. SO^+ (Sulfur Monoxide Cation)

The detection of SO^+ was reported by Turner (1992a) toward IC 443G using the NRAO 12 m telescope. The Λ-doubled $^2\Pi_{1/2}$, $J = 5/2 \rightarrow 3/2$ and $9/2 \rightarrow 7/2$ transitions at 116 and 209 GHz, respectively, were observed. The frequencies of the $5/2 \rightarrow 3/2$ transitions were measured by Amano et al. (1991), while those of the $9/2 \rightarrow 7/2$ transitions were calculated from the constants given therein.

3.25. CO^+ (Carbon Monoxide Cation)

CO^+ was first observed toward M17SW and NGC 7027 using the NRAO 12 m telescope by Latter et al. (1993). The $N = 2 \rightarrow 1$, $J = 3/2 \rightarrow 1/2$ and $5/2 \rightarrow 3/2$ near 236 GHz and the $3 \rightarrow 2$, $5/2 \rightarrow 3/2$ were observed based on the laboratory work of Sastry et al. (1981b). An earlier reported detection of the $2 \rightarrow 1$, $5/2 \rightarrow 3/2$ transition in Orion by Erickson et al. (1981), based on the laboratory data of Dixon & Woods (1975), was later definitely assigned to transitions of $^{13}CH_3OH$ by Blake et al. (1984).

3.26. HF (Hydrogen Fluoride)

Neufeld et al. (1997) reported the detection of the $J = 2 \rightarrow 1$ transition of HF at 2.5 THz toward Sgr B2 using *ISO*. The rest frequencies were measured in the laboratory by Nolt et al. (1987).

3.27. N_2 (Nitrogen)

Knauth et al. (2004) observed the $c_4'\,^1\Sigma_u^+ – X^1\Sigma_g^+$ and $c_3^1\Sigma_u^+ – X^1\Sigma_g^+$ transitions of N_2 at 958.6 and 960.3 Å , respectively, using FUSE observations toward HD 124314. The oscillator

strengths of the $c_4'\,^1\Sigma_u^+$–$X^1\Sigma_g^+$ transition were obtained from Stark et al. (2000), and the $c_3\,^1\Sigma_u^+$–$X^1\Sigma_g^+$ transition from a private communication with G. Stark.

3.28. CF^+ (Fluoromethylidynium Cation)

The detection of CF^+ was reported by Neufeld et al. (2006) using IRAM 30 m and APEX 12 m observations of the $J = 1 \rightarrow 0$, $2 \rightarrow 1$, and $3 \rightarrow 2$ transitions at 102.6, 205.2, and 307.7 GHz, respectively, toward the Orion Bar. The laboratory frequencies were reported by Plummer et al. (1986).

3.29. PO (Phosphorous Monoxide)

Tenenbaum et al. (2007) reported the detection of the Λ-doubled $J = 11/2 \rightarrow 9/2$ and $13/2 \rightarrow 11/2$ transitions of PO at 240 and 284 GHz, respectively, using SMT 10 m observations of VY Canis Majoris. Although not cited, the frequencies were presumably obtained from the laboratory work of Kawaguchi et al. (1983) and Bailleux et al. (2002).

3.30. O_2 (Oxygen)

A tentative detection of molecular oxygen was reported by Goldsmith et al. (2002) in SWAS observations of ρ Oph, with further evidence provided by Larsson et al. (2007) using observations of the $N_J = 1_1 \rightarrow 1_0$ transition at 118750 MHz with the Odin satellite toward ρ Oph A. Although no citation is provided, the frequencies were presumably obtained from the laboratory work of Endo & Mizushima (1982). Later, Goldsmith et al. (2011) reported the observation of the $N_J = 3_3 \rightarrow 1_2$, $5_4 \rightarrow 3_4$, and $7_6 \rightarrow 5_6$ transitions at 487, 774, and 1121 GHz, respectively, using *Herschel*/HIFI observations of Orion. Although there appears to be no citation for the laboratory data, these transition frequencies were likely taken from Drouin et al. (2010).

3.31. AlO (Aluminum Monoxide)

Tenenbaum & Ziurys (2009) reported the detection of the $N = 7 \rightarrow 6$, $6 \rightarrow 5$, and $4 \rightarrow 3$ transitions of AlO at 268, 230, and 153 GHz, respectively, toward VY Canis Majoris using the SMT 10 m telescope. The laboratory frequencies were reported in Yamada et al. (1990).

3.32. CN^- (Cyanide Anion)

The detection of CN^- was reported by Agúndez et al. (2010) in observations of IRC+10216 using the IRAM 30 m telescope. The $J = 1 \rightarrow 0$, $2 \rightarrow 1$, and $3 \rightarrow 2$ lines at 112.3, 224.5, and 336.8 GHz were observed, based on the laboratory work of Amano (2008).

3.33. OH^+ (Hydroxyl Cation)

OH^+ was detected by Wyrowski et al. (2010) using APEX 12 m observations of Sgr B2. The $N = 1 \rightarrow 0$, $J = 0 \rightarrow 1$ transitions were detected in absorption at 909 GHz based on the laboratory work of Bekooy et al. (1985). Nearly simultaneously, Benz et al. (2010) reported the detection of the $1 \rightarrow 0$, $3/2 \rightarrow 1/2$ transitions at 1033 GHz toward W3 IRS5 using *Herschel*/HIFI, and Gerin et al. (2010) reported a detection along the LOS to W31C, also with *Herschel*/HIFI.

3.34. SH^+ (Sulfanylium Cation)

Benz et al. (2010) reported the detection of the $N_J = 1_2 \rightarrow 0_1$ transition of SH^+ at 526 GHz using *Herschel*/HIFI observations of W3. Although only a reference to the CDMS database is given, the frequency was almost certainly based on the laboratory work of Hovde & Saykally (1987) and Brown & Müller (2009). Although published after Benz et al. (2010), the first *submitted* detection appears to be that of Menten et al. (2011), who reported the detection of SH^+ in absorption toward Sgr B2, using the APEX 12 m telescope. The $N_J = 1_1 \rightarrow 0_1$ transition at 683 GHz was observed based on the laboratory work of Hovde & Saykally (1987) and Brown & Müller (2009). Benz et al. (2010) acknowledged the earlier submission of Menten et al. (2011) in their work.

3.35. HCl^+ (Hydrogen Chloride Cation)

The detection of HCl^+ was reported by De Luca et al. (2012) in *Herschel*/HIFI observations of W31C and W49N. Hyperfine and Λ-doubling structure was observed in the $^2\Pi_{3/2}$ $J = 5/2 \rightarrow 3/2$ transition of $H^{35}Cl^+$ at 1.444 THz toward both sources, and the same transition of $H^{37}Cl^+$ was also observed toward W31C. The laboratory work was described in Gupta et al. (2012).

3.36. SH (Mercapto Radical)

Neufeld et al. (2012) reported the detection of the $^2\Pi_{3/2}$ $J = 5/2 \rightarrow 3/2$ Λ-doubled transition of SH at 1383 GHz along the LOS to W49A using the GREAT instrument on SOFIA. The transition frequencies relied upon the work of Morino & Kawaguchi (1995) and Klisch et al. (1996).

3.37. TiO (Titanium Monoxide)

TiO was detected in VY Canis Majoris by Kamiński et al. (2013) using a combination of SMA and PdBI observations. Several fine structure components in the $J = 11 \rightarrow 10$, $J = 10 \rightarrow 9$, $J = 9 \rightarrow 8$, and $J = 7 \rightarrow 6$ transitions were observed between 221 and 352 GHz based on the laboratory work of Namiki et al. (1998).

3.38. ArH^+ (Argonium)

Although a feature was initially observed in several *Herschel* data sets near 618 GHz (Neill et al. 2014), the attribution to $^{36}ArH^+$ was not readily apparent. On Earth, ^{40}Ar is 300 times more abundant than ^{36}Ar (Lee et al. 2006), and as no signal from $^{40}ArH^+$ was visible, $^{36}ArH^+$ seemed to be an unlikely carrier. Barlow et al. (2013), however, recognized that ^{36}Ar is the dominant isotope in the ISM (Cameron 1973), and identified the $J = 1 \rightarrow 0$ and $2 \rightarrow 1$ rotational lines of $^{36}ArH^+$ at 617.5 and 1234.6 GHz, respectively, in *Herschel*/SPIRE spectra of the Crab Nebula. A citation is only given for the CDMS database, as no laboratory data appear to exist for $^{36}ArH^+$. Instead, it is derived in the database to observational accuracy using isotopic scaling factors from other isotopologues.

3.39. NS^+ (Nitrogen Sulfide Cation)

Cernicharo et al. (2018) reported both the laboratory spectroscopy and astronomical identification of NS^+. The $J = 2 \rightarrow 1$ line has been observed with the IRAM 30 m telescope

toward numerous sightlines, several of which came with confirming observations of the $3 \rightarrow 2$ and $5 \rightarrow 4$ lines.

Three-atom Molecules

3.40. H_2O (Water)

Cheung et al. (1969) reported the detection of the $J_{K_a,K_c} = 6_{1,6} \rightarrow 5_{2,3}$ transition of H_2O at 22.2 GHz using the Hat Creek Observatory toward Sgr B2, Orion, and W49. No citation to the laboratory data appears to be given, but presumably it was obtained from the work of Golden et al. (1948).

3.41. HCO^+ (Formylium Cation)

Buhl & Snyder (1970) first reported the discovery of a bright emission feature at 89190 MHz toward Orion, W51, W3(OH), L134, and Sgr A in observations with the NRAO 36 ft telescope, and named the carrier "X-ogen." Shortly thereafter, Klemperer (1970) suggested the attribution of this line to HCO^+. The detection and attribution were confirmed by the laboratory observation of HCO^+ by Woods et al. (1975).

3.42. HCN (Hydrogen Cyanide)

The first reported detection of HCN was that of Snyder & Buhl (1971), who observed the ground state $J = 1 \rightarrow 0$ transition at 88.6 GHz toward W3(OH), Orion, Sgr A, W49, W51, and DR 21 using the NRAO 36 ft telescope. The enabling laboratory spectroscopy was reported by Delucia & Gordy (1969).

3.43. OCS (Carbonyl Sulfide)

Emission from the $J = 9 \rightarrow 8$ transition of OCS at 109463 MHz toward Sgr B2 was reported by Jefferts et al. (1971) using the NRAO 36 ft telescope. The laboratory spectroscopy was reported in King & Gordy (1954).

3.44. HNC (Hydrogen Isocyanide)

Both Zuckerman et al. (1972) and Snyder & Buhl (1972a) observed an unidentified emission signal at 90.7 GHz using the NRAO 36 ft telescope toward W51 and NGC 2264, respectively. Snyder & Buhl (1972a) suggested this line to be due to HNC, which was confirmed four years later with the first measurement of the $J = 1 \rightarrow 0$ transition in the laboratory by Blackman et al. (1976).

3.45. H_2S (Hydrogen Sulfide)

Thaddeus et al. (1972) reported the detection of the $J_{K_a,K_c} = 1_{1,0} \rightarrow 1_{0,1}$ transition of *ortho*-H_2S at 168.7 GHz toward a number of sources with the NRAO 36 ft telescope. The laboratory transition frequencies were measured by Cupp et al. (1968).

3.46. N_2H^+ (Protonated Nitrogen)

Turner (1974) first reported an unidentified emission line at 93.174 GHz in NRAO 36 ft telescope toward a number of sources, including Sgr B2, DR 21(OH), NGC 2264, and NGC 6334N. In a companion letter, Green et al. (1974) suggested the carrier was N_2H^+, based on theoretical calculations. Thaddeus & Turner (1975) claimed the following year to have confirmed the detection by observing an exceptional match to the predicted ^{14}N hyperfine splitting. Laboratory work by Saykally et al. (1976) solidified the detection.

3.47. C_2H (Ethynyl Radical)

The detection of C_2H was reported by Tucker et al. (1974) through observation of four λ-doubled, hyperfine components of the $N = 1 \rightarrow 0$ transition near 87.3 GHz in NRAO 36 ft telescope observations of Orion and numerous other sources. The assignment was made based on a calculated rotational constant under the assumption that the C–H and C≡C bonds had the same length as those already known in acetylene (C_2H_2). A linear structure was assumed based on the laboratory work of Cochran et al. (1964) and Graham et al. (1974). The confirming laboratory microwave spectroscopy was later reported by Sastry et al. (1981a).

3.48. SO_2 (Sulfur Dioxide)

SO_2 was reported in NRAO 36 ft telescope observations toward Orion and Sgr B2 by Snyder et al. (1975). The $J_{K_a,K_c} = 8_{1,7} \rightarrow 8_{0,8}$, $8_{3,5} \rightarrow 9_{2,8}$, and $7_{3,5} \rightarrow 8_{2,6}$ transitions at 83.7, 86.6, and 97.7 GHz, respectively, were observed in emission. The enabling laboratory microwave spectroscopy work was performed by Steenbeckeliers (1968) with additional computation analysis performed by Kirchhoff (1972).

3.49. HCO (Formyl Radical)

Snyder et al. (1976) reported the detection of the $N_{K_-,K_+} = 1_{0,1}$–$0_{0,0}$, $J = 3/2 \rightarrow 1/2$, $F = 2 \rightarrow 1$ transition of HCO at 86671 MHz toward W3, NGC 2024, W51, and K3-50 using the NRAO 36 ft telescope. The laboratory microwave spectroscopy was reported by Saito (1972).

3.50. HNO (Nitroxyl Radical)

The detection of HNO was first reported by Ulich et al. (1977), who observed the $J_{K_a,K_c} = 1_{0,1} \rightarrow 0_{0,0}$ transition at 81477 MHz toward Sgr B2 and NGC 2024 using the NRAO 36 ft telescope. The laboratory frequency was measured by Saito & Takagi (1973). The initial detection was subject to significant controversy in the literature (see Snyder et al. 1993). Subsequent observation of additional lines by Hollis et al. (1991) and Ziurys et al. (1994c) confirmed the initial detection, aided by the laboratory work of Sastry et al. (1984).

3.51. HCS^+ (Protonated Carbon Monosulfide)

Thaddeus et al. (1981) reported the detection of four harmonically spaced, unidentified lines in NRAO 36 ft and Bell 7 m telescope observations of Orion and Sgr B2. Based on the harmonic pattern, the lines were assigned to the $J = 2 \rightarrow 1$, $3 \rightarrow 2$, $5 \rightarrow 4$, and $6 \rightarrow 5$ transitions of HCS^+ at 85, 128, 213, and 256 GHz, respectively. The confirming laboratory measurements were presented in a companion letter by Gudeman et al. (1981).

3.52. HOC^+ (Hydroxymethyliumylidene)

HOC^+ was reported by Woods et al. (1983) in FCRAO and Onsala observations toward Sgr B2. The $J = 1 \rightarrow 0$ transition at 89478 MHz was identified based on the laboratory work of Gudeman & Woods (1982). The detection was confirmed by

Ziurys & Apponi (1995), who observed the $J = 2 \rightarrow 1$, and $3 \rightarrow 2$ transitions at 179 and 268 GHz, respectively.

3.53. c-SiC_2 (Silacyclopropynylidene)

Thaddeus et al. (1984) reported the detection of c-SiC_2 in NRAO 36 ft and Bell 7 m telescope observations of IRC +10216. Nine transitions between 93 and 171 GHz were observed and assigned based on the laboratory work of Michalopoulos et al. (1984), who derived rotational constants from rotationally resolved optical transitions. Thaddeus et al. (1984) noted that a number of these transitions had previously been observed in IRC+10216 and classified as unidentified by various other researchers as early as 1976. Suenram et al. (1989) and Gottlieb et al. (1989) subsequently reported the laboratory observation of the pure rotational spectrum. c-SiC_2 was the first molecular ring molecule identified in the ISM.

3.54. C_2S (Dicarbon Sulfide)

The detection of C_2S ($^3\Sigma^-$) was reported toward TMC-1 and Sgr B2 by Saito et al. (1987) using the Nobeyama 45 m telescope. The laboratory measurements were also performed by Saito et al. (1987). Although published a month earlier than Saito et al. (1987), Cernicharo et al. (1987d) reported the detection of C_2S in IRC+10216 using the laboratory results of Saito et al. (1987) from a preprint article.

3.55. C_3 (Tricarbon)

Hinkle et al. (1988) reported the detection of C_3 in KPNO 4 m telescope observations of IRC+10216. The ν_3 band of C_3 was observed and assigned based on combination differences from the work of Gausset et al. (1965) near 2030 cm^{-1}.

3.56. CO_2 (Carbon Dioxide)

D'Hendecourt & Jourdain de Muizon (1989) reported the observation of the ν_2 bending mode of CO_2 ice in absorption at 15.2 μm using archival spectra from the IRAS database toward AFGL 961, AFGL 989, and AFGL 890. The assignment was based on laboratory spectroscopy of mixed CO_2 ices (D'Hendecourt & Allamandola 1986). Gas-phase CO_2 was later observed toward numerous sightlines with *ISO* as a sharp absorption feature near 15 μm superimposed on a broad solid-phase absorption feature near the same frequency (van Dishoeck et al. 1996). The frequencies were obtained from Paso et al. (1980), while the band strengths used were taken from Reichle & Young (1972).

3.57. CH_2 (Methylene)

CH_2 was first detected by Hollis et al. (1989) in NRAO 12 m telescope observations of Orion. Several hyperfine components of the $N_{K_a,K_c} = 4_{0,4} \rightarrow 3_{1,3}$ transition were observed at 68 and 71 GHz and were assigned based on the laboratory work of Lovas et al. (1983). The detection was later confirmed by Hollis et al. (1995).

3.58. C_2O (Dicarbon Monoxide)

The detection of C_2O was reported by Ohishi et al. (1991) toward TMC-1 using the Nobeyama 45 m telescope. The $N_J = 1_2 \rightarrow 0_1$ and $2_3 \rightarrow 1_2$ transitions at 22 and 46 GHz, respectively, were assigned based on the laboratory data of Yamada et al. (1985).

3.59. MgNC (Magnesium Isocyanide)

Kawaguchi et al. (1993) successfully assigned a series of three, unidentified harmonically spaced doublet emission lines detected by Guélin et al. (1986) in IRAM 30 m observations of IRC+10216 to the $N = 7 \rightarrow 6$, $8 \rightarrow 7$, and $9 \rightarrow 8$ transitions of MgNC based on their own laboratory spectroscopy of the species. MgNC was the first magnesium-containing molecule to be detected in the ISM.

3.60. NH_2 (Amidogen Radical)

The detection of NH_2 was reported by van Dishoeck et al. (1993) toward Sgr B2 using CSO observations of five components of the $J = 3/2 \rightarrow 3/2, 1/2 \rightarrow 1/2$, and $3/2 \rightarrow 1/2$ transitions at 426, 469, and 461 GHz, respectively, based on the laboratory work of Burkholder et al. (1988) and Charo et al. (1981). Some hyperfine splitting was resolved.

3.61. NaCN (Sodium Cyanide)

The detection of NaCN was reported by Turner et al. (1994) using NRAO 12 m telescope observations of IRC+10216. The $J_{K_a,K_c} = 5_{0,5} \rightarrow 4_{0,4}$, $6_{0,6} \rightarrow 5_{0,5}$, $7_{0,7} \rightarrow 6_{0,6}$, and $9_{0,9} \rightarrow 8_{0,8}$ transitions at 78, 93, 108, and 139 GHz, respectively, were observed. The assignments were based on predictions from the rotational constants derived in van Vaals et al. (1984).

3.62. N_2O (Nitrous Oxide)

Ziurys et al. (1994a) reported the detection of the $J = 3 \rightarrow 2$, $4 \rightarrow 3$, $5 \rightarrow 4$, and $6 \rightarrow 5$ transitions of N_2O at 75, 100, 125, and 150 GHz, respectively, in NRAO 12 m observations toward Sgr B2. The laboratory frequencies were obtained from Lovas (1978).

3.63. MgCN (Magnesium Cyanide Radical)

The detection of the MgCN radical was reported by Ziurys et al. (1995) in NRAO 12 m and IRAM 30 m observations of IRC+10216. The $N = 11 \rightarrow 10$, $10 \rightarrow 9$, and $9 \rightarrow 8$ transitions were observed, some with resolved spin-rotation splitting, based on the accompanying laboratory work of Anderson et al. (1994).

3.64. H_3^+

First suggested as a possible interstellar molecule in Martin et al. (1961), H_3^+ was detected 35 years later in absorption toward GL 2136 and W33A by Geballe & Oka (1996) using UKIRT to observe three transitions of the ν_2 fundamental band near 3.7 μm. The laboratory work was performed by Oka (1980).

3.65. SiCN (Silicon Monocyanide Radical)

Guélin et al. (2000) reported the detection of the SiCN radical in IRAM 30 m observations of IRC+10216. Three Λ-doubled transitions at 83, 94, and 105 GHz were detected based on the laboratory work by Apponi et al. (2000).

3.66. AlNC (Aluminum Isocyanide)

The detection of AlNC toward IRC+10216 with the IRAM 30 m telescope was reported by Ziurys et al. (2002). Five transitions between 132 and 251 GHz were assigned based on the laboratory work of Robinson et al. (1997).

3.67. SiNC (Silicon Monoisocyanide Radical)

Guélin et al. (2004) reported the detection of the SiNC radical in IRAM 30 m telescope observations of IRC+10216. Four rotational transitions between 83 and 134 GHz were observed and assigned based on the laboratory work of Apponi et al. (2000).

3.68. HCP (Phosphaethyne)

Agúndez et al. (2007) reported the detection of four transitions ($J = 4 \rightarrow 3$ through $7 \rightarrow 6$) of HCP toward IRC +10216 using the IRAM 30 m telescope. The enabling laboratory work was performed by Bizzocchi et al. (2001) and references therein.

3.69. CCP (Dicarbon Phosphide Radical)

The detection of the CCP radical in ARO 12 m observations of IRC+10216 was reported by Halfen et al. (2008). Five transitions with partially resolved hyperfine splitting were identified and assigned based on laboratory work described in the same manuscript.

3.70. AlOH (Aluminum Hydroxide)

AlOH was detected in ARO 12 m and SMT observations of VY Canis Majoris by Tenenbaum & Ziurys (2010). The $J = 9 \rightarrow 8$, $7 \rightarrow 6$, and $5 \rightarrow 4$ transitions at 283, 220, and 157 GHz, respectively, were identified based on the enabling laboratory work of Apponi et al. (1993).

3.71. H_2O^+ (Oxidaniumyl Cation)

H_2O^+ was identified in *Herschel*/HIFI spectra toward DR21, Sgr B2, and NGC 6334 by Ossenkopf et al. (2010). Six hyperfine components of the $N_{K_a,K_c} = 1_{1,1} \rightarrow 0_{0,0}$, $J = 3/2 \rightarrow 1/2$ transition in the $^2B_1$ electronic ground state at 1.115 THz were observed. The assignments were based on a synthesis, re-analysis, and extrapolation of the laboratory work by Strahan et al. (1986) and Mürtz et al. (1998) Nearly simultaneously, Gerin et al. (2010) reported the observation of H_2O^+ along the LOS to W31C, also using *Herschel*/HIFI.

3.72. H_2Cl^+ (Chloronium Cation)

Lis et al. (2010) reported the observation of the $J_{K_a,K_c} = 2_{1,2} \rightarrow 1_{0,1}$ transitions of ortho-$H_2^{35}Cl^+$ and ortho-$H_2^{37}Cl^+$ near 781 GHz, and the $J_{K_a,K_c} = 1_{1,1} \rightarrow 0_{0,0}$ transition of para-$H_2^{35}Cl^+$ near 485 GHz in absorption toward NGC 6334I and Sgr B2 using *Herschel*/HIFI. The frequencies were derived from the rotational constants determined in the laboratory work of Araki et al. (2001).

3.73. KCN (Potassium Cyanide)

The detection of KCN was reported by Pulliam et al. (2010) using ARO 12 m, IRAM 30 m, and SMT observations of IRC +10216. More than a dozen transitions between 85 and 250 GHz were assigned based on the laboratory work of Törring et al. (1980).

3.74. FeCN (Iron Cyanide)

Zack et al. (2011) reported the detection of six transitions of FeCN between 84 and 132 GHz in ARO 12 m observations of IRC+10216. The enabling laboratory spectroscopy was reported in Flory & Ziurys (2011), which was not yet published at the time of the publication of Zack et al. (2011).

3.75. HO_2 (Hydroperoxyl Radical)

The detection of HO_2 was reported in IRAM 30 m and APEX observations toward ρ Oph A by Parise et al. (2012). Several hyperfine components were observed in the $N_{K_a,K_c} = 2_{0,2} \rightarrow 1_{0,1}$ and $4_{0,4} \rightarrow 3_{0,3}$ transitions at 130 and 261 GHz, respectively. The laboratory work was performed by Beers & Howard (1975), Saito (1977), and Charo & De Lucia (1982).

3.76. TiO_2 (Titanium Dioxide)

TiO_2 was detected by Kamiński et al. (2013) in SMA and PdBI observations of VY Canis Majoris. More than two dozen transitions of TiO_2 were observed between 221 and 351 GHz based on the laboratory work of Brünken et al. (2008) and Kania et al. (2011).

3.77. CCN (Cyanomethylidyne)

Anderson & Ziurys (2014) reported the detection of CCN in ARO 12 m and SMT observations of IRC+10216. The $J = 9/2 \rightarrow 7/2$, $13/2 \rightarrow 11/2$, and $19/2 \rightarrow 17/2$ Λ-doubled transitions near 106, 154, and 225 GHz, respectively, were identified and assigned based on the laboratory work of Anderson et al. (2015), which was published several months later.

3.78. SiCSi (Disilicon Carbide)

As reported by Cernicharo et al. (2015), 112 transitions of SiCSi were observed in IRAM 30 m telescope observations of IRC+10216 between 80 and 350 GHz. The transition frequencies were derived based on the contemporaneous laboratory work of McCarthy et al. (2015).

3.79. S_2H (Hydrogen Disulfide)

Fuente et al. (2017) reported the detection of S_2H in IRAM 30 m observations of the Horsehead PDR region. Although Fuente et al. (2017) do not not provide quantum numbers, they detect four lines corresponding to the unresolved hyperfine doublets of the $J_{K_a,K_c} = 6_{0,6} \rightarrow 5_{0,5}$ and $7_{0,7} \rightarrow 6_{0,6}$ transitions near 94 and 110 GHz, respectively. The laboratory analysis was described in Tanimoto et al. (2000).

3.80. HCS (Thioformyl Radical)

The detection of HCS was reported by Agúndez et al. (2018b) in IRAM 30 m observations of L483. Five resolved hyperfine components of the $N_{K_a,K_c} = 2_{0,2} \rightarrow 1_{0,1}$ transition of HCS near 81 GHz were identified based on the laboratory work of Habara et al. (2002).

3.81. HSC (Sulfhydryl Carbide Radical)

The detection of HSC was reported by Agúndez et al. (2018b) in IRAM 30 m observations of L483. Two resolved hyperfine components of the $N_{K_a,K_c} = 2_{0,2} \rightarrow 1_{0,1}$ transition of HSC near 81 GHz were identified based on the laboratory work of Habara & Yamamoto (2000).

3.82. NCO (Isocyanate Radical)

Marcelino et al. (2018) reported the detection of the NCO radical in IRAM 30 m observations of L483. Several hyperfine components of the $J = 7/2 \rightarrow 5/2$ and $9/2 \rightarrow 7/2$ transitions near 81.4 and 104.6 GHz were identified and assigned based on the laboratory work of Saito & Amano (1970) and Kawaguchi et al. (1985).

Four-atom Molecules

3.83. NH_3 (Ammonia)

The first detection of NH_3 was reported by Cheung et al. (1968) by observation of its $(J, K) = (1, 1)$ and $(2, 2)$ inversion transitions in the Galactic Center using a 20 m radio telescope located at Hat Creek Observatory. No references to the laboratory data are given, but the frequencies were likely derived from the accumulated works of Cleeton & Williams (1934), Gunther-Mohr et al. (1954), Kukolich (1965), and Kukolich (1967).

3.84. H_2CO (Formaldehyde)

Snyder et al. (1969) reported the detection of H_2CO in NRAO 140 ft telescope observations of more than a dozen interstellar sources. The $J_{K_a,K_c} = 1_{1,1} \rightarrow 1_{1,0}$ transition at 4830 MHz was observed without hyperfine splitting, based on the laboratory data of Shigenari (1967).

3.85. HNCO (Isocyanic Acid)

HNCO was observed in NRAO 36 ft observations of Sgr B2 by Snyder & Buhl (1972b). The $J_{K_a,K_c} = 4_{0,4} \rightarrow 3_{0,3}$ transition at 87925 MHz was detected and assigned based on the laboratory work of Kewley et al. (1963). The detection was confirmed in a companion article with the observation of the $1_{0,1} \rightarrow 0_{0,0}$ transition by Buhl et al. (1972).

3.86. H_2CS (Thioformaldehyde)

Sinclair et al. (1973) reported the detection of H_2CS through Parkes 64 m observations of Sgr B2. The $J_{K_a,K_c} = 2_{1,1} \rightarrow 2_{1,2}$ transition at 3139 MHz was identified and assigned based on the laboratory work of Johnson & Powell (1970).

3.87. C_2H_2 (Acetylene)

The detection of C_2H_2 was reported by Ridgway et al. (1976) in Mayall 4 m telescope observations of IRC+10216. The $\nu_1 + \nu_5$ combination band of acetylene at 4091 cm^{-1} was identified based on the laboratory work of Baldacci et al. (1973).

3.88. C_3N (Cyanoethynyl Radical)

Guélin & Thaddeus (1977) reported the tentative detection of C_3N in NRAO 36 ft observations of IRC+10216. They observed two sets of doublet transitions, with the center frequencies at 89 and 99 GHz. Based on calculated rotational constants, they tentatively assigned the emission to C_3N. Friberg et al. (1980) later confirmed the detection by observing the predicted $N = 3 \rightarrow 2$ transitions near 30 GHz. The laboratory spectra were subsequently measured by Gottlieb et al. (1983).

3.89. HNCS (Isothiocyanic Acid)

HNCS was detected by observation of the $J = 11 \rightarrow 10$, $9 \rightarrow 8$, and $8 \rightarrow 7$ transitions, among others, at 192, 106, and 94 GHz, respectively, in Bell 7 m and NRAO 36 ft telescope observations of Sgr B2 by Frerking et al. (1979). The laboratory frequencies were measured by Kewley et al. (1963).

3.90. $HOCO^+$ (Protonated Carbon Dioxide)

Thaddeus et al. (1981) reported the observation of a series of three lines in Bell 7 m observations of Sgr B2 they assigned to the $J = 6 \rightarrow 5$, $5 \rightarrow 4$, and $4 \rightarrow 3$ transitions of $HOCO^+$ at 128, 107, and 86 GHz, respectively, based on ab initio calculations by Green et al. (1976). The detection was later confirmed by laboratory observation of the rotational spectrum by Bogey et al. (1984).

3.91. C_3O (Tricarbon Monoxide)

The detection of C_3O was reported by Matthews et al. (1984) through NRAO 140 ft telescope observations of TMC-1. The $J = 2 \rightarrow 1$ transition at 19244 MHz was observed and assigned based on laboratory work by Brown et al. (1983). Three further transitions up to $J = 9 \rightarrow 8$ were observed in a follow-up study in the same source by Brown et al. (1985b). The detection was confirmed by Kaifu et al. (2004) with the observation of numerous additional lines in Nobeyama 45 m observations of TMC-1.

3.92. l-C_3H (Propynylidyne Radical)

The l-C_3H radical was detected toward TMC-1 and IRC +10216 through a combination of observations with the Bell 7 m, University of Massachusetts 14 m, NRAO 36 ft, and Onsala 20 m telescopes as reported in Thaddeus et al. (1985a). A number of transitions between 33 and 103 GHz were identified based on the accompanying laboratory work of Gottlieb et al. (1985).

3.93. $HCNH^+$ (Protonated Hydrogen Cyanide)

$HCNH^+$ was reported in NRAO 12 m and MWO 4.9 m telescope observations of Sgr B2 by Ziurys & Turner (1986). The $J = 1 \rightarrow 0$, $2 \rightarrow 1$, and $3 \rightarrow 2$ transitions were targeted at 74, 148, and 222 GHz, respectively, based on frequencies estimated from the laboratory work of Altman et al. (1984) and confirmed during the course of publication by the laboratory work of Bogey et al. (1985b).

3.94. H_3O^+ (Hydronium Cation)

Wootten et al. (1986) and Hollis et al. (1986) nearly simultaneously reported the detection of H_3O^+. Wootten et al. (1986) used the NRAO 12 m telescope to search for the $J_K = 1_1 \rightarrow 2_1$ transition at 307.2 GHz in Orion and Sgr B2, reporting a detection in each. Hollis et al. (1986) also observed the same transition in both Orion and Sgr B2 with the NRAO 12 m telescope. Later, Wootten et al. (1991) reported the

detection of a confirming line in Orion and Sgr B2 with the identification of the $3_2 \rightarrow 2_2$ transition of ortho-H_3O^+ using the CSO. These detections were based on the laboratory work of Plummer et al. (1985), Bogey et al. (1985a), and Liu & Oka (1985).

3.95. C_3S (Tricarbon Monosulfide Radical)

The detection of C_3S was reported by Yamamoto et al. (1987a). The authors measured the laboratory rotational spectrum of the molecule, and assigned the $^1\Sigma$ $J = 4 \rightarrow 3$, $7 \rightarrow 6$, and $8 \rightarrow 7$ lines at 23, 40, and 46 GHz, respectively to previously unidentified lines in the observations of Kaifu et al. (1987) toward TMC-1 using the Nobeyama 45 m telescope.

3.96. c-C_3H (Cyclopropenylidene Radical)

Yamamoto et al. (1987b) reported the detection of the hyperfine components of the $J = 5/2 \rightarrow 3/2$ and $3/2 \rightarrow 1/2$ transitions at 91.5 and 91.7 GHz, respectively, in Nobeyama 45 m observations of TMC-1. The enabling laboratory spectroscopy was presented in the same manuscript.

3.97. HC_2N (Cyanocarbene Radical)

Guélin & Cernicharo (1991) reported the detection of nine lines of HC_2N in IRAM 30 m observations of IRC+10216 between 72 and 239 GHz. The enabling laboratory work was presented in Saito et al. (1984) and Brown et al. (1990).

3.98. H_2CN (Methylene Amidogen Radical)

The detection of H_2CN was reported in NRAO 12 m observations of TMC-1 by Ohishi et al. (1994), who observed two hyperfine components of the $N_{K_a,K_c} = 1_{0,1} \rightarrow 0_{0,0}$ transition at 73.3 GHz. The laboratory spectroscopy was conducted by Yamamoto & Saito (1992).

3.99. SiC_3 (Silicon Tricarbide)

Apponi et al. (1999a) reported the detection of SiC_3 in NRAO 12 m observations of IRC+10216. Nine transitions of SiC_3 between 81 and 103 GHz were observed and assigned based on laboratory work by the same group, published shortly thereafter in McCarthy et al. (1999) and Apponi et al. (1999b).

3.100. CH_3 (Methyl Radical)

The detection of CH_3 was reported by Feuchtgruber et al. (2000) using *ISO* observations of the ν_2 Q-branch line at 16.5 μm and the $R(0)$ line at 16.0 μm toward Sgr A*. The enabling laboratory work was performed by Yamada et al. (1981). The first ground-based detection of CH_3 was described later by Knez et al. (2009).

3.101. C_3N^- (Cyanoethynyl Anion)

Both the laboratory spectroscopy and astronomical detection of C_3N^- were presented in Thaddeus et al. (2008). The anion was detected in IRAM 30 m observations of IRC+10216 in the $J = 10 \rightarrow 9$, $11 \rightarrow 10$, $14 \rightarrow 13$, and $15 \rightarrow 14$ transitions at 97, 107, 136, and 146 GHz, respectively.

3.102. PH_3 (Phosphine)

Agúndez et al. (2008) and Tenenbaum & Ziurys (2008) simultaneously and independently reported the tentative detection of PH_3. Tenenbaum & Ziurys (2008) observed emission from the $J_K = 1_0 \rightarrow 0_0$ transition at 267 GHz toward IRC+10216 and CRL 2688 using the SMT telescope. Agúndez et al. (2008) observed the same transition toward IRC+10216 using the IRAM 30 m telescope, and searched for the $J = 3 \rightarrow 2$ transition at 801 GHz using the CSO, unsuccessfully. These detections were confirmed by Agúndez et al. (2014a) through successful observation of the 534 GHz $J = 2 \rightarrow 1$ line toward IRC+10216 with *Herschel*/HIFI. The laboratory spectroscopy was presented in Cazzoli & Puzzarini (2006), Sousa-Silva et al. (2013), and Müller (2013).

3.103. HCNO (Fulminic Acid)

The discovery of HCNO was reported by Marcelino et al. (2009) through observation of the $J = 5 \rightarrow 4$ and $4 \rightarrow 3$ transitions at 92 and 115 GHz, respectively, in IRAM 30 m observations of TMC-1, L1527, B1-b, L1544, and L183. The laboratory rotational spectra were reported in Winnewisser & Winnewisser (1971).

3.104. HOCN (Cyanic Acid)

The laboratory rotational spectrum and tentative astronomical identification of HOCN were reported by Brünken et al. (2009a) toward Sgr B2 using archival survey data. The $J_{K_a,K_c} = 5_{0,5} \rightarrow 4_{0,4}$ and $6_{0,6} \rightarrow 5_{0,5}$ transitions at 104.9 and 125.8 GHz, respectively, were observed in Bell 7 m observations by Cummins et al. (1986). The $4_{0,4} \rightarrow 3_{0,3}$ transition at 83.9 GHz was observed in the survey of Turner (1989) using the NRAO 36 ft telescope, but misassigned in that work to a transition of CH_3OD. These detections were confirmed shortly thereafter by Brünken et al. (2010) using IRAM 30 m observations of Sgr B2 to self-consistently observe the $4_{0,4} \rightarrow 3_{0,3}$ through $8_{0,8} \rightarrow 7_{0,7}$ transitions.

3.105. HSCN (Thiocyanic Acid)

Halfen et al. (2009) reported the detection of HSCN in ARO 12 m observations of Sgr B2. Six lines between 69–138 GHz were observed and assigned to the $J_{K_a,K_c} = 6_{0,6} \rightarrow 5_{0,5}$ through $12_{0,12} \rightarrow 11_{0,11}$ transitions based on the laboratory work of Brünken et al. (2009b).

3.106. HOOH (Hydrogen Peroxide)

The detection of HOOH was reported by Bergman et al. (2011) in APEX 12 m observations toward ρ Oph A. Three lines corresponding to the $J_{K_a,K_c} = 3_{0,3} \rightarrow 2_{1,1}$ $\tau = 4 \rightarrow 2$, $6_{1,5} \rightarrow 5_{0,5}$ $2 \rightarrow 4$, and $5_{0,5} \rightarrow 4_{1,3}$ $4 \rightarrow 2$ torsion-rotation transitions at 219, 252, and 318 GHz, respectively, were assigned based on the laboratory work of Helminger et al. (1981) and Petkie et al. (1995).

3.107. l-C_3H^+ (Cyclopropynylidynium Cation)

Pety et al. (2012) first reported the detection of a series of eight harmonically spaced unidentified lines in IRAM 30 m observations of the Horsehead PDR region, which seemed to correspond to the $J = 4 \rightarrow 3$ through $12 \rightarrow 11$ transitions of a linear or quasi-linear molecule. Based on the comparison of

their derived rotational constants to ab initio values calculated by Ikuta (1997), they tentatively assigned the carrier of these lines to the l-C_3H^+ cation. Using the derived spectroscopic parameters, McGuire et al. (2013a) subsequently detected the $1 \rightarrow 0$ and $2 \rightarrow 1$ transitions at 22.5 and 45 GHz, respectively, in absorption toward Sgr B2 using the GBT 100 m telescope. Contemporaneously, Huang et al. (2013) and Fortenberry et al. (2013) challenged the attribution to l-C_3H^+, suggesting that the C_3H^- anion was a more likely candidate, based on better agreement between the distortion constants from their high-level quantum chemical calculations to those derived by Pety et al. (2012). This assertion was challenged by McGuire et al. (2014), who argued that the formation and destruction chemistry in the high-UV environments the molecule was found strongly favored l-C_3H^+ over C_3H^-. The assignment to l-C_3H^+ was shortly thereafter confirmed by the laboratory observation and characterization of the rotational spectrum of the cation by Brünken et al. (2014).

3.108. HMgNC (Hydromagnesium Isocyanide)

Cabezas et al. (2013) reported the laboratory and astronomical identification of HMgNC in IRAM 30 m observations of IRC+10216. The $J = 8 \rightarrow 7$ through $13 \rightarrow 12$ transitions between 88 and 142 GHz were observed and assigned based on predicted values from the laboratory observations of the hyperfine split $1 \rightarrow 0$ and $2 \rightarrow 1$ transitions at 11 and 22 GHz, respectively.

3.109. HCCO (Ketenyl Radical)

The detection of HCCO was reported by Agúndez et al. (2015b) using IRAM 30 m observations of Lupus-1A and L483. Four fine and hyperfine components of the $N = 4 \rightarrow 3$ transition of HCCO were resolved near 86.7 GHz and assigned based on the laboratory work of Endo & Hirota (1987) and Ohshima & Endo (1993).

3.110. CNCN (Isocyanogen)

Agúndez et al. (2018a) reported the detection of CNCN in L483 using IRAM 30 m observations. The $J = 8 \rightarrow 7$, $9 \rightarrow 8$, $10 \rightarrow 9$ transitions at 82.8, 93.1, and 103.5 GHz were observed and assigned based on the laboratory work of Winnewisser et al. (1992) and Gerry et al. (1990). A tentative detection in TMC-1 was also reported in the same work.

Five-atom Molecules

3.111. HC_3N (Cyanoacetylene)

Turner (1971) reported the detection of the $F = 2 \rightarrow 1$ and $1 \rightarrow 1$ hyperfine components of the $J = 1 \rightarrow 0$ transition of HC_3N at 9098 and 9097 MHz, respectively, in NRAO 140 ft telescope observations of Sgr B2. The assignment was based on the laboratory work of Tyler & Sheridan (1963). The detection was confirmed the following year by Dickinson (1972) through observation of two hyperfine components of the $J = 2 \rightarrow 1$ transition at 18 GHz in Haystack Observatory 120 ft telescope observations of Sgr B2.

3.112. HCOOH (Formic Acid)

The detection of HCOOH was reported by Zuckerman et al. (1971) in Sgr B2 using the NRAO 140 ft telescope. The $J_{K_a,K_c} = 1_{1,1} \rightarrow 1_{1,0}$ transition at 1639 MHz was identified and assigned based on laboratory work presented in the same manuscript. Later, Winnewisser & Churchwell (1975) confirmed the detection by observation of the $2_{1,1} \rightarrow 2_{1,2}$ transition at 4.9 GHz in Sgr B2 using the MPIfR 100 m telescope. This identification was based on the laboratory work of Bellet et al. (1971b) and Bellet et al. (1971a, in French).

3.113. CH_2NH (Methanimine)

Godfrey et al. (1973) reported the detection of CH_2NH in Sgr B2 using the Parkes 64 m telescope. The $J = 1_{1,0} \rightarrow 1_{1,1}$ transition at 5.2 GHz was observed and assigned based on laboratory work presented in the same manuscript, and building on the earlier laboratory efforts of Johnson & Lovas (1972). CH_2NH is also referred to as methylenimine.

3.114. NH_2CN (Cyanamide)

Turner et al. (1975) described the detection of NH_2CN in Sgr B2 by observation of its $J_{K_a,K_c} = 5_{1,4} \rightarrow 4_{1,3}$ and $4_{1,3} \rightarrow 3_{1,2}$ transitions at 100.6 and 80.5 GHz, respectively, using the NRAO 36 ft telescope. The assignment was based on the work of Lide (1962), Millen et al. (1962), and Tyler et al. (1972), and subsequently confirmed in the laboratory by Johnson et al. (1976).

3.115. H_2CCO (Ketene)

The detection of H_2CCO was reported by Turner (1977) in NRAO 36 ft telescope observations of Sgr B2. The $J_{K_a,K_c} = 5_{1,4} \rightarrow 4_{1,3}$, $5_{1,5} \rightarrow 4_{1,4}$, and $4_{1,3} \rightarrow 3_{1,2}$ transitions at 102, 100, and 82 GHz, respectively, were observed and assigned based on the laboratory work of Johnson & Strandberg (1952) and Johns et al. (1972).

3.116. C_4H (Butadiynyl Radical)

Guélin et al. (1978) reported the tentative detection of C_4H using NRAO 36 ft observations of IRC+10216 in combination with the previously published observations of Scoville & Solomon (1978) and Liszt (1978) in complementary frequency ranges. In total, four sets of spin doublet lines were observed between 86 and 114 GHz, and assigned to the $N = 9 \rightarrow 8$ through $N = 12 \rightarrow 11$ transitions of C_4H based on comparison to the theoretical rotational constants calculated by Wilson & Green (1977). The detection was subsequently confirmed through the laboratory efforts of Gottlieb et al. (1983).

3.117. SiH_4 (Silane)

The detection of SiH_4 was reported by Goldhaber & Betz (1984) in IRTF observations toward IRC+10216. Thirteen absorption lines in the ν_4 band near 917 cm^{-1} were assigned based on laboratory work described in the same manuscript.

3.118. c-C_3H_2 (Cyclopropenylidene)

The laboratory spectroscopy and interstellar detection of c-C_3H_2 was described in a pair of papers by Thaddeus et al. (1985b) and Vrtilek et al. (1987). After the report of Thaddeus et al. (1985b), the molecule began to be detected in numerous sources, with the best detections, as reported in Vrtilek et al. (1987) being in Sgr B2, Orion, and TMC-1 with the Bell 7 m

telescope. A total of 11 transitions between 18 and 267 GHz were initially assigned.

3.119. CH_2CN (Cyanomethyl Radical)

Irvine et al. (1988b) reported the detection of the CH_2CN radical in TMC-1 and Sgr B2 using a combination of observations from the FCRAO 14 m, NRAO 140 ft, Onsala 20 m, and Nobeyama 45 m telescopes. Numerous hyperfine-resolved components of the $N_{K_a,K_c} = 1_{0,1} \rightarrow 0_{0,0}$ and $2_{0,2} \rightarrow 1_{0,1}$ transitions at 20 and 40 GHz, respectively, were observed in TMC-1, as well as an unresolved detection of the $4_{0,4} \rightarrow 4_{0,3}$ transition at 101 GHz. The assignments were made based on laboratory work presented in a companion paper from Saito et al. (1988). Five partially resolved components were also detected in Sgr B2 between 40 and 101 GHz.

3.120. C_5 (Pentacarbon)

The detection of C_5 was reported by Bernath et al. (1989) in KPNO 4 m telescope observations of IRC+10216. More than a dozen *P*- and *R*-branch transitions of the ν_3 asymmetric stretching mode near 2164 cm^{-1} were detected, guided by the laboratory work of Vala et al. (1989).

3.121. SiC_4 (Silicon Tetracarbide)

Ohishi et al. (1989) reported the detection of SiC_4 in Nobeyama 45 m observations of IRC+10216. Their search was initially guided by quantum chemical calculations they carried out, the results of which led to the assignment of five astronomically observed features between 37 and 89 GHz to the $J = 12 \rightarrow 11, 13 \rightarrow 12, 14 \rightarrow 13, 16 \rightarrow 15$, and $28 \rightarrow 27$ transitions of SiC_4. In the same work, they confirmed the detection by conducting laboratory microwave spectroscopy of the $J = 42 \rightarrow 41$ through $48 \rightarrow 47$ transitions.

3.122. H_2CCC (Propadienylidene)

The detection of H_2CCC was reported by Cernicharo et al. (1991a) in IRAM 30 m telescope observations and archival Effelsberg 100 m telescope observations (Cernicharo et al. 1987b) of TMC-1. The $J_{K_a,K_c} = 1_{0,1} \rightarrow 0_{0,0}$ transition of para-H_2CCC at 21 GHz, and three transitions of ortho-H_2CCC between 103 and 147 GHz were identified based on the laboratory work of Vrtilek et al. (1990).

3.123. CH_4 (Methane)

CH_4 was detected in both the gas phase and solid phase in IRTF observations toward NGC 7538 IRS 9 by Lacy et al. (1991). The gas-phase *R*(0) line and two blended *R*(2) lines at 1311.43, 1322.08, and 1322.16 cm^{-1} were observed and assigned based on the laboratory work of Champion et al. (1989). The solid-phase absorption of the ν_4 mode near 7.7 μm was observed and assigned based on the laboratory work of D'Hendecourt & Allamandola (1986).

3.124. HCCNC (Isocyanoacetylene)

Kawaguchi et al. (1992a) reported the detection of HCCNC, also known as isocyanoethyne and ethynyl isocyanide, in Nobeyama 45 m observations of TMC-1. The $J = 4 \rightarrow 3$, $5 \rightarrow 4$, and $9 \rightarrow 8$ transitions at 40, 50, and 89 GHz, respectively, were identified and assigned based on the laboratory work of Krueger et al. (2010).

3.125. HNCCC

Kawaguchi et al. (1992b) reported both the laboratory spectroscopy and astronomical identification of HNCCC in Nobeyama 45 m telescope observations of TMC-1. The $J = 3 \rightarrow 2$, $4 \rightarrow 3$, and $5 \rightarrow 4$ transitions at 28, 37, and 47 GHz, respectively, were assigned and identified.

3.126. H_2COH^+ (Protonated Formaldehyde)

The detection of H_2COH^+ was reported by Ohishi et al. (1996) in Nobeyama 45 m and NRAO 12 m telescope observations of Sgr B2, Orion, and W51. Six transitions between 32 and 174 GHz were observed and assigned based on the laboratory work of Chomiak et al. (1994).

3.127. C_4H^- (Butadiynyl Anion)

Cernicharo et al. (2007) reported the detection of C_4H^- in IRAM 30 m observations of IRC+10216 through observation of five transitions between 84 and 140 GHz. The detection was enabled by the laboratory work of Gupta et al. (2007).

3.128. CNCHO (Cyanoformaldehyde)

CNCHO was detected in GBT 100 m observations of Sgr B2(N) by Remijan et al. (2008a). A total of seven transitions between 2.1 and 41 GHz were identified and assigned based on the laboratory work of Bogey et al. (1988) and Bogey et al. (1995). CNCHO is also referred to as formyl cyanide.

3.129. HNCNH (Carbodiimide)

McGuire et al. (2012) reported the detection of HNCNH in GBT 100 m observations of Sgr B2. Four sets of transitions were identified to arise from maser action, while several other stronger transitions incapable of masing were not observed. The assignments were made based on the laboratory work of Birk et al. (1989), Wagener et al. (1995), and Jabs et al. (1997).

3.130. CH_3O (Methoxy Radical)

The detection of CH_3O was reported in IRAM 30 m observations of B1-b by Cernicharo et al. (2012). Several hyperfine components of the $N = 1 \rightarrow 0$ transition near 82.4 GHz were identified and assigned based on the laboratory work of Endo et al. (1984) and Momose et al. (1988). Components of the $2 \rightarrow 1$ transition are shown, but no frequency information is provided other than that the transitions are at 2 mm.

3.131. NH_3D^+ (Deuterated Ammonium Cation)

The detection of NH_3D^+ was reported toward Orion and B1-b in IRAM 30 m observations by Cernicharo et al. (2013b). A single line with unresolved hyperfine structure was observed and assigned to the $J_K = 1_0 \rightarrow 0_0$ transition of NH_3D^+ based on laboratory results presented in the same manuscript. A companion article by Domenech et al. (2013) detailed the laboratory results.

3.132. H_2NCO^+ (Protonated Isocyanic Acid)

Gupta et al. (2013) reported a tentative detection of H_2NCO^+ in GBT 100 m observations of Sgr B2. Based on laboratory work presented in the same manuscript, they identified and assigned the $J_{K_a,K_c} = 0_{0,0} \rightarrow 1_{0,1}$ and $1_{1,0} \rightarrow 2_{1,1}$ transitions of para- and ortho-H_2NCO^+ at 20.2 and 40.8 GHz, respectively. The detection was confirmed by Marcelino et al. (2018) in IRAM 30 m observations of L483. They observed six additional transitions of H_2NCO^+ between 80 and 116 GHz.

3.133. $NCCNH^+$ (Protonated Cyanogen)

Agúndez et al. (2015a) reported the detection of $NCCNH^+$ in TMC-1 and L483 using IRAM 30 m and Yerbes 40 m observations. The $J = 5 \rightarrow 4$ and $10 \rightarrow 9$ transitions at 44.3 and 88.8 GHz, respectively, were identified and assigned based on the laboratory work of Amano & Scappini (1991) and Gottlieb et al. (2000).

3.134. CH_3Cl (Chloromethane)

CH_3Cl, also called methyl chloride, was detected in ALMA observations of IRAS 16293-2422, and in ROSINA mass spectrometry measurements of comet 67P/Churyumov–Gerasimenko, by Fayolle et al. (2017). Both the ^{35}Cl and ^{37}Cl isotopologues were detected through observation and assignment of the $J_K = 13_K \rightarrow 12_K$ $K = 0$ to 4 transitions between 340 and 360 GHz. The laboratory work was presented by Wlodarczak et al. (1986).

Six-atom Molecules

3.135. CH_3OH (Methanol)

Ball et al. (1970) reported the detection of CH_3OH in NRAO 140 ft observations of Sgr A and Sgr B2. The $J_{K_a,K_c} = 1_{1,0} \rightarrow 1_{1,1}$ transition at 834 MHz was observed and assigned based on laboratory work described in the same manuscript.

3.136. CH_3CN (Methyl Cyanide)

CH_3CN was detected by Solomon et al. (1971) in Sgr B2 and Sgr A using the NRAO 36 ft telescope. Two fully resolved, and two blended K components of the $J = 6 \rightarrow 5$ transition near 110.4 GHz were identified and assigned based on the laboratory data cataloged in Cord et al. (1968). It is likely that the frequencies listed in Cord et al. (1968) were obtained from, or relied heavily upon, the prior work by Kessler et al. (1950). CH_3CN is also referred to as acetonitrile.

3.137. NH_2CHO (Formamide)

The detection of NH_2CHO was reported by Rubin et al. (1971) in NRAO 140 ft observations of Sgr B2. The $J_{K_a,K_c} = 2_{1,1} \rightarrow 2_{1,2}$, $F = 2 \rightarrow 2$ and $1 \rightarrow 1$ hyperfine components were resolved, while the $3 \rightarrow 3$ was detected as part of a blend with the H112α transition. The enabling laboratory spectroscopy was reported in the same manuscript. NH_2CHO was the first interstellar molecule detected containing H, C, N, and O.

3.138. CH_3SH (Methyl Mercaptan)

Linke et al. (1979) reported the detection of CH_3SH in Bell 7 m telescope observations of Sgr B2. Six transitions between 76 and 102 GHz were identified and assigned based on the laboratory work of Kilb (1955) and unpublished data of D.R. Johnson. This latter data set was analyzed and formed the foundation of the more extensive work of Lees & Mohammadi (1980).

3.139. C_2H_4 (Ethylene)

The detection of C_2H_4 was reported by Betz (1981) toward IRC+10216 using the 1.5 m McMath Solar Telescope. Three rotationally resolved ro-vibrational transitions were observed in the ν_7 state: the $J_{K_a,K_c} = 5_{1,5} \rightarrow 5_{0,5}$ at 28.5 THz was assigned based on the laboratory work of Lambeau et al. (1980), while the $1_{1,0} \rightarrow 0_{0,0}$ and $8_{0,8} \rightarrow 8_{1,8}$ were assigned based on laboratory work described in Betz (1981).

3.140. C_5H (Pentynylidyne Radical)

A tentative detection of C_5H was reported by Cernicharo et al. (1986b) in IRAM 30 m observations of IRC+10216. They identified a series of lines that could be assigned to a radical species in a $^2\Pi$ ground state with quantum numbers $J = 31/2 \rightarrow 29/2$ and $35/2 \rightarrow 33/2$ through $43/2 \rightarrow 41/2$ between 74 and 103 GHz. Based on comparison of the derived rotational constant ($B_0 = 2387$ MHz) to a calculated rotational constant ($B_0 = 2375$ MHz) described in the same manuscript, they tentatively assigned the emission to the C_5H radical. The subsequent laboratory work by Gottlieb et al. (1986) confirmed the assignment, and the interstellar identifications were extended shortly thereafter by Cernicharo et al. (1986a, 1987c).

3.141. CH_3NC (Methyl Isocyanide)

A tentative detection of CH_3NC was reported by Cernicharo et al. (1988) in IRAM 30 m observations of Sgr B2. A somewhat blended signal was observed near the frequencies corresponding to the $J = 4 \rightarrow 3$, $5 \rightarrow 4$, and $7 \rightarrow 6$ transitions at 80.4, 100.5, and 140.7 GHz, respectively. Although no reference is given for these frequencies, they were presumably enabled by the laboratory work of Kukolich (1972) and Ring et al. (1947). The detection was confirmed nearly two decades later in GBT 100 m observations of Sgr B2 by Remijan et al. (2005), who observed the $J_K = 1_0 \rightarrow 0_0$ transition in absorption at 20.1 GHz and by Gratier et al. (2013), who observed three lines in the $J = 5 \rightarrow 4$ transition at 100.5 GHz with the IRAM 30 m toward the Horsehead PDR.

3.142. HC_2CHO (Propynal)

Irvine et al. (1988a) reported the detection of HC_2CHO in NRAO 140 ft and Nobeyama 45 m observations of TMC-1. The $J_{K_a,K_c} = 2_{0,2} \rightarrow 1_{0,1}$ and $4_{0,4} \rightarrow 3_{0,3}$ transitions at 18.7 and 37.3 GHz, respectively, were assigned based on the laboratory work of Winnewisser (1973).

3.143. H_2C_4 (Butatrienylidene)

Cernicharo et al. (1991b) reported the detection of the H_2C_4 carbene molecule in IRAM 30 m observations of IRC+10216. Eight transitions with J values between 8 and 15 were identified and assigned between 80 and 135 GHz based on the laboratory spectroscopy of Killian et al. (1990).

3.144. C_5S (Pentacarbon Monosulfide Radical)

The C_5S radical was tentatively detected by Bell et al. (1993) in NRAO 140 ft telescope observations of IRC+10216. A weak line corresponding to the $J = 13 \rightarrow 12$ transition of C_5S was identified near 23960 MHz based on the laboratory work of Kasai et al. (1993). The detection was confirmed in Agúndez et al. (2014b) with IRAM 30 m observations of IRC+10216. The $J = 44 \rightarrow 43$, $45 \rightarrow 44$, and $46 \rightarrow 45$ transitions at 81.2, 83.0, and 84.9 GHz, respectively, were identified and assigned based on the laboratory work of Gordon et al. (2001).

3.145. HC_3NH^+ (Protonated Cyanoacetylene)

Kawaguchi et al. (1994) reported the detection of HC_3NH^+ in Nobeyama 45 m observations of TMC-1. The $J = 4 \rightarrow 3$ and $5 \rightarrow 4$ transitions at 34.6 and 43.3 GHz, respectively, were identified and assigned based on the frequencies reported by Lee & Amano (1987) from infrared difference frequency laser spectroscopy. Using the astronomically detected pure rotational lines as a guide, the rotational spectrum was then measured in the laboratory by Gottlieb et al. (2000).

3.146. C_5N (Cyanobutadiynyl Radical)

The C_5N radical was detected by Guélin et al. (1998) in Effelsberg 100 m and IRAM 30 m observations of TMC-1. Two sets of hyperfine components of the $J = 17/2 \rightarrow 15/2$ and $65/2 \rightarrow 63/2$ transitions of C_5N at 25.2 and 89.8 GHz, respectively, were identified and assigned based on the laboratory work of Kasai et al. (1997).

3.147. HC_4H (Diacetylene)

Cernicharo et al. (2001) reported the detection of HC_4H in *ISO* observations of CRL 618 near 15.9 μm. The observed absorption signal was identified and assigned to the ν_8 fundamental bending mode of HC_4H based on the laboratory work of Arié & Johns (1992).

3.148. HC_4N

The HC_4N radical was detected by Cernicharo et al. (2004) in IRAM 30 m observations of IRC+10216. A dozen transitions beteween 83 and 97 GHz were identified and assigned based on the laboratory work of Tang et al. (1999).

3.149. c-H_2C_3O (Cyclopropenone)

Hollis et al. (2006b) reported the detection of c-H_2C_3O in GBT 100 m observations of Sgr B2. Six transitions between 9.3 and 44.6 GHz were identified and assigned based on the laboratory work of Benson et al. (1973) and Guillemin et al. (1990).

3.150. CH_2CNH (Ketenimine)

The detection of CH_2CNH was reported by Lovas et al. (2006a) using GBT 100 m telescope observations of Sgr B2. The $J_{K_a,K_c} = 9_{1,8} \rightarrow 10_{0,10}$, $8_{1,7} \rightarrow 9_{0,9}$, and $7_{1,6} \rightarrow 8_{0,8}$ transitions at 4.9, 23.2, and 41.5 GHz, respectively, were identified and assigned based on the laboratory work of Rodler et al. (1984, 1986).

3.151. C_5N^- (Cyanobutadiynyl Anion)

Cernicharo et al. (2008) reported the detection of C_5N^- in IRAM 30 m observations of IRC+10216. They identified and assigned 11 lines to the $J = 29 \rightarrow 28$ through $40 \rightarrow 39$ transitions of C_5N^- by comparison to the calculated rotational constants presented in Botschwina & Oswald (2008). To date, there does not appear to be a published pure rotational laboratory spectrum of this species.

3.152. HNCHCN (E-cyanomethanimine)

HNCHCN was detected in GBT 100 m telescope observations of Sgr B2 as reported by Zaleski et al. (2013). Nine transitions between 9.6 and 47.8 GHz were identified and assigned based on laboratory spectroscopy presented in the same manuscript.

3.153. SiH_3CN (Silyl Cyanide)

The tentative detection of SiH_3CN was reported by Agúndez et al. (2014b) in IRAM 30 m observations of IRC+10216 through the identification of three weak emission features that they assign to the $J = 9 \rightarrow 8$, $10 \rightarrow 9$, and $11 \rightarrow 10$ transitions of SiH_3CN at 89.5, 99.5, and 109.4 GHz, respectively, based on the laboratory work of Priem et al. (1998). The detection was confirmed by Cernicharo et al. (2017) through the detection of additional, higher-frequency transitions in this source.

Seven-atom Molecules

3.154. CH_3CHO (Acetaldehyde)

The detection of the $J_{K_a,K_c} = 1_{1,1} \rightarrow 1_{1,0}$ transition of CH_3CHO at 1065 MHz was reported by Gottlieb (1973) in NRAO 140 ft observations of Sgr B2 and Sgr A. The assignment was made based on the laboratory work of Kilb et al. (1957) and Souter & Wood (1970). Fourikis et al. (1974a) reported a confirming observation of the $2_{1,1} \rightarrow 2_{1,2}$ transition in Parkes 64 m observations of Sgr B2 at 3195 MHz.

3.155. CH_3CCH (Methyl Acetylene)

Buhl & Snyder (1973) reported the detection of the $J_K = 5_0 \rightarrow 4_0$ transition of CH_3CCH at 85.4 GHz in NRAO 36 ft telescope observations of Sgr B2. Although no reference to the source of the frequency is given, it was presumably obtained from the laboratory work of Trambarulo & Gordy (1950). Subsequent confirming transitions were observed at higher frequencies by Hollis et al. (1981) and Kuiper et al. (1984).

3.156. CH_3NH_2 (Methylamine)

The detection of CH_3NH_2 was simultaneously reported by Fourikis et al. (1974b) and Kaifu et al. (1974). Kaifu et al. (1974) used the Mitaka 6 m and NRAO 36 ft telescopes to observe CH_3NH_2 toward Sgr B2 and Orion. The *a*, $J_{K_a,K_c} = 5_{1,5} \rightarrow 5_{0,5}$ and *s*, $4_{1,4} \rightarrow 4_{0,4}$ transitions at 73 and 86 GHz, respectively, were assigned based on the laboratory work of Takagi & Kojima (1973). Using the same laboratory work, Fourikis et al. (1974b) reported the detection of the *a*, $2_{0,2} \rightarrow 1_{1,0}$ transition at 8.8 GHz using the Parkes 64 m telescope, also toward Sgr B2 and Orion.

3.157. CH_2CHCN (Vinyl Cyanide)

CH_2CHCN, also known as acrylonitrile, was detected by Gardner & Winnewisser (1975) in Parkes 64 m observations of Sgr B2. The $J_{K_a,K_c} = 2_{1,1} \rightarrow 2_{1,2}$ transition at 1372 MHz was identified and assigned based on the laboratory work of Gerry & Winnewisser (1973). Several additional confirming transitions were later observed in NRAO 140 ft telescope observations of TMC-1 by Matthews & Sears (1983).

3.158. HC_5N (Cyanodiacetylene)

Avery et al. (1976) reported the detection of HC_5N in Algonquin Radio Observatory 46 m telescope observations of Sgr B2. They observed and assigned the $J = 4 \rightarrow 3$ transition at 10651 MHz based on the laboratory work of Alexander et al. (1976). Later that year, Broten et al. (1976) observed the $1 \rightarrow 0$ and $8 \rightarrow 7$ transitions with the same facility, also in Sgr B2.

3.159. C_6H (Hexatriynyl Radical)

The first detection of the C_6H radical was made by Suzuki et al. (1986) in Nobeyama 45 m observations of TMC-1. The authors observed three sets of doublet transitions at 23.6, 40.2, and 43.0 GHz, which they assigned to the hyperfine-split, Λ-doubled $J = 17/2 \rightarrow 15/2$, $29/2 \rightarrow 27/2$, and $31/2 \rightarrow 29/2$ transitions, respectively, of C_6H based on a comparison to the quantum chemical work of Murakami et al. (1987). The detection was confirmed the following year with the measurement of the laboratory rotational spectrum by Pearson et al. (1988).

3.160. c-C_2H_4O (Ethylene Oxide)

Dickens et al. (1997) reported the detection of c-C_2H_4O in Nobeyama 45 m, Haystack 140 ft, and SEST 15 m telescope observations of Sgr B2. Nine transitions between 39.6 and 254.2 GHz were identified and assigned based on the laboratory rotational spectroscopy performed by Hirose (1974).

3.161. CH_2CHOH (Vinyl Alcohol)

Turner & Apponi (2001) reported the detection of both syn- and anti-vinyl alcohol in NRAO 12 m observation of Sgr B2. The syn conformer of CH_2CHOH is the more stable, but only two lines, the $J_{K_a,K_c} = 2_{1,2} \rightarrow 1_{0,1}$ and $3_{1,3} \rightarrow 2_{0,2}$ transitions at 86.6 and 103.7 GHz, respectively, were identified and assigned based on the laboratory work of Kaushik (1977). In contrast, five transitions of the anti-conformer were identified between 71.8 and 154.5 GHz based on the laboratory work of Rodler (1985).

3.162. C_6H^- (Hexatriynyl Anion)

The first molecular anion to be detected in the ISM, McCarthy et al. (2006) described both the observation and laboratory spectroscopic identification of C_6H^-. More than a decade prior, Kawaguchi et al. (1995) had noted the presence of a series of unidentified, harmonically spaced emission features in their Nobeyama 45 m survey of IRC+10216 dubbed B1377. Based on their laboratory work, McCarthy et al. (2006) successfully assigned the carrier of these transitions to C_6H^-. They also identified the $J = 4 \rightarrow 3$ and $5 \rightarrow 4$ transitions at 11.0 and 13.8 GHz, respectively, in GBT 100 m telescope observations of TMC-1.

3.163. CH_3NCO (Methyl Isocyanate)

The detection of CH_3NCO was reported by Halfen et al. (2015) in ARO 12 m and SMT observations of Sgr B2. They observed 17 uncontaminated emission lines of CH_3NCO between 68 and 116 GHz and assigned them based on laboratory work described in the same manuscript. The following year, Cernicharo et al. (2016) reported the detection of the molecule in IRAM 30 m and ALMA data toward Orion, as well as extending the laboratory spectroscopy.

3.164. HC_5O (Butadiynylformyl Radical)

McGuire et al. (2017a) reported the detection of HC_5O in GBT 100 m observations of TMC-1. Four hyperfine-resolved components of the $J = 17/2 \rightarrow 15/2$ transition at 21.9 GHz were detected and assigned based on the laboratory work of Mohamed et al. (2005).

Eight-atom Molecules

3.165. $HCOOCH_3$ (Methyl Formate)

Brown et al. (1975a) reported the detection of *cis*-$HCOOCH_3$ in Parkes 64 m telescope observations of Sgr B2. Based on laboratory work presented in the same paper, they identified and assigned the *A*-state $J_{K_a,K_c} = 1_{1,0} \rightarrow 1_{1,1}$ transition of *cis*-$HCOOCH_3$ at 1610.25 MHz. Several months later, Churchwell & Winnewisser (1975) confirmed the detection of the *A*-state line and additionally observed the *E*-state line of the same transition at 1610.9 MHz using the Effelsberg 100 m telescope. Nearly three decades later, Neill et al. (2012) reported the tentative identification of the higher-energy trans conformer of $HCOOCH_3$ in GBT 100 m telescope observations of Sgr B2, based on laboratory spectroscopy presented in the same work. A total of seven transitions between 9.1 and 27.4 GHz were observed.

3.166. CH_3C_3N (Methylcyanoacetylene)

The detection of CH_3C_3N was reported by Broten et al. (1984) in NRAO 140 ft observations of TMC-1. A total of seven components of the $J = 5 \rightarrow 4$ through $8 \rightarrow 7$ transitions of CH_3C_3N between 20.7 and 33.1 GHz were resolved and assigned based on the laboratory work of Moïses et al. (1982).

3.167. C_7H (Heptatriynylidyne Radical)

Guélin et al. (1997) reported the detection of the C_7H radical in IRAM 30 m telescope observations of IRC+10216. Based on the laboratory spectroscopy of Travers et al. (1996a), they identified and assigned five rotational transitions between 83 and 86.6 GHz.

3.168. CH_3COOH (Acetic Acid)

The detection of CH_3COOH was reported by Mehringer et al. (1997) in BIMA and OVRO observations of Sgr B2. The $J_{K_a,K_c} = 8_{*,8} \rightarrow 7_{*,7}$ *A* and *E*-state lines of CH_3COOH around 90.2 GHz, and the $9_{*,9} \rightarrow 8_{*,8}$ *E*-state line at 100.9 GHz were identified and assigned based on the work of Tabor (1957) and Wlodarczak & Demaison (1988).

3.169. H_2C_6 (Hexapentaenylidene)

Langer et al. (1997) reported the detection of H_2C_6 in Goldstone 70 m telescope observations of TMC-1. The $J_{K_a,K_c} = 7_{1,7} \rightarrow 6_{1,6}$ and $8_{1,8} \rightarrow 7_{1,7}$ transitions of H_2C_6 at 18.8 and 21.5 GHz, respectively, were identified and assigned based on the laboratory work of McCarthy (1997).

3.170. CH_2OHCHO (Glycolaldehyde)

The detection of CH_2OCHO was reported by Hollis et al. (2000) in NRAO 12 m observations of Sgr B2. A total of five transitions between 71.5 and 103.7 GHz were identified and assigned based on the laboratory work of Marstokk & Møllendal (1973). Despite numerous claims in the astronomical literature, glycolaldehyde is not a true sugar, and is instead a diose, a two-carbon monosaccharide, making it the simplest sugar-related molecule.

3.171. HC_6H (Triacetylene)

Cernicharo et al. (2001) reported the detection of HC_6H in *ISO* observations of CRL 618. The ν_{11} fundamental bending mode of HC_6H at 16.1 μm was observed and assigned based on the laboratory work of Haas et al. (1994).

3.172. CH_2CHCHO (Propenal)

A tentative detection of CH_2CHCHO was reported by Dickens et al. (2001a) in NRAO 12 m and SEST 15 m observations of G327.3-0.6 and Sgr B2. They tentatively assigned six emission lines between 88.5 and 107.5 GHz to CH_2CHCHO, based on the laboratory work of Winnewisser et al. (1975). The detection was confirmed by Hollis et al. (2004b) in GBT 100 m telescope observations of Sgr B2. They observed and assigned the $J_{K_a,K_c} = 2_{1,1} \rightarrow 1_{1,0}$ and $3_{1,3} \rightarrow 2_{1,2}$ transitions at 18.2 and 26.1 GHz, respectively, based on the laboratory work of Blom et al. (1984). CH_2CHCHO is also referred to as acrolein.

3.173. CH_2CCHCN (Cyanoallene)

Lovas et al. (2006b) reported the detection of CH_2CCHCN in GBT 100 m observations of TMC-1. Four transitions between 20.2 and 25.8 GHz with partially resolved hyperfine structure were identified and assigned based on the laboratory work of Bouchy et al. (1973) and Schwahn et al. (1986).

3.174. NH_2CH_2CN (Aminoacetonitrile)

The detection of NH_2CH_2CN was reported by Belloche et al. (2008) in IRAM 30 m, PdBI, and ATCA observations of Sgr B2. A total of 51 emission features between 80 and 116 GHz were identified and assigned to transitions of NH_2CH_2CN based on the laboratory work of Bogey et al. (1990). As part of their work, Belloche et al. (2008) refined the spectroscopic fit for the molecule based on the work of Bogey et al. (1990) and references therein.

3.175. CH_3CHNH (Ethanimine)

Loomis et al. (2013) reported the detection of CH_3CHNH in GBT 100 m observations of Sgr B2. More than two dozen transitions of the molecule between 13.0 and 47.2 GHz were identified and assigned based on laboratory spectroscopy work presented in the same manuscript.

3.176. CH_3SiH_3 (Methyl Silane)

The detection of CH_3SiH_3 was reported by Cernicharo et al. (2017) in IRAM 30 m observations of IRC+10216. Ten transitions between 80 and 350 GHz were identified and assigned based on the laboratory work of Meerts & Ozier (1982) and Wong et al. (1983).

Nine-atom Molecules

3.177. CH_3OCH_3 (Dimethyl Ether)

Snyder et al. (1974) reported the detection of CH_3OCH_3 in NRAO 36 ft, and Maryland Point Observatory NRL 85 ft observations of Orion. The $J_{K_a,K_c} = 6_{0,6} \rightarrow 5_{1,5}$, $2_{1,1} \rightarrow 2_{0,2}$, and $2_{2,0} \rightarrow 2_{1,1}$ transitions at 90.2, 31.1, and 88.2 GHz, respectively, were observed and assigned based on the laboratory work of Kasai & Myers (1959) and Blukis et al. (1963).

3.178. CH_3CH_2OH (Ethanol)

The detection of trans-CH_3CH_2OH was reported by Zuckerman et al. (1975) in NRAO 36 ft telescope observations of Sgr B2. The $J_{K_a,K_c} = 6_{0,6} \rightarrow 5_{1,5}$, $4_{1,4} \rightarrow 3_{0,3}$, and $5_{1,5} \rightarrow 4_{0,4}$ transitions at 85.3, 90.1, and 104.8 GHz, respectively, were identified and assigned based on the laboratory work of Takano et al. (1968). The gauche substates of CH_3CH_2OH were later identified as the carriers of 14 previously unidentified emission features in the Nobeyama 45 m observations of Orion presented in Ohishi et al. (1988) based on the laboratory work of Pearson et al. (1997).

3.179. CH_3CH_2CN (Ethyl Cyanide)

Johnson et al. (1977) reported the detection of CH_3CH_2CN in NRAO 36 ft observations of Orion, and weakly in Sgr B2. Two dozen emission features between 88 and 116 GHz were identified and assigned to CH_3CH_2CN in Orion. The foundational laboratory spectroscopy was reported by Heise et al. (1974), Mäder et al. (1974), and Laurie (1959). Based on this work, additional higher-frequency lines were measured and assigned in Johnson et al. (1977).

3.180. HC_7N (Cyanotriacetylene)

Reports of the detection of HC_7N were made nearly simultaneously by Little et al. (1978) (January 4) and Kroto et al. (1978) (February 1), although the former acknowledges an earlier report by Kroto et al. (1977; June 13). A few months later (October 5), Winnewisser & Walmsley (1978) also reported the detection of HC_7N.

The observations of Kroto et al. (1977) and Kroto et al. (1978) were conducted toward TMC-1 using both the Algonquin 46 m and Haystack 36.6 m telescopes. Kroto et al. (1977) reported the observation of the $J = 9 \rightarrow 8$ transition at 10.2 GHz, while Kroto et al. (1978) additionally observed the $21 \rightarrow 20$ transition at 23.7 GHz. The assignments were based on laboratory work carried out by a subset of the authors of Kroto et al. (1978), which they would later report in Kirby et al. (1980).

Little et al. (1978) used the SRC Appleton Laboratory 25 m telescope to observe the $22 \rightarrow 21$ transition at 24.8 GHz in both TMC-1 and TMC-2. The rotational constants required for the detection were provided by H. W. Kroto.

The work of Winnewisser & Walmsley (1978) was presumably carried out independently, as there were no references to the previous three manuscripts in this paper. They reported the detection of the 21 → 20 transition in IRC +10216. Although the facility used for the observations is not named in the main portion of the manuscript, the authors acknowledge the operators of Effelsberg, and cite a beam size of 40″ near 24 GHz, which is reasonably close to that of a 100 m telescope. There is also no reference given to the source of the rotational transition frequency, nor is a frequency actually given.

3.181. CH_3C_4H (Methyldiacetylene)

The detection of CH_3C_4H was nearly simultaneously reported by Walmsley et al. (1984; March 22) and MacLeod et al. (1984; July 15). Later that year, Loren et al. (1984; November 1) also reported an independent detection, having received word of the earlier work during the publication process.

Walmsley et al. (1984) reported the detection in observations of TMC-1 using the Effelsberg 100 m telescope. They observed and assigned the $K = 0$ and $K = 1$ components of the $J = 6 \rightarrow 5$ and $5 \rightarrow 4$ transitions at 24.4 and 20.3 GHz, respectively. Their assignments were based on the laboratory work of Heath et al. (1955), although they suggested the astronomical observations might be used to refine those measurements moving forward.

Both MacLeod et al. (1984) and Loren et al. (1984) observed the same transitions in TMC-1, the former using the Haystack 36.6 m and NRAO 140 ft telescopes, while the latter used solely the NRAO 140 ft.

3.182. C_8H (Octatriynyl Radical)

Cernicharo & Guélin (1996) reported the detection of the C_8H radical in IRAM 30 m observations of IRC+10216, as well as in the archival Nobeyama 45 m observations of Kawaguchi et al. (1995). They identified and assigned 10 transitions between 31.1 and 83.9 GHz based on comparison to calculated rotational constants from Pauzat et al. (1991). The detection and assignment was confirmed in an accompanying letter by the laboratory work of McCarthy et al. (1996).

3.183. CH_3CONH_2 (Acetamide)

The detection of CH_3CONH_2 was reported toward Sgr B2 by Hollis et al. (2006a) using the GBT 100 m telescope. A total of eight transitions between 9.3 and 47.4 GHz were identified and assigned based on the laboratory work of Suenram et al. (2001) and Ilyushin et al. (2004).

3.184. C_8H^- (Octatriynyl Anion)

Brünken et al. (2007) and Remijan et al. (2007) simultaneously reported the detection of C_8H^-. Both detections were made with the GBT 100 m telescope; the former described the detection in TMC-1, while the latter was toward IRC+10216. Remijan et al. (2007) detected the $J = 22 \rightarrow 21$ and $35 \rightarrow 34$ through $38 \rightarrow 37$ transitions between 25.7 and 44.3 GHz based on the laboratory work of Gupta et al. (2007). Brünken et al. (2007) observed the $11 \rightarrow 10$ through $13 \rightarrow 12$, and the $16 \rightarrow 15$ transitions between 12.8 and 18.7 GHz, based on the same laboratory work.

3.185. CH_2CHCH_3 (Propylene)

The detection of CH_2CHCH_3, also referred to as propene, was reported by Marcelino et al. (2007) in IRAM 30 m observations of TMC-1. A total of 13 rotational transitions between 84.2 and 103.7 GHz were identified and assigned based on the laboratory work of Wlodarczak et al. (1994) and Pearson et al. (1994).

3.186. CH_3CH_2SH (Ethyl Mercaptan)

Kolesniková et al. (2014) reported the detection of CH_3CH_2SH in IRAM 30 m observations of Orion. A total of 77 unblended lines between 80 and 280 GHz were identified and assigned based on laboratory spectroscopy presented in the same manuscript. Subsequent attempts to identify the molecule in Sgr B2(N) by Müller et al. (2016) were unsuccessful.

3.187. HC_7O (Hexadiynylformyl Radical)

McGuire et al. (2017a) reported the tentative detection of the HC_7O radical in GBT 100 m observations of TMC-1. Based on the laboratory work of Mohamed et al. (2005), a weak detection of the $J = 35/2 \rightarrow 33/2$ transition with partially resolved hyperfine structure was observed near 19.2 GHz. The detection was confirmed in Cordiner et al. (2017) by the observation of several additional weak features, without hyperfine structure, corresponding to the $33/2 \rightarrow 31/2$ transitions near 18.1 GHz. A composite average of these lines, plus the data from McGuire et al. (2017a), provided a 9.5σ detection.

Ten-atom Molecules

3.188. $(CH_3)_2CO$ (Acetone)

Combes et al. (1987) reported the detection of $(CH_3)_2CO$ in IRAM 30 m, NRAO 140 ft, and NRAO 12 m observations of Sgr B2. A total of 11 transitions between 18.7 and 112.4 GHz were identified and assigned based on the laboratory work of Vacherand et al. (1986).

3.189. $HO(CH_2)_2OH$ (Ethylene Glycol)

The detection of the $g'Ga$ conformer of $HO(CH_2)_2OH$ was reported by Hollis et al. (2002) in NRAO 12 m observations of Sgr B2. Four transitions between 75.1 and 93.0 GHz were identified and assigned based on the laboratory work of Christen et al. (1995). The higher-energy aGg' conformer was later detected by Rivilla et al. (2017) in GBT 100 m, IRAM 30 m, and SMA observations of G31.41+0.31.

3.190. CH_3CH_2CHO (Propanal)

Hollis et al. (2004b) reported the detection of CH_3CH_2CHO in GBT 100 m observations of Sgr B2. A total of five transitions between 19.2 and 22.2 GHz were identified and assigned based on the laboratory work of Butcher & Wilson (1964). CH_3CH_2CHO is also referred to as propionaldehyde.

3.191. CH_3C_5N (Methylcyanodiacetylene)

The detection of CH_3C_5N was reported by Snyder et al. (2006) in GBT 100 m telescope observations of TMC-1. Ten transitions between 18.7 and 24.9 GHz were identified and assigned to the $K = 0$ and $K = 1$ components of the

$J_K = 12_* \rightarrow 11_*$ through $16_* \rightarrow 15_*$ transitions of CH_3C_5N based on the laboratory work of Alexander et al. (1978) and Chen et al. (1998).

3.192. CH_3CHCH_2O (Propylene Oxide)

McGuire et al. (2016) reported the detection of CH_3CHCH_2O in GBT 100 m and Parkes 64 m observations of Sgr B2. The $J_{K_a,K_c} = 1_{1,0} \rightarrow 1_{0,1}$, $2_{1,1} \rightarrow 2_{0,2}$, and $3_{1,2} \rightarrow 3_{0,3}$ transitions at 12.1, 12.8, and 14.0 GHz, respectively, were identified and assigned based on laboratory spectroscopy presented in the same manuscript. CH_3CHCH_2O was the first chiral molecule detected in the ISM.

3.193. CH_3OCH_2OH (Methoxymethanol)

The detection of CH_3OCH_2OH was reported by McGuire et al. (2017b) in ALMA observations of NGC 6334I. More than two dozen largely unblended transitions between 239 and 349 GHz were identified and assigned based on the laboratory work of Motiyenko et al. (2018), which was in press at the time.

Eleven-atom Molecules

3.194. HC_9N (Cyanotetraacetylene)

Broten et al. (1978) reported the detection of HC_9N in TMC-1 using the Algonquin Radio Observatory 46 m and NRAO 140 ft telescopes. The $J = 18 \rightarrow 17$ and $25 \rightarrow 24$ transitions at 10.5 and 14.5 GHz, respectively, were identified on the basis of theoretical calculations described in the same manuscript. The detection was later confirmed by the laboratory spectroscopy performed by Iida et al. (1991).

3.195. CH_3C_6H (Methyltriacetylene)

The detection of CH_3C_6H was reported by Remijan et al. (2006) in GBT 100 m observations of TMC-1. Ten spectral lines corresponding to the $K = 0$ and $K = 1$ components of the $J_K = 12_* \rightarrow 11_*$ through $16_* \rightarrow 15_*$ transitions between 18.7 and 24.9 GHz were identified and assigned based on the laboratory work of Alexander et al. (1978).

3.196. CH_3CH_2OCHO (Ethyl Formate)

Belloche et al. (2009) reported the detection of trans-CH_3CH_2OCHO in IRAM 30 m observations of Sgr B2. A total of 41 unblended transitions of trans-CH_3CH_2OCHO between 80 and 268 GHz were identified and assigned based on the laboratory data of Medvedev et al. (2009). The subsequent detection of the gauche-conformer was reported by Tercero et al. (2013) in IRAM 30 m observations of Orion. They identified and assigned 38 unblended transitions between 80 and 281 GHz based on the laboratory work of Demaison et al. (1984).

3.197. CH_3COOCH_3 (Methyl Acetate)

The detection of CH_3COOCH_3 was reported by Tercero et al. (2013) in IRAM 30 m observations of Orion. A total of 215 unblended transitions of CH_3COOCH_3 between 80 and 281 GHz were identified and assigned based on the laboratory work of Tudorie et al. (2011).

Twelve-atom Molecules

3.198. C_6H_6 (Benzene)

Cernicharo et al. (2001) reported the detection of C_6H_6 in *ISO* observations of CRL 618. The ν_4 bending mode of C_6H_6 near 14.8 μm was identified and assigned based on the laboratory work of Lindenmayer et al. (1988).

3.199. n-C_3H_7CN (n-propyl Cyanide)

The detection of n-C_3H_7CN, also referred to as n-butyronitrile, was reported by Belloche et al. (2009) in IRAM 30 m observations of Sgr B2. A total of 50 unblended transitions of the anti-conformer of n-C_3H_7CN were identified and assigned based on an extensive re-analysis of the literature spectra presented in the same manuscript.

3.200. i-C_3H_7CN ($i$so-propyl Cyanide)

Belloche et al. (2014) reported the detection of i-C_3H_7CN in ALMA observations of Sgr B2 between 84 and 111 GHz, based on the laboratory work of Müller et al. (2011). This was the first branched carbon-chain molecule detected in the ISM.

Thirteen-atom Molecules

3.201. C_6H_5CN (Benzonitrile)

McGuire et al. (2018) reported the detection of C_6H_5CN in GBT 100 m observations of TMC-1. A total of nine transitions, some with resolved ^{14}N hyperfine structure, between 18.4 and 23.2 GHz were identified and assigned on the basis of laboratory work described in the same paper, as well as that of Wohlfart et al. (2008).

Fullerene Molecules

3.202. C_{60} (Buckminsterfullerene)

Cami et al. (2010) reported the detection of C_{60} in *Spitzer* observations of Tc 1. Strong emission features from C_{60} at 7.0, 85, 17.4, and 18.9 μm were identified and assigned based on the work of Martin et al. (1993) and Fabian (1996).

3.203. C_{60}^+ (Buckminsterfullerene Cation)

Berné et al. (2013) reported the detection of C_{60}^+ in *Spitzer* observations toward NGC 7023. Two emission features at 7.1 and 6.4 μm were assigned to C_{60}^+ based on the laboratory matrix-isolation work of Kern et al. (2013). A number of additional features were assigned based on theoretical calculations performed and described in Berné et al. (2013). Subsequent laboratory work by Campbell et al. (2015) confirmed the presence of C_{60}^+ in the ISM by measuring the gas-phase spectrum of C_{60}^+. Based on those results, they determined that C_{60}^+ was the carrier of the 9632 and 9577 Å DIBs, the first definitive molecular assignment of a carrier of one of these bands. Follow-up observational and laboratory studies by Walker et al. (2015) and Campbell et al. (2016) solidified the identification.

3.204. C_{70} (Rugbyballene)

Cami et al. (2010) reported the detection of C_{70} in *Spitzer* observations of Tc 1. They identified and assigned four emission features between 12 and 22 μm to C_{70} based on the

work of Nemes et al. (1994), von Czarnowski & Meiwes-Broer (1995), and Stratmann et al. (1998).

4. Tentative Detections

This section contains those molecules for which a detection has been classified by the authors as tentative. Those molecules once viewed as tentative that have since been confirmed are listed in Section 3.

4.1. C_2H_5N (Aziridine)

Dickens et al. (2001b) reported the tentative detection of the $J_{K_a,K_c} = 5_{5,0} \rightarrow 4_{4,1}$ transition of C_2H_5N, also known as ethylenimine, at 226 GHz toward Sgr B2, G34.3+.2, G10.47 +0.03, and G327.3-0.6 in observations made with the SEST 15 m, NRAO 12 m, and NASA Deep Space Network 70 m telescopes. The laboratory data were reported by Thorwirth et al. (2000).

4.2. SiH (Silicon Hydride)

Schilke et al. (2001) reported the tentative detection of two features in a CSO line survey of Orion that were coincident with transitions of SiH. Two groups of hyperfine transitions in the $^2\Pi_{1/2}$ state at 625 and 628 GHz fell within range of the observations. The lower set is significantly blended with other emitting species, whereas the higher-frequency set appears unblended, and may show partially resolved hyperfine structure. The laboratory frequencies were from Brown et al. (1985a).

4.3. FeO (Iron Monoxide)

Walmsley et al. (2002) identified an absorption feature in IRAM 30 m observations of Sgr B2 at 153 GHz that they tentatively assign to the $J = 5 \rightarrow 4$, $\Omega = 4$ transition of FeO, based on the laboratory work of Allen et al. (1996). Later, Furuya et al. (2003) used the Nobeyama Millimeter Array to confirm the detection of this line, but no additional transitions were observed. Most recently, Decin et al. (2018) reported a tentative detection of the $11 \rightarrow 10$, $\Omega = 4$ transition in ALMA observations of R Dor at 337 GHz.

4.4. OCN^- (Cyanate Anion)

There is a long history of attempts to identify the carrier of the "XCN" feature in astrophyiscal ice observations near 2167 cm^{-1}. On the basis of extensive laboratory work (see, e.g., Schutte & Greenberg 1997), van Broekhuizen et al. (2005) claimed an identification of OCN^- in ices along numerous sightlines to low-mass YSO's using the Very Large Telescope (VLT). Only a single absorption feature could be ascribed to OCN^-. As this is a single feature detection, and no gas-phase detection has been claimed, OCN^- has been listed as a tentative interstellar species in this census.

4.5. C_6H_5OH (Phenol)

Kolesniková et al. (2013) reported the laboratory rotational spectroscopy of C_6H_5OH, and identified a number of coincidences between transitions of C_6H_5OH and unassigned lines in IRAM 30 m observations of Orion between 80 and 280 GHz (Tercero et al. 2012).

4.6. NO^+ (Nitrosylium Cation)

Cernicharo et al. (2014) reported the tentative detection of a single line ($J = 2 \rightarrow 1$) of NO^+ at 238 GHz toward B1-b using the IRAM 30 m telescope. The assignment was made based on laboratory rotational spectroscopy described in the same paper.

4.7. $(NH_2)_2CO$ (Urea)

Remijan et al. (2014) reported on the evidence for a tentative detection of $(NH_2)_2CO$ in observations of Sgr B2. The data, covering 100–250 GHz, were obtained from the BIMA, CARMA, NRAO 12 m, SEST 15 m, and IRAM 30 m telescopes. The laboratory data were from Brown et al. (1975b), Kasten & Dreizler (1986), and Kretschmer et al. (1996). A single set of physical parameters reproduced the features across all observational sets within a factor of two, and interferometric maps of individual transitions showed a consistent spatial structure. The lack of a sufficiently large set of unblended transitions precluded a definitive detection.

4.8. MgCCH (Magnesium Monoacetylide)

Agúndez et al. (2014b) reported the tentative detection of MgCCH in IRAM 30 m observations of IRC+10216. They identified and assigned two sets of features corresponding to *l*-doubled transitions of the $^2\Sigma^+$ ground electronic state of MgCCH at 89 and 99 GHz based on the laboratory work of Brewster et al. (1999).

4.9. NCCP (Cyanophosphaethyne)

Agúndez et al. (2014b) reported the tentative detection of NCCP in IRAM 30 m observations of IRC+10216. They identified and tentatively assigned three signals in their spectra to the $J = 15 \rightarrow 14$, $16 \rightarrow 15$, and $18 \rightarrow 17$ transitions of NCCP at 81, 87, and 97 GHz, respectively, based on the laboratory work of Bizzocchi et al. (2001).

4.10. $C_2H_5OCH_3$ (trans-Ethyl Methyl Ether)

Charnley et al. (2001) indicated a tentative detection of $C_2H_5OCH_3$ in NRAO 12 m and BIMA observations of Orion-KL and Sgr B2(N). A detection of $C_2H_5OCH_3$ was then later reported by Fuchs et al. (2005) in IRAM 30 m and SEST 15 m observations of W51e2. This detection was disputed by Carroll et al. (2015), who re-observed both W51e2 and Sgr B2(N) using the ARO 12 m and GBT 100 m telescopes, and failed to detect $C_2H_5OCH_3$, setting an upper limit column density substantially lower than the reported value of Fuchs et al. (2005). Evidence supporting the tentative detection in Orion-KL was later reported by Tercero et al. (2015) using IRAM 30 m and ALMA observations of the region, although the authors claim the detection should still be viewed as tentative. The laboratory spectroscopy was performed by Hayashi & Kuwada (1975) and Fuchs et al. (2003).

4.11. CH_3NHCHO (N-methylformamide)

A tentative detection of CH_3NHCHO was reported toward Sgr B2(N2) by Belloche et al. (2017) using ALMA observations in the range 84–114 GHz. The laboratory rotational spectroscopy are provided in the same reference.

5. Disputed Detections

This section contains those molecules for which a detection has been claimed and subsequently disputed in the literature. Those species that were disputed but later confirmed are listed in Section 3. Species for which a tentative detection has been claimed and also disputed are not listed.

5.1. $HC_{11}N$ (Cyanopentaacetylene)

Bell et al. (1997) reported a detection of $HC_{11}N$ in NRAO 140-foot observations of TMC-1. They assigned two emission features at 12848.728 MHz and 13186.853 MHz to the $J = 38 \rightarrow 37$ and $39 \rightarrow 38$ transitions of $HC_{11}N$ based on the laboratory work of Travers et al. (1996b). The detection was later disputed by Loomis et al. (2016), who re-observed TMC-1 using the 100 m GBT. They targeted six transitions of $HC_{11}N$, including those originally reported by Bell et al. (1997), and detected no signal at any of these frequencies. They suggest correlator artifacts may have been responsible for the signals seen in Bell et al. (1997). Subsequently, Cordiner et al. (2017) confirmed the findings of Loomis et al. (2016), setting a yet lower upper limit with more sensitive data.

5.2. NH_2CH_2COOH (Glycine)

Kuan et al. (2003) reported a detection of 27 lines of NH_2CH_2COOH in observations toward Orion, Sgr B2, and W51 using the NRAO 12 m telescope. Each source contained 13–16 of the 27 features; three features were seen in common between the sources. The frequencies were obtained from the rotational constants measured and reported in Suenram & Lovas (1980) and Lovas et al. (1995). The detection was later disputed by Snyder et al. (2005), who claimed to have identified a number of issues with the analysis. Notably, Snyder et al. (2005) argued that the frequency predictions used by Kuan et al. (2003) were extrapolated too far above the measured laboratory transitions. Snyder et al. (2005) used laboratory frequencies from Ilyushin et al. (2005) that covered the observed frequency range, and examined archival NRAO 12 m and SEST 15 m observations of Orion, Sgr B2, and W51. They reported a number of "missing" transitions of NH_2CH_2COOH that they predicted should have been strongly detected, if the detection of Kuan et al. (2003) held. Subsequent searches by Jones et al. (2007), Cunningham et al. (2007), and Belloche et al. (2008) using both interferometers and single-dish facilities failed to detect NH_2CH_2COOH, and set upper limits to the column density lower than that claimed in the detection of Kuan et al. (2003; see Belloche et al. 2008 Section 4.4 for a detailed discussion).

6. Species Detected in External Galaxies

A remarkable fraction (67/204; ~33%) of the known interstellar and circumstellar molecules have also been detected in observations of external galaxies. A list of these species is given in Table 4. For most species, the provided reference is to the earliest claim of a detection in the literature. In some cases, additional references are provided for context. Molecules for which a tentative detection in external galaxies have been claimed are indicated. In the case of fullerene molecules, there has been some debate in the literature over the claimed identification of these molecules (Duley & Hu 2012), thus these are not included in this table at this time.

A few notable absences stand out. The detection of H_2Cl^+ (Muller et al. 2014a) hints that the detections of HCl and HCl^+ may be achievable, assuming the extragalactic abundances follow those seen in our galaxy where these species are within factors of 1–3 of each other (Monje et al. 2013). Similarly, the presence of SH^+ would indicate that SH is a likely candidate, given its marginally higher abundance in galactic sightlines (see, e.g., Neufeld et al. 2012). The very recent detections of the much larger species $HCOOCH_3$ and CH_3OCH_3 (Qiu et al. 2018; Sewiło et al. 2018) suggest a reservoir of complex molecules may also be observable.

The complete list of external galaxies in which these detections were made is included in the Supplementary Information Python database. By far the largest contributors to these detections are NGC 253 (24 molecules), the LOS to PKS 1830-211 (15 molecules), and M82 (14 molecules).

7. Species Detected in Interstellar Ices

Observations of ices require a background illuminating source for absorption, limiting the number of sightlines that are available for study. Further complications arise when comparing with laboratory spectra, as the peak positions, line widths, and intensities of molecular ices features are known to be sensitively dependent on temperature, crystal structure of the ice (or lack thereof), and mixing or layering with other species (see, e.g., Ehrenfreund et al. 1997; Schutte et al. 1999, and Cooke et al. 2016). As a result, only a handful of species (H_2O, CO, CO_2, CH_4, CH_3OH, and NH_3) have been definitively detected in interstellar ices.

The first molecular ice detection was reported by Gillett & Forrest (1973), who observed an absorption feature at 3.1 μm toward Orion-KL which they attribute to H_2O based on comparison to the laboratory work of Irvine & Pollack (1968). Soifer et al. (1979) then reported the detection of CO at 4.61 μm in absorption toward W33A, based on the laboratory work of Mantz et al. (1975).

The laboratory work of D'Hendecourt & Allamandola (1986) was then used to detect a further four species. As mentioned in Section 3.56, CO_2 was detected by D'Hendecourt & Jourdain de Muizon (1989), based on their own laboratory work, in absorption at 15.2 μm toward several IRAS sources. Also discussed previously (Section 3.123), CH_4 was simultaneously detected in the gas and solid phases by Lacy et al. (1991) toward NGC 7538 IRS 9. A feature was attributed to CH_4 at 7.7 μm. That same year, Grim et al. (1991) identified and assigned an absorption feature at 3.53 μm in UKIRT observations toward W33A to CH_3OH. Finally, the detection of NH_3 was reported by Lacy et al. (1998), who assigned an absorption feature at 1110 cm^{-1} toward NGC 7538 IRS 9.

Several more species have been tentatively identified due to the coincidence of a spectral feature with laboratory data for a molecule under certain temperature or mixture conditions. Palumbo et al. (1995) and Palumbo et al. (1997) identified an absorption feature at 4.90 μm toward a number of sources that corresponded to OCS when mixed with CH_3OH, based on their own laboratory work. As discussed in Section 4.4, van Broekhuizen et al. (2005) claim an identification of OCN^- based on a lengthy history of laboratory work (e.g., Schutte & Greenberg 1997).

Finally, a number of additional molecular carriers have been suggested or tentatively assigned, but have not yet been definitively confirmed. These possible interstellar molecules

Table 4
List of Molecules Detected in External Galaxies with References to the First Detections

2 Atoms		3 Atoms		4 Atoms		5 Atoms	
Species	Ref.	Species	Ref.	Species	Ref.	Species	Ref.
CH	47	H_2O	3	NH_3	16	HC_3N	20, 13
CN	13	HCO^+	41	H_2CO	6	CH_2NH	25
CH^+	15	HCN	37	HNCO	32	NH_2CN	18
OH	45	OCS	22	H_2CS	18	H_2CCO	25
CO	36	HNC	13	C_2H_2	19	C_4H	25
H_2	42	H_2S	10	$HOCO^+$	1, 18	c-C_3H_2	39
SiO	23	N_2H^+	23	l-C_3H	25	CH_2CN	25
CS	11	C_2H	13	H_3O^+	48	H_2CCC	25
SO	14, 33	SO_2	17	c-C_3H[a]	18		
NS	17	HCO	38, 5				
C_2	46	HCS^+	26				
NO	17	HOC^+	43				
NH	8	C_2S	18				
SO^+	25	C_3	46				
CO^+	4	NH_2	27				
HF	49, 35, 24	H_3^+	7				
CF^+	30	H_2O^+	44				
OH^+	49, 35, 9	H_2Cl^+	28				
SH^+	31						
ArH^+	29						

6 Atoms		7 Atoms		8 Atoms		9 Atoms		12 Atoms	
Species	Ref.	Species	Ref.	Species	Ref.	Species	Ref.	Species	Ref.
CH_3OH	12	CH_3CHO	25	$HCOOCH_3$	40	CH_3OCH_3	34, 40	C_6H_6	2
CH_3CN	21	CH_3CCH	21	HC_6H	2				
NH_2CHO	26	CH_3NH_2	25						
HC_4H	2	HC_5N[a]	1						

Note. Tentative detections are indicated, and some extra references are occasionally provided for context.
[a] Tentative detection.

References. [1] Aladro et al. (2015), [2] Bernard-Salas et al. (2006), [3] Churchwell et al. (1977), [4] Fuente et al. (2006), [5] García-Burillo et al. (2002), [6] Gardner & Whiteoak (1974), [7] Geballe et al. (2006), [8] González-Alfonso et al. (2004), [9] González-Alfonso et al. (2013), [10] Heikkilä et al. (1999), [11] Henkel & Bally (1985), [12] Henkel et al. (1987), [13] Henkel et al. (1988), [14] Johansson (1991), [15] Magain & Gillet (1987), [16] Martin & Ho (1979), [17] Martín et al. (2003), [18] Martín et al. (2006), [19] Matsuura et al. (2002), [20] Mauersberger et al. (1990), [21] Mauersberger et al. (1991), [22] Mauersberger et al. (1995), [23] Mauersberger & Henkel (1991), [24] Monje et al. (2011), [25] Muller et al. (2011), [26] Muller et al. (2013), [27] Muller et al. (2014b), [28] Muller et al. (2014a), [29] Müller et al. (2015), [30] Muller et al. (2016), [31] Muller et al. (2017), [32] Nguyen-Q-Rieu et al. (1991), [33] Petuchowski & Bennett (1992), [34] Qiu et al. (2018), [35] Rangwala et al. (2011), [36] Rickard et al. (1975), [37] Rickard et al. (1977), [38] Sage & Ziurys (1995), [39] Seaquist & Bell (1986), [40] Sewiło et al. (2018), [41] Stark & Wolff (1979), [42] Thompson et al. (1978), [43] Usero et al. (2004), [44] Weiß et al. (2010), [45] Weliachew (1971), [46] Welty et al. (2012), [47] Whiteoak et al. (1980), [48] van der Tak et al. (2007), [49] van der Werf et al. (2010).

are discussed in some detail in a review article by Boogert et al. (2015).

8. Species Detected in Protoplanetary Disks

Compared to the molecular clouds from which they form, the detected molecular inventory of protoplanetary disks is relatively sparse. A list of species detected in disks, including isotopologues, is given in Table 5, along with early and/or representative detection references. The detections of H_2D^+ and HDO that were reported by Ceccarelli et al. (2004) and Ceccarelli et al. (2005), but were later disputed by Guilloteau et al. (2006), are not included.

The (relatively) low number of gas-phase species detected so far in disks can likely be attributed to a combination of factors:

1. Often narrow ranges of physical environments conducive to a large gas-phase abundance. For example, many complex molecules are likely locked into ices in the cold, shielded mid-plane of the disk and are liberated into the gas phase for detection in only certain, narrow regions of the disk (Walsh et al. 2014).
2. Conversely, gas-phase molecules that reach the upper layers of the disk are subject to the harsh, PDR-like radiation environment of the star and the resulting photodestructive processes (Henning et al. 2010).
3. The angular extent of these sources on the sky is small (of order arcseconds; Brogan et al. 2015), largely degrading the utility of the most sensitive single-dish facilities due to beam dilution. As a result of the overall low abundance, the required surface brightness sensitivity likewise limits the effectiveness of many small and mid-scale interferometers. The most complex and low-abundance species are therefore being detected exclusively with ALMA, and are already pushing the limits of the instrument (Loomis et al. 2018).

Detection and analysis of the most complex molecules seen to date, CH_3OH and CH_3CN (Öberg et al. 2015; Walsh et al. 2016), have benefited from velocity stacking and newly developed matched-filtering techniques to extract useful

Table 5
List of Molecules, Including Rare Isotopic Species, Detected in Protoplanetary Disks, with References to Representative Detections

2 Atoms		3 Atoms		4 Atoms		5 Atoms		6 Atoms	
Species	Ref.	Species	Ref.	Species	Ref.	Species	Ref.	Species	Ref.
CN	10, 21	H_2O	5, 31, 19	NH_3	30	HCOOH	12	CH_3CN	24
$C^{15}N$	18	HCO^+	10, 21	H_2CO	10	*c*-C_3H_2	29	CH_3OH	36
CH^+	35	DCO^+	8	C_2H_2	22	CH_4	14		
OH	23, 31	$H^{13}CO^+$	37, 8	HC_3N	7				
CO	2	HCN	10, 21						
^{13}CO	32	DCN	28						
$C^{18}O$	9	$H^{13}CN$	17						
$C^{17}O$	33, 16	$HC^{15}N$	17						
H_2	34	HNC	10						
HD	3	H_2S	26						
CS	25, 4, 15	N_2H^+	27, 11						
$C^{34}S$	1	N_2D^+	20						
SO	13	C_2H	10						
CO_2	6								

Note. The earliest reported detection of a species in the literature is provided on a best-effort basis. Tentative and disputed detections are not included (see the text).
References. [1] Artur de la Villarmois et al. (2018), [2] Beckwith et al. (1986), [3] Bergin et al. (2013), [4] Blake et al. (1992), [5] Carr et al. (2004), [6] Carr & Najita (2008), [7] Chapillon et al. (2012), [8] van Dishoeck et al. (2003), [9] Dutrey et al. (1994), [10] Dutrey et al. (1997), [11] Dutrey et al. (2007), [12] Favre et al. (2018), [13] Fuente et al. (2010), [14] Gibb & Horne (2013), [15] Guilloteau et al. (2012), [16] Guilloteau et al. (2013), [17] Guzmán et al. (2015), [18] Hily-Blant et al. (2017), [19] Hogerheijde et al. (2011), [20] Huang & Öberg (2015), [21] Kastner et al. (1997), [22] Lahuis et al. (2006), [23] Mandell et al. (2008), [24] Öberg et al. (2015), [25] Ohashi et al. (1991), [26] Phuong et al. (2018), [27] Qi et al. (2003), [28] Qi et al. (2008), [29] Qi et al. (2013), [30] Salinas et al. (2016), [31] Salyk et al. (2008), [32] Sargent & Beckwith (1987), [33] Smith et al. (2009), [34] Thi et al. (1999), [35] Thi et al. (2011), [36] Walsh et al. (2016), [37] van Zadelhoff et al. (2001).

signal-to-noise ratios (Loomis et al. 2018). While these techniques are likely to produce a number of new detections of lower-abundance molecules in the coming years, astrochemical models combined with sensitivity analyses currently suggest that the total number of molecules detectable with complexity greater than CH_3OH and CH_3CN may be small (Walsh et al. 2017).

9. Species Detected in Exoplanetary Atmospheres

Although exoplanet atmospheres have now been observed for some time (Charbonneau et al. 2002), only a handful of molecules have been detected in these environments. That number, and the ability to robustly measure molecules in exoplanetary atmospheres, is expected to increase somewhat with the launch of the *James Webb Space Telescope* (Schlawin et al. 2018). Table 6 lists those molecules for which a consensus seems to have been reached in the literature as being detected. There is extensive debate in the literature as to the robustness of many claimed detections (see Madhusudhan et al. 2016 for a thorough overview). Thus, references are provided both to some early detections, for historical context, and to some more recent literature. The reference list is intended to be representative, not exhaustive.

Table 6
List of Molecules Detected in Exoplanetary Atmospheres, with References to Representative Detections (Tentative and Disputed Detections Are Not Included)

Species	References
CO	9, 1, 7, 2
TiO	4, 11, 10
H_2O	14, 3, 5, 6, 8
CO_2	12, 9, 7
CH_4	13, 1, 12, 2

References. [1] Barman et al. (2011), [2] Barman et al. (2015), [3] Deming et al. (2013), [4] Haynes et al. (2015), [5] Kreidberg et al. (2014), [6] Kreidberg et al. (2015), [7] Lanotte et al. (2014), [8] Lockwood et al. (2014), [9] Madhusudhan et al. (2011), [10] Nugroho et al. (2017), [11] Sedaghati et al. (2017), [12] Stevenson et al. (2010), [13] Swain et al. (2008), [14] Tinetti et al. (2007).

10. Analysis and Discussion

As of publication, a total of 204 individual molecules have been detected in the ISM. Here, several graphical representations of the census results presented above are shown and briefly discussed.

10.1. Cumulative Detection Rates

The cumulative number of known interstellar molecules with time is presented in Figure 1, as well as the commissioning dates of a number of key observational facilities. Although the first molecules were detected between 1937 and 1941 (see Sections 3.1–3.3), and OH in 1963 (Section 3.4), it was not until the late 1960s with the development of high-resolution radio receivers optimized for line observations that detections began in earnest. Since 1968, the rate of detections has remained remarkably constant at ∼3.7 new molecules per year.

Notably, beginning in 2005 there is some evidence that this detection rate has increased. A fit of the data solely between 2005 and 2018 yields a rate of ∼5.4 molecules per year. This would appear to be consistent with the advent of the GBT as a molecule-detection telescope, and a significant uptick in the rate of detections from IRAM, as discussed further below.

Figure 2 displays the same data as Figure 1, broken down by the cumulative detections of molecules containing *n* atoms, while Table 7 and Figure 3 display the rates of new detections per year sorted by the number of atoms per molecule. These rates show a steady decrease between 2 and 6 atom molecules,

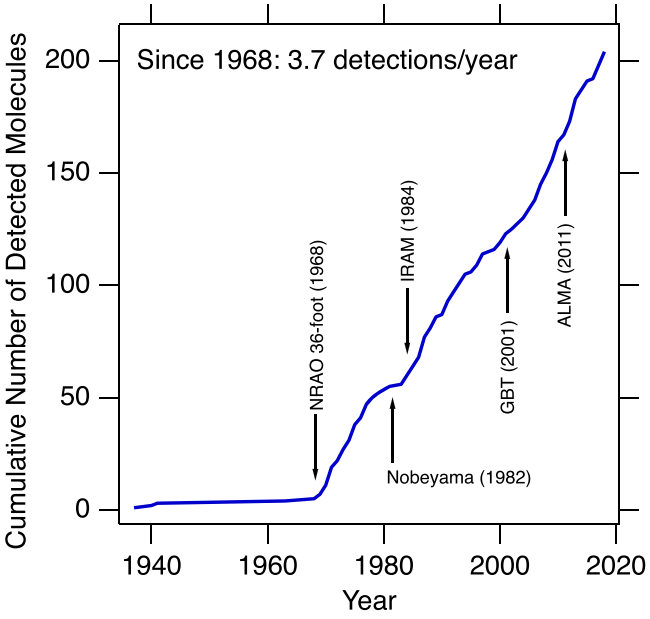

Figure 1. Cumulative number of known interstellar molecules over time. After the birth of molecular radio astronomy in the 1960s, there have been on average 3.7 new detections per year ($R^2 = 0.991$ for a linear fit beginning in 1968). The commissioning dates of several major contributing facilities are noted with arrows.

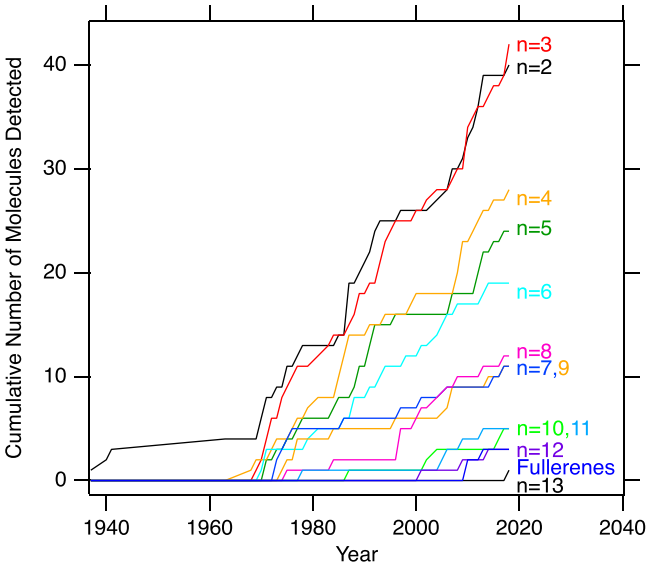

Figure 2. Cumulative number of known interstellar molecules with 2–13 atoms, as well as fullerene molecules, as a function of time. The traces are color-coded by number of atoms, and labeled on the right.

at which point the rate appears to flatten to an average of about one new detection every five years. Of note, molecules with 10 or more atoms did not begin to be routinely detected until the early 2000s.

10.2. Detecting Facilities

Table 8 lists the total number of detections by each facility listed in Section 3. When two or more telescopes were used for a detection, each was given full credit. In total, 48 different facilities have contributed to the detection of at least one new species. Acronym definitions for these are given in Table 1 or in the text.

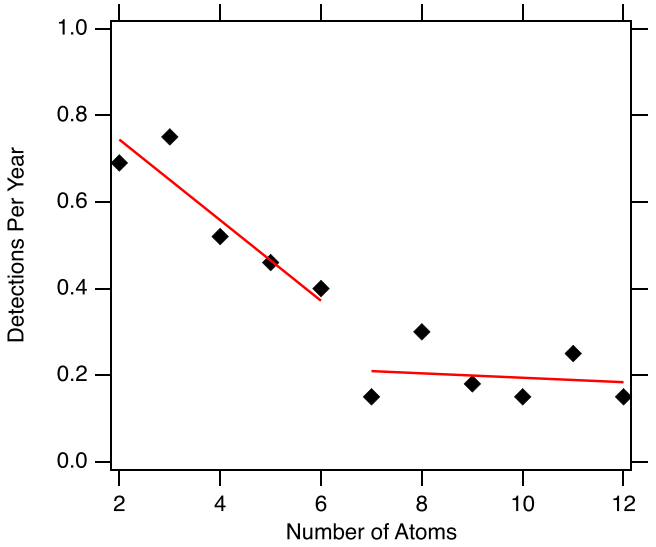

Figure 3. Number of detections per year for a molecule with a given number of atoms. The data can be visually divided into a gradually decreasing trend from 2 to 6 atom molecules, while molecules with 7 to 12 atoms have a steady average detection rate of ∼0.2 per year.

Table 7
Rates (m) of Detection of New Molecules per Year, Sorted by Number of Atoms per Molecule Derived from Linear fits to the Data Shown in Figure 2 as well as the R^2 Values of the fits, for Molecules with 2–12 Atoms

# Atoms	m (yr^{-1})	R^2	Onset Year
2	0.69	0.97	1968
3	0.75	0.99	1968
4	0.52	0.98	1968
5	0.46	0.96	1971
6	0.40	0.98	1970
7	0.15	0.93	1973
8	0.30	0.91	1975
9	0.18	0.91	1974
10	0.15	0.67	2001
11	0.25	0.83	2004
12	0.15	0.85	2001

Note. The start year was chosen by the visual onset of a steady detection rate, and is given for each fit.

The Nobeyama 45 m, GBT, ARO/NRAO 12 m, NRAO 36 ft, and IRAM 30 m telescopes have cumulatively contributed to more than half of the new molecular detections. It is worth examining the impact of a facility on the new detections over its operational lifetime. For instance, while the IRAM 30 m telescope clearly dominates in the total number of detections, the NRAO 36 ft telescope produced more detections per year of its operational life. Figure 4 shows this information graphically for the top six contributing facilities; in this case, the NRAO 12 m and ARO 12 m have been combined, despite being operated by different organizations over its lifetime. During its operation, the NRAO 36 ft contributed to more than half of all new molecular detections. Of the currently operating facilities, the IRAM 30 m telescope is contributing the largest percentage of new detections (43%), followed by the GBT 100 m telescope (29%).

Figure 5 presents this data in another way, displaying the cumulative number of detections over time by each facility with more than 10 total detections. During its prime, the NRAO

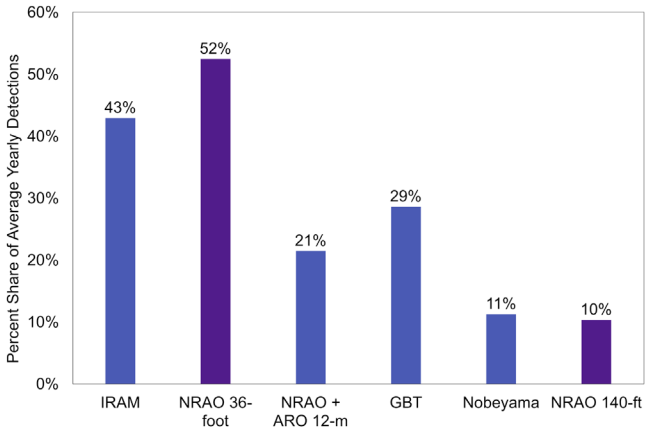

Figure 4. Percentage share of the yearly detections (3.7) that a facility contributed (or is contributing) over its operational lifetime. For example, over its operational career, the NRAO 36 ft antenna accounted for 52% of the annual detections. Facilities no longer in operation are colored purple, while current facilities are in blue.

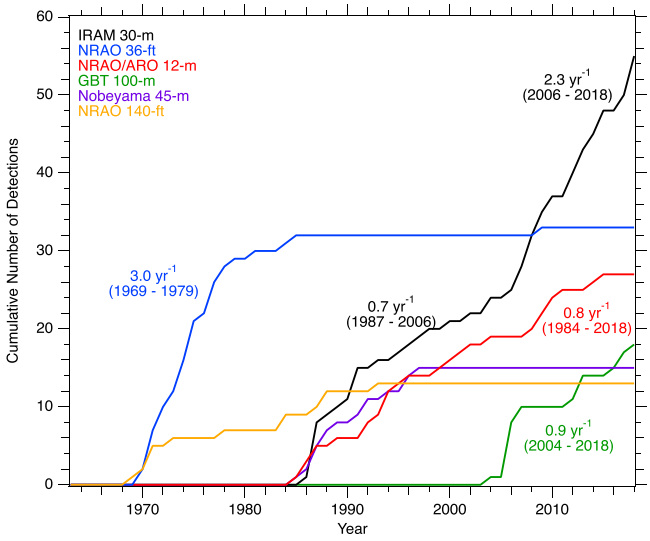

Figure 5. Cumulative number of detections per facility by year. For clarity, only those facilities with more than 10 total detections are shown. The detection rates for several facilities over selected time periods are highlighted.

Table 8
Total Number of Detections for Each Facility Listed in Section 3

Facility	#	Facility	#
ALMA	3	Mayall 4 m	1
APEX	4	McMath Solar Telescope	1
ARO 12 m	7	Millstone Hill	1
ATCA	1	Mitaka 6 m	1
Aerobee-150 Rocket	1	Mt Hopkins	1
Algonquin 46 m	3	Mt Wilson	3
BIMA	1	NRAO 12 m	20
Bell 7 m	8	NRAO 140 ft	13
CSO	2	NRAO 36 ft	33
Effelsberg 100 m	4	NRL 85 ft	1
FCRAO 14 m	4	Nobeyama	15
FUSE	1	OVRO	2
GBT	18	Odin	1
Goldstone 70 m	1	Onsala	4
Hat Creek	2	Parkes 64 m	5
Haystack	3	PdBI	2
Herschel	7	SEST 15 m	2
IRAM	55	SMA	2
IRAS	1	SMT	7
IRTF	2	SOFIA	1
ISO	5	Spitzer	3
KPNO 4 m	3	U Mass 14 m	1
Kuiper	1	UKIRT	1
MWO 4.9 m	2	Yebes 40 m	1

36 ft telescope was producing an average of three new detections a year, a rate that has not been matched since, although the IRAM 30 m has shown a significant increase in its detection rate since 2006, more than tripling its yearly detections. Indeed, if this modern detection rate for the IRAM 30 m is used instead, the percentage share shown in Figure 4 increases to 59% for that facility.

10.3. Molecular Composition

Carbon, hydrogen, nitrogen, and oxygen dominate the elemental composition of interstellar molecules, with sulfur and silicon in a distant second tier. Indeed, the entirety of the known molecular inventory is constructed out of a mere 16 of the 118 known elements. Figure 6 provides a visual representation of this composition.

Also of note is the relationship between the mass of the known molecules and the wavelength ranges that have contributed to their detection (Figure 7). As might be expected, there is little dependence on mass in the number of infrared detections, as the effects of increasing mass on vibrational frequencies are unlikely to shift these modes significantly enough to push them entirely out of the infrared region. Rotational transitions, however, are heavily dependent on mass. For a given rotational temperature, and to first order, the strongest rotational transitions of a molecule shift to lower frequencies with increasing mass (see Section 2.1 and Appendix A). This trend is reflected in the distribution of atomic masses detected by centimeter, millimeter, and submillimeter instruments. There is a marked preference for low-mass species to be seen at high frequencies, and for high-mass species, especially those with mass >80 amu, to be detected at the lowest frequencies. For a more complete discussion of the effects of increased mass and complexity on the wavelength ranges where the strongest transitions occur, see Appendix A.

This trend is also borne out in the number of atoms in a molecule detected at each wavelength (Figure 8). The centimer range has the peak of its distribution at five atoms, but extends heavily to larger numbers. The millimeter range shows a lower peak (3) atoms, but also sees a distribution to larger numbers. As might be expected, the infrared shows a rather flat distribution, as the vibrational transitions of molecules probed here will all generally fall within the IR, regardless of mass or number of atoms. Interestingly, all molecules detected in the visible and UV are diatomics.

Another interesting metric is the distribution of saturated and unsaturated hydrocarbon molecules detected. A fully saturated hydrocarbon is one where no π bonds (double or triple bonds) and no rings exist, with these electrons fully dedicated to bonding other elements (usually hydrogen). A simple formula for calculating the degree of unsaturation (DU) or equivalently the total number of rings and π bonds in a hydrocarbon

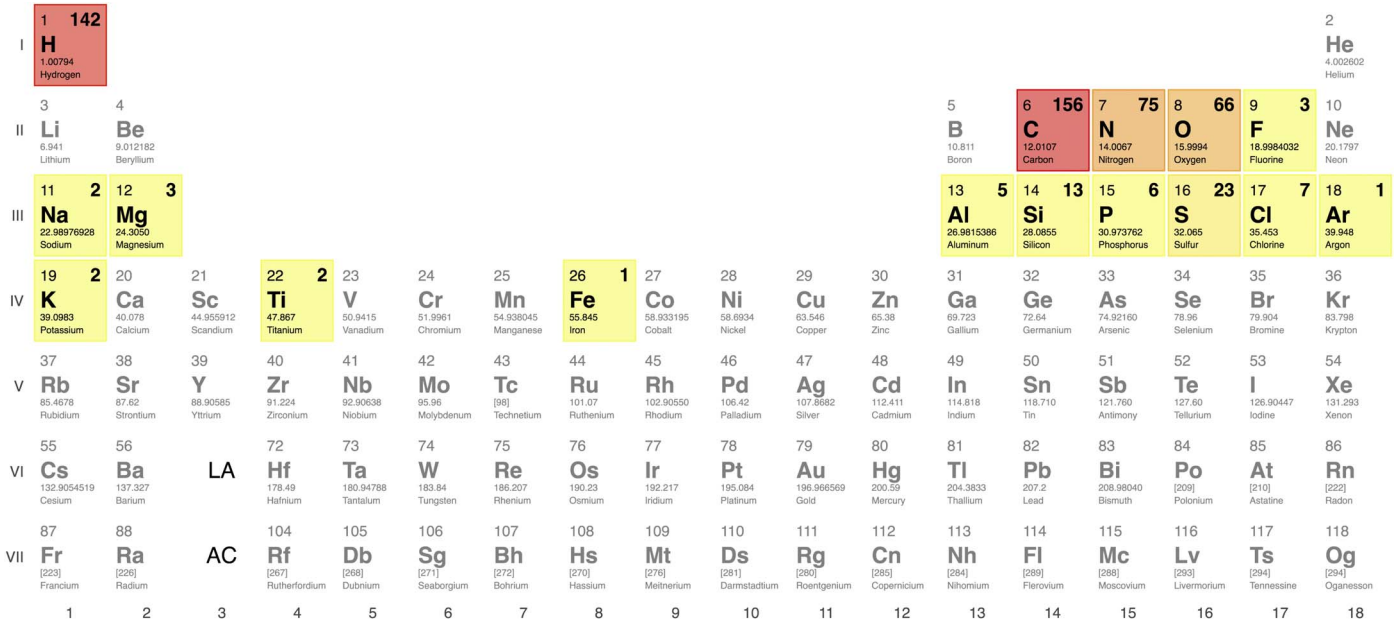

Figure 6. Periodic table of the elements, absent the lathanide and actinide series, color-coded by number of detected species containing each element. For those elements with detected ISM molecules, that number is displayed in the upper right of each cell.

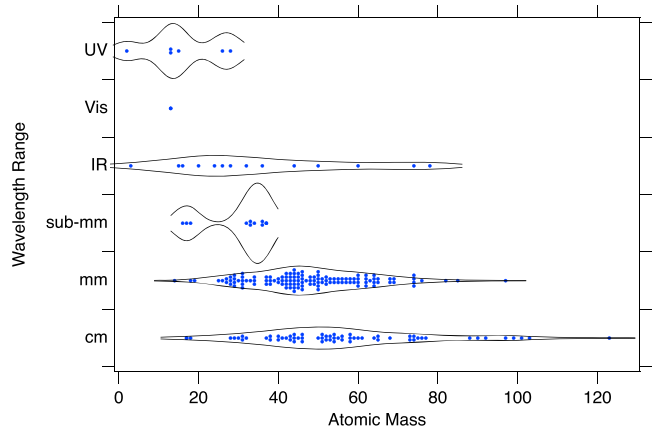

Figure 7. Violin plot of the mass of molecules detected in each wavelength range. In some cases, the initial detection was reported in two or more wavelength ranges (see text), and credit was given to each for this analysis. The frequency ranges for centimeter, millimeter, and submillimeter used were 0–50, 50–300, and 300+ GHz, respectively.

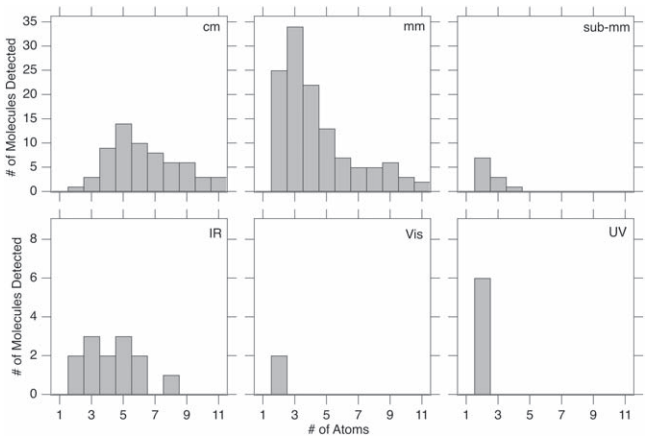

Figure 8. Histograms of the number of molecules detected in each wavelength range with a given number of atoms. In some cases, the initial detection was reported in two or more wavelength ranges (see the text), and credit was given to each for this analysis. The fullerene molecules are not included here.

molecule is given by Equation (4):

$$\mathrm{DU} = 1 + n(\mathrm{C}) + \frac{n(\mathrm{N})}{2} - \frac{n(\mathrm{H})}{2} - \frac{n(\mathrm{X})}{2}, \qquad (4)$$

where n is the number of each element in the molecule, and X is a halogen (F or Cl). Here, each atom contributes $x-2$ to the DU, where x is its valence; thus, the divalent elements O and S do not contribute. A visual representation of this distribution for interstellar hydrocarbons is shown as a histogram in Figure 9. With the exception of the fullerenes (not shown), HC_9N is the most unsaturated interstellar molecule, while only 10 species are fully saturated: CH_4, CH_3Cl, CH_3OH, CH_3SH, CH_3NH_2, CH_3OCH_3, CH_3CH_2OH, CH_3CH_2SH, $HOCH_2CH_2OH$, and CH_3OCH_2OH. The most common DUs are 1.0 and 2.0, representing one or two rings and/or π bonds. In total, 93% of all interstellar hydrocarbons are unsaturated to some degree.

Figure 10 provides a visual breakdown of the number of known interstellar molecules that are neutral, cationic, anionic, radical species, or cyclic. Many molecules fall into more than one of these categories. An analysis of the rates of detection of these various types of molecules in differing types of interstellar sources is provided in Section 10.4.

10.4. Detection Sources, Source Types, and Trends

More than 90% of the detections can be readily classified as being made in a source that falls into the generalized type of either a carbon star (e.g., IRC+10216), dark cloud (e.g., TMC-1), a diffuse/translucent/dense cloud along the LOS to a background source (hereafter "LOS Cloud"), or a star-forming region (SFR; e.g., Sgr B2). Figure 11 displays the percentage of interstellar molecules that were detected in each source type. Note that because some molecules were simultaneously detected in more than one source type, these percentages add to >100%. The

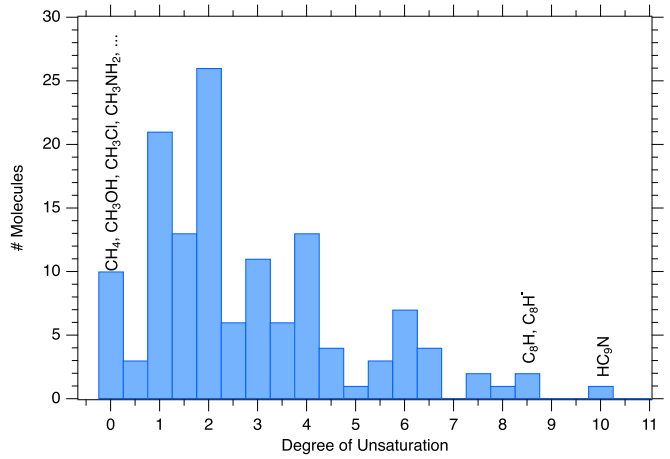

Figure 9. Histogram of the degree of unsaturation, or alternatively the number of rings and π-bonds (see the text), for hydrocarbon molecules containing only H, O, N, C, Cl, or F. Only seven interstellar hydrocarbons are fully saturated with no rings or π bonds. Most molecules contain one or two rings or π bonds (a double bond is one π bond, and a triple bond is two π bonds). The fullerene molecules are not shown.

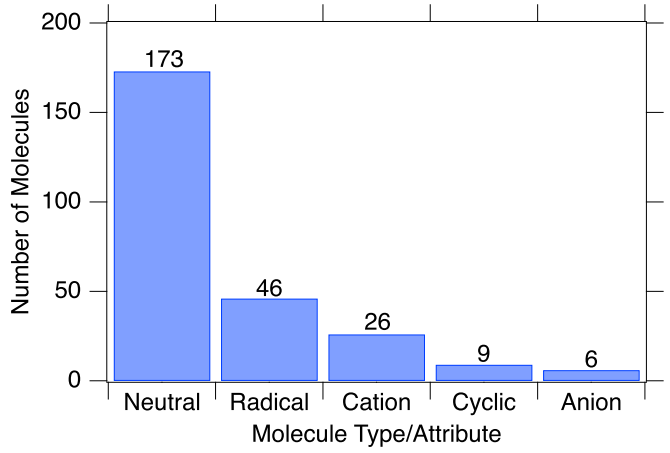

Figure 10. Number of known interstellar molecules that are neutral, cationic, anionic, radical species, or cyclic. Many molecules fall into more than one of these categories (e.g., most radical species have a net neutral charge).

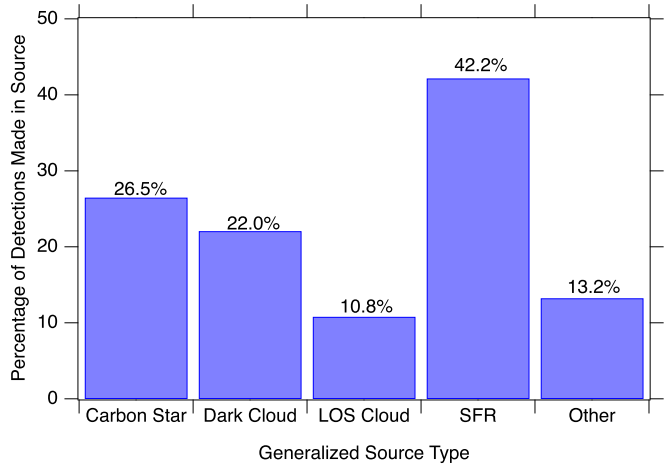

Figure 11. Percentage of known molecules that were detected for the first time in carbon stars, dark clouds, LOS clouds, and SFRs (see the text). Some molecules were simultaneously detected in multiple source types (e.g., C_8H^- in TMC-1 and IRC+10216).

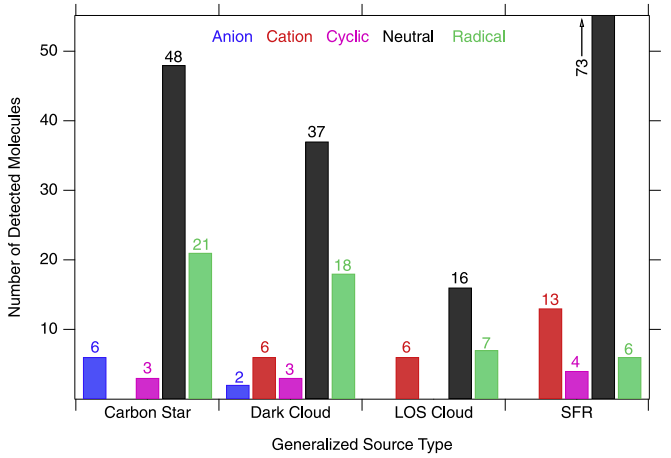

Figure 12. Number of known interstellar molecules that are neutral, cationic, anionic, radical species, or cyclic detected in four generalized source types. A small number of detections that did not fit easily into one of these categories (e.g., ArH^+ in the Crab Nebula supernova remnant) are excluded. As with Figure 10, species falling into more than one molecule type are counted for each of that type.

Table 9
Total Number of Detections that Each Source Contributed to for the Molecules Listed in Section 3

Source	#	Source	#
Sgr B2	67	NGC 7023	2
IRC+10216	51	TC 1	2
TMC-1	34	W49	2
Orion	24	CRL 2688	1
LOS Clouds	22	Crab Nebula	1
L483	8	DR 21(OH)	1
W51	8	Galactic Center	1
VY Ca Maj	5	IC 443G	1
B1-b	4	IRAS 16293	1
DR 21	4	K3-50	1
NGC 6334	4	L134	1
Sgr A	4	L1527	1
CRL 618	3	L1544	1
NGC 2264	3	L183	1
W3(OH)	3	Lupus-1A	1
rho Oph A	3	M17SW	1
Horsehead PDR	2	NGC 7027	1
NGC 2024	2	NGC 7538	1

Note. Detections made in clouds along the line of sight to a background source have been consolidated into "LOS clouds," and detections in closely location regions have been grouped together as well (e.g., Sgr B2(OH), Sgr B2(N), Sgr B2(S), and Sgr B2(M) are all considered Sgr B2).

number of detections in each individual source is listed in Table 9.

The distribution of molecules, as categorized by their attributes in Figure 10, across the generalized source types, is shown in Figure 12. Immediately obvious from this is that no molecular anions were first detected outside of carbon stars and dark clouds, a fact that remains the case even outside of first detections.

This may not be surprising when also considering the average degree of unsaturation across these generalized source types (Figure 13). The maximum degree of unsaturation of

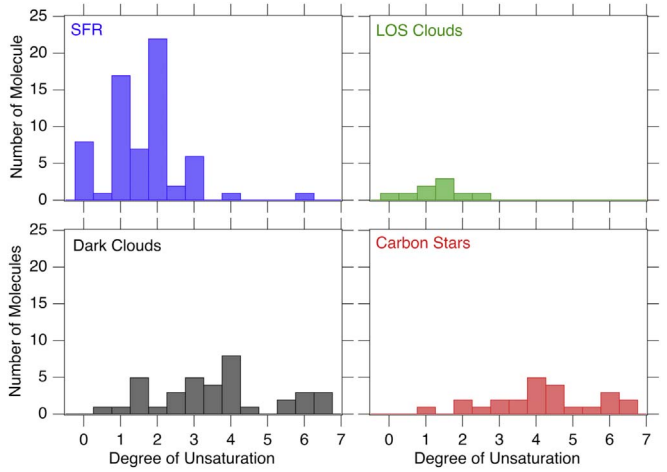

Figure 13. Histograms of the degree of unsaturation of molecules across the four generalized source types.

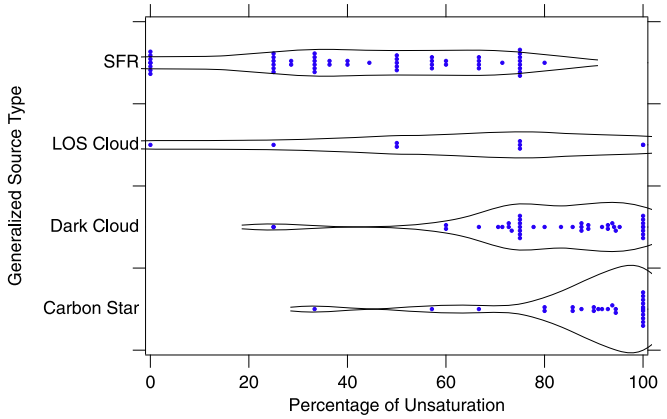

Figure 14. Violin plot of the percentage of unsaturation of molecules across the same source types.

molecules is molecule-dependent, meaning that the distribution of DU by source type is biased by the length/size of molecules seen there. This can be mitigated by examining the relative degree of unsaturation—meaning how close to fully unsaturated the molecules in a source type are. This is shown in Figure 14, where the percentage of unsaturation is the molecule's DU divided by the DU for a fully unsaturated version of that species.

In both cases, and with very few exceptions, molecules detected in carbon stars and dark clouds are on average highly unsaturated compared to other sources, and the six known molecular anions, CN^-, C_3N^-, C_4H^-, C_5N^-, C_6H^-, and C_8H^- are no exception. As shown in Figure 15, the molecules detected in these sources also tend to be the most massive.

A possible explanation for this trend is the influence of grain-surface/ice-mantle chemistry in SFRs. One of the most efficient pathways for increasing the saturation of species in the ISM is through direct hydrogenation on grain surfaces. A substantial amount of laboratory (e.g., Linnartz et al. 2015 and Fedoseev et al. 2015), quantum chemical (e.g., Woon 2002), and chemical modeling (e.g., Garrod et al. 2008) work suggests that these hydrogenation processes are efficient in the ISM, often even at low temperatures. In carbon stars, the bulk of the ice is thought to have been long since evaporated, with any hydrogenation occurring via catalysis on the (mostly) bare

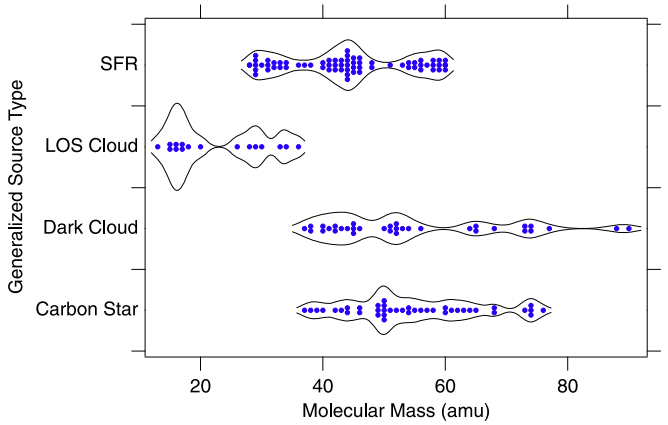

Figure 15. Violin plot of the molecular masses of non-fullerene molecules detected in each of the four generalized source types. The highest and lowest 10% of values (minimum 1) have been dropped from each data set.

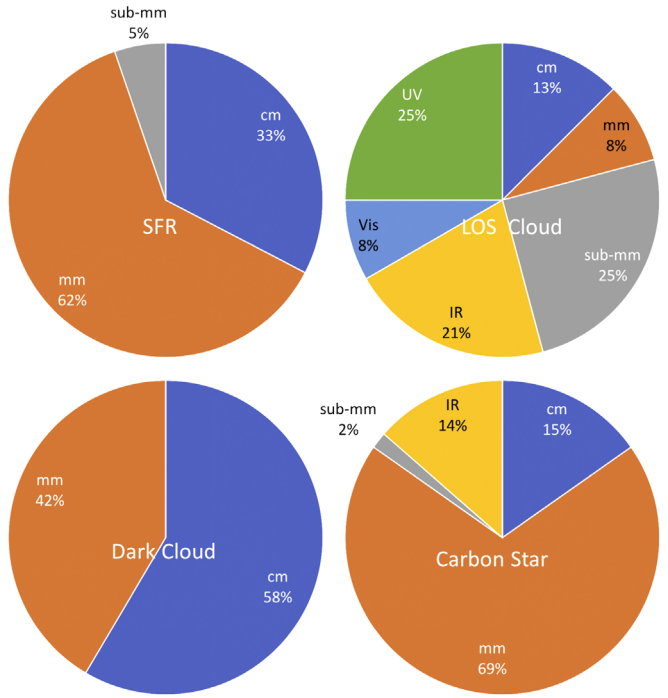

Figure 16. Percentage of first detections in each generalized source type that were made at centimeter, millimeter, submillimeter, infrared, visible, and ultraviolet wavelengths.

grain surfaces (Willacy 2003). In dark clouds, the temperatures are so low that although chemistry is likely occurring in ice mantles, there is no readily apparent mechanism for liberating these molecules into the gas phase for detection. Some recent work in this area has suggested that cosmic-ray impacts could non-thermally eject this material in these sources (Ribeiro et al. 2015), but this is certainly not as efficient a process as the shock-induced (Requena-Torres et al. 2006) or thermal desorption that play significant roles in SFRs.

Looking back at Figure 12, a few other trends are apparent. First, the fraction of species detected in SFRs that are radicals is substantially lower (5%) than seen in the other environments (11% to as high as 30% [dark clouds]). Radicals tend to be highly chemically reactive species, and perhaps are being depleted as more reaction partners are being liberated from the surface of ice mantles in these regions. Second, it bears noting

that the only source type in which all five types of species discussed here were first detected are dark clouds, perhaps suggesting that these regions are more chemically complex than they may appear at first glance, especially given the prominence of SFRs like Sgr B2 and Orion in the detection of new molecules.

It is also worth examining the wavelength ranges that contributed to first detections in each of these generalized source types (Figure 16). As discussed in Sections 2.2 and 2.3, detections in the IR, visible, and UV portions of the spectrum are nearly always performed in absorption, necessitating both a background source and an optically thin absorbing medium. LOS clouds satisfy both of these requirements, and thus these regions show the greatest diversity in wavelengths used for detection, whereas SFR and dark clouds, which are often optically thick, have not yet seen a first detection at wavelengths shorter than the far-infrared.

11. Conclusions

In summary, 204 individual molecular species have been detected in the ISM. A further 11 molecules are considered to be tentatively detected, while 2 species have had their detections disputed. These detections have been dominated by radioastronomical observations, with the IRAM 30 m, GBT 100 m, Nobeyama 45 m, and NRAO/ARO 12 m telescopes the most prolific extant facilities. Beginning in 1968, the rate of new detections per year can be well-fit to a linear trend of 3.7 new molecules per year, although there is evidence for an increase in this rate in the last decade, due to the onset of GBT detections and a tripling of the rate of IRAM detections. A substantial fraction (∼33%) of known molecules have now been seen in external galaxies, while the numbers of molecules known in protoplanetary disks (23), interstellar ices (6), and exoplanet atmospheres (5) are much smaller due to observational challenges.

B.A.M. sincerely thanks the five anonymous referees for their careful reading and suggestions, which have substantially improved the quality of this manuscript. B.A.M. also thanks J. Mangum for helpful discussions regarding the history of NRAO telescope facilities, L.I. Cleeves for discussions of molecules in protoplanetary disks, and A. Burkhardt for a critical reading of the appendix. The National Radio Astronomy Observatory is a facility of the National Science Foundation operated under cooperative agreement by Associated Universities, Inc. Support for B.A.M. was provided by NASA through Hubble Fellowship grant #*HST*-HF2-51396 awarded by the Space Telescope Science Institute, which is operated by the Association of Universities for Research in Astronomy, Inc., for NASA, under contract NAS5-26555.

Appendix A
Sources of Molecular Complexity and Their Impact on Detectability

The purpose of this appendix is to examine a number of the factors that affect the detectability of molecules in the ISM. When considering a molecule that has not yet been detected in the ISM (or in protoplanetary disks, etc.), examining each of the factors presented here should provide an informed first-look at the reasons why detection may be challenging, beyond merely a potential low abundance. The list of factors outlined here is not exhaustive, but instead focuses on those that commonly affect molecules observed in interstellar sources. Furthermore, while some quantitative measures and analytical formulas will be presented, this discussion is intended to be primarily qualitative in nature. Some concepts will be presented as zeroth- or first-order approximations. The terminology may not always be quantum mechanically rigorous.

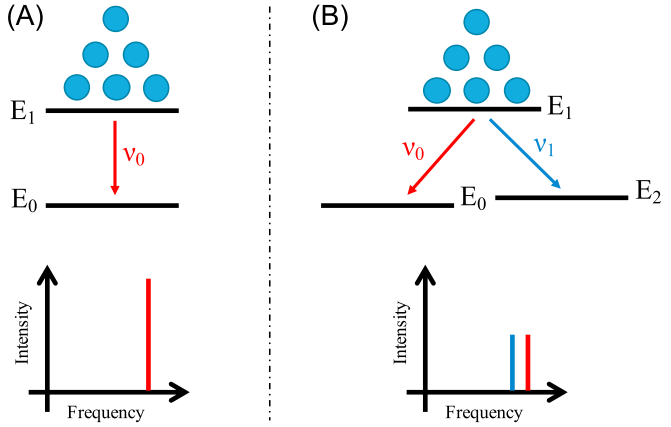

Figure 17. Idealized examples of the effects of having additional energy levels to undergo transitions. In case A, all six molecules can undergo transition ν_0. In case B, about half the molecules will undergo transition ν_0, but the other half will undergo transition ν_1. In case B, the intensity of transition ν_0 is therefore half of what it is in case A.

In the last decade, the common astrochemical parlance defining a complex organic molecule (COM) has been any molecule with six or more atoms, with methanol (CH_3OH) being the prototypically simplest COM (Herbst & van Dishoeck 2009). This definition, while arbitrary, has proven a useful aid in the discussion of structural complexity. The detectability of molecules, however, is affected by much more than the number of atoms. Indeed, as will be shown later, a low-abundance linear molecule may be far easier to observe than a higher-abundance, asymmetric top containing far fewer atoms. Similarly, a low-abundance, structurally complex molecule may be more readily detected than a highly abundant, structurally simple molecule with very weak transitions.

As discussed in the main text, the bulk of new detections are made via observation of rotational transitions in the radio, so that will be the focus of this discussion. Emission or absorption signals from molecules in the centimeter, millimeter, and submillimeter regimes almost always arise from rotational transitions as a molecule moves between two rotational energy levels. The intensity of any given signal is dependent on numerous factors, many of which will be discussed here, but these can largely be broken down into three primary components:

1. intrinsic, quantum-mechanical properties of the molecule;
2. telescope and radioastronomical source properties; and
3. the absolute number of molecules undergoing that transition.

The molecular, instrumental, and source properties (1 and 2) will vary from line to line, molecule to molecule, and source to source, but the effects of abundance (3), excluding a number of edge cases, are universal. There are only so many molecules available to undergo a transition, and produce an observable signal, in a source.

While this may seem like a triviality, the effects are far-reaching. Figure 17 describes two cases for a molecule

undergoing a transition and emitting light to be detected by a telescope looking for frequency ν_0. In the first case, where all the population undergoes the transition, the light observed at frequency ν_0 is twice as great as that of the second case, where the molecule can now undergo a similar transition at a different frequency because of the presence of an additional energy level. As will become clear in the following sections, the true complexity of a species is largely measured in the number of rotational energy levels the population is distributed over, and undergoing transitions between. The more levels, the fewer photons that are produced at any given transition frequency, and the more complex the spectrum becomes as additional transition frequencies appear. While a simple linear molecule like CO may have a few dozen energy levels populated at 300 K, a truly complex molecule may have hundreds of thousands.

Thus, a reasonable measure of the level of complexity is the number of rotational energy levels that can be expected to have a non-trivial fraction of the total number of that molecule in a source. Because these levels vary in energy, the fraction of the molecules in each state is dependent on the average energy of the population of molecules, which is described by an excitation temperature. In many cases, this distribution is governed by a Boltzmann distribution, where the fraction (F_n) of molecules in any given energy (E_n) state n is governed by Equation (5), and the ratio of population between any two states (E_n, E_m) is governed by Equation (6), at an excitation temperature $T_{\rm ex}$:

$$F_n \propto e^{-\frac{E_n}{kT_{\rm ex}}}, \tag{5}$$

$$\frac{F_n}{F_m} = e^{\frac{E_m - E_n}{kT_{\rm ex}}}. \tag{6}$$

The rigorous accounting of states with a significant F_n at a given temperature is expressed through the temperature-dependent partition function, which is discussed explicitly in Appendix A.11. While the partition function is often used as a practical proxy for the number of non-trivially populated energy levels, for the purposes of this initial discussion, a simpler approximation can be adopted. Drawing on Equations (5) and (6), the nth energy level of a molecule having energy $E_n = 5kT$ will have $F_n = e^{-5}$, or ~1% relative to the ground state ($E_0 = 0kT$) population. Thus, the number of states with energies $<5kT$ is an excellent approximation for the number of states that will have a non-trivial population at any given temperature.

As discussed above, the number of possible transitions increases with the number of states that have a non-trivial population: more states, more transitions, lower intensity for any given one. Thus, when examining the individual factors that affect the detectability of a molecule (i.e., the overall intensity of transitions and the number of those transitions), the number of states below $5kT$ can provide a gross approximation of the magnitude of an effect on detectability.

A.1. Number of Atoms

The number of atoms in a given molecule is a good first approximation of spectral complexity. The energy levels of a molecule are determined by the molecular structure and reflected in the moments of inertia. Consider a simple linear molecule, whose energy levels are given, to zeroth-order, by Equation (7), where B is the rotational constant (often

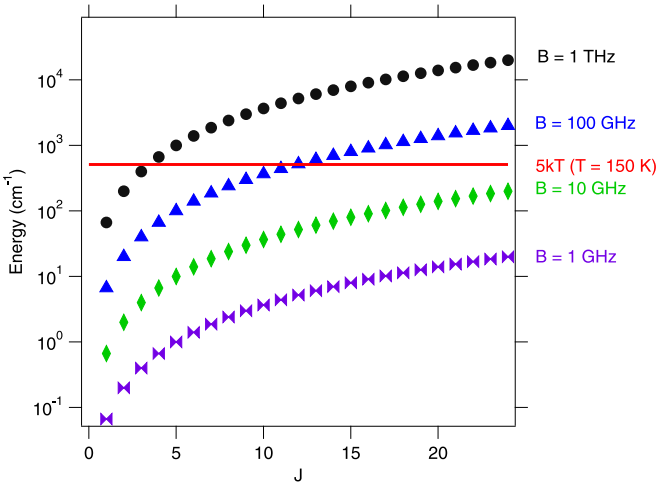

Figure 18. Rotational energy levels for molecules with rotational constants B = 1000, 100, 10, and 1 GHz. The red line is drawn at 521 cm^{-1}, the value of $5kT$ at T = 150 K; energy levels below this value are non-trivially populated.

expressed in units of MHz or cm^{-1}), and J is a quantum number representing the total rotational angular momentum (Bernath 2005):

$$E_J = BJ(J+1). \tag{7}$$

The rotational constant B is then related to the moment of inertia, I, along the molecular axis by Equation (8) (Bernath 2005):

$$B = \frac{h^2}{8\pi^2 I}. \tag{8}$$

The moment of inertia is proportional to the amount of torque needed to rotate a molecule, and is determined by the spatial distribution of mass from the axis of rotation, going as the square of the distance. A longer molecule will therefore, in general, have a larger I (and a correspondingly small B) than a shorter molecule with similar constituent atoms. This means for a given value of J, the energy of that level will be lower. In turn, there are more energy levels accessible $<5kT$, and the total population will be spread more thinly among them. Figure 18 shows the number of levels which fall beneath $5kT$ for four hypothetical molecules with rotational constants spanning four orders of magnitude.

A more specific example is the HC$_x$N family of linear molecules, with astronomically observed constituents as large as HC$_9$N (Broten et al. 1978; Loomis et al. 2016). Table 10 gives the rotational constants and number of energy levels below kT for these molecules. It is clear that the number of populated energy levels increases with decreasing B, increasing the spectral complexity by a density of lines argument alone. Additionally, however, consider that for an equivalent population of HCN and HC$_7$N, the HC$_7$N molecules are distributed over almost an order of magnitude more energy levels. As a result, the number of molecules undergoing a single rotational transition (and thus producing detectable signal) is overall lower for HC$_7$N, resulting in weaker signals.

This can be seen most easily by examining the rotational spectra of these molecules at T = 150 K. Figure 19 shows a comparison of the spectra of HCN and HC$_7$N at T = 150 K, assuming the same number of molecules for each. Not only is the HC$_7$N spectrum far more spectrally dense, but the intensities are so low that they must be scaled by a factor of

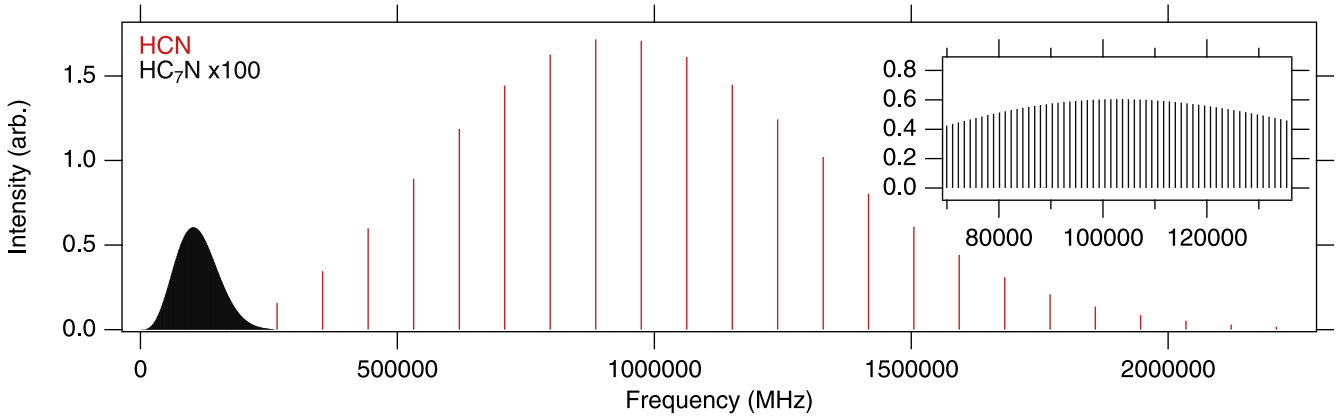

Figure 19. Rotational spectra of HCN (red) and HC_7N (black) at $T = 150$ K for the same number of molecules of each. Hyperfine has not been considered. The inset shows a magnified portion of the HC_7N to show detail as to the density of lines. In both the main plot and the inset, the intensities of the HC_7N lines are multiplied by a factor of 100.

Table 10
Rotational Constants and Number of Energy Levels below kT at 150 K for All HC_xN Species Detected in the ISM

Molecule	B (MHz)	# Levels[a] $<kT$ @ 150 K	Lab Ref.
HCN	44316	18	1
HC_2N	10986	36	2
HC_3N	4549	58	3
HC_4N	2302	80	4
HC_5N	1331	107	5
HC_7N	564	166	6
HC_9N	290	231	7

Note.
[a] Hyperfine splitting not considered, for simplicity.
References. [1] Ahrens et al. (2002), [2] Saito et al. (1984), [3] de Zafra (1971), [4] Tang et al. (1999), [5] Alexander et al. (1976), [6] Kirby et al. (1980), [7] McCarthy et al. (2000).

100 to be readily visible on the graph. The strongest transition of HCN at this temperature is the $J = 10-9$, while the strongest transition of HC_7N is the $J = 91-90$. The strongest HCN transition is nearly 300 times stronger than that of HC_7N. A further consequence is that the frequency of a given transition shifts to lower and lower frequency as the number of atoms increases, increasing the moment of inertia, and decreasing the rotational constant. This is clearly seen in Figure 19, where the strongest HCN transitions are arising in the ~900 GHz region, while for HC_7N these are at ~100 GHz.

In general, for families of molecules with similar elemental compositions, adding additional atoms will increase the spectral complexity (line density), decrease the overall intensity of these lines, and shift the lines to lower frequency.

A.2. Geometry and Symmetry

The previous discussion focused exclusively on linear molecules as the prime example, but few molecules commonly considered complex by interstellar standards are linear (although certainly this is a debatable position). When additional atoms are added off of the primary axis, additional complexity can be introduced, dependent on whether additional components to the dipole moment are manifest. One of the underlying causes of the relative simplicity of linear molecular rotational spectra is the inherent symmetry of a linear molecule.

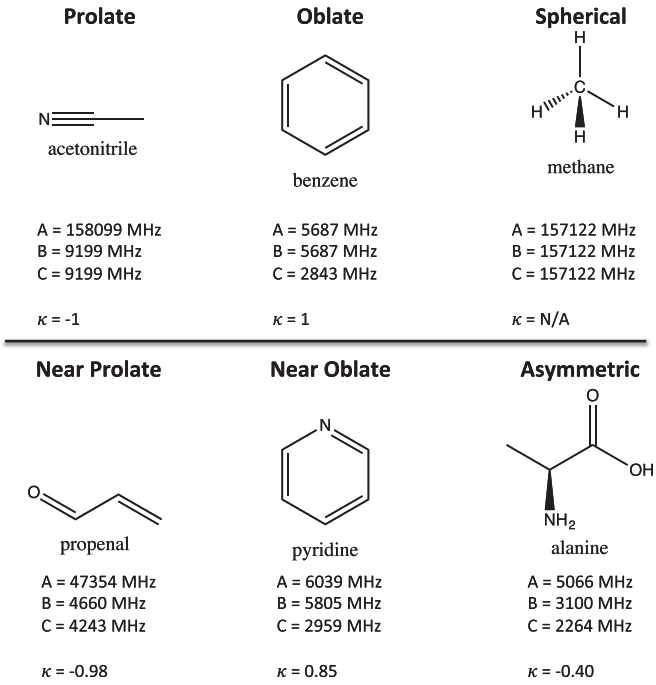

Figure 20. Examples of different molecular symmetries demonstrate equivalencies in rotational constants and the corresponding Ray's asymmetry parameters.

An allowed rotational transition can only occur when a permanent electric dipole moment is present. Due to symmetry, linear molecules can only ever possess at most a single component of the electric dipole moment, oriented along the linear axis. The addition of off-axis atoms introduces, in most cases, a degree of asymmetry.

A convenient measure for assessing the degree of asymmetry introduced is κ, the Ray's asymmetry parameter (Ray 1932), given in Equation (9), where A, B, and C are the rotational constants of the molecule.

$$\kappa = \frac{2B - A - C}{A - C}. \tag{9}$$

A number of example molecules displaying symmetry, or near symmetry, are shown in Figure 20. A completely spherically

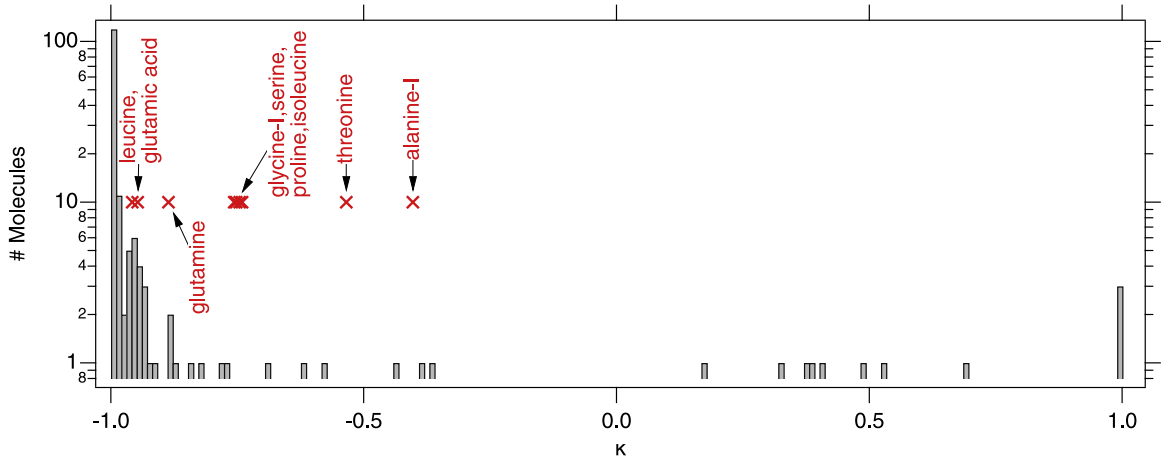

Figure 21. Histogram of all detected interstellar molecules by their Ray's Asymmetry Parameter, κ. Prolate rotors have $\kappa = -1$, while oblate rotors have $\kappa = 1$. A selection of amino acids are overlaid in red.

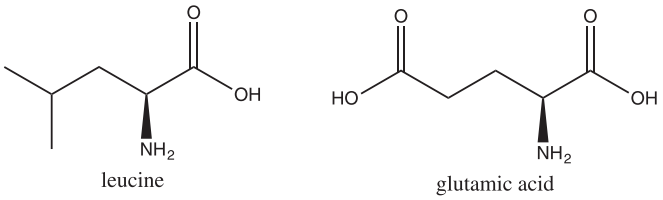

Figure 22. Structures of the amino acids leucine and glutamic acid.

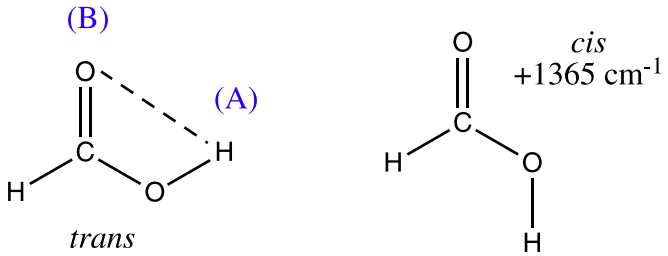

Figure 23. The cis and trans conformers of formic acid. The hydrogen-bonding interaction of the hydroxyl hydrogen (A) with the carbonyl oxygen (B) in the trans form substantially stabilizes (by 1365 cm^{-1}; Hocking 1976) the conformer relative to the cis form.

symmetric molecule, such as methane (CH_4), will have $A = B = C$, and thus κ is undefined.

Among the known interstellar molecules, the most commonly occurring symmetric top species are prolate (commonly thought of as cigar-shaped) with $\kappa = -1$, and $I_a < I_b = I_c$. Linear molecules are the most common prolate symmetric tops; however, any near-linear molecule in which the off-axis mass is symmetrically distributed, such as methyl cyanide (acetonitrile, CH_3CN), resulting in $I_b = I_c$, are also prolate. As a consequence of this symmetry, no additional permanent dipole components are introduced, and prolate symmetric tops behave largely like linear molecules as complexity increases.

Figure 21 displays the distribution of known interstellar molecules by their κ values. It is clear that the vast majority ($\sim$90%) of detected interstellar molecules are prolate or near-prolate. Only 24 molecules have $\kappa > -0.9$. To first order, therefore, it is reasonable to claim that the more prolate a potential interstellar molecule is, the more likely it is to be detectable. For the sake of comparison, also plotted on Figure 21 are a number of amino acids, molecules not detected in space but highly sought and widely considered truly complex. In the case of glycine and alanine, the simplest amino acids by number of atoms, both are quite asymmetric ($\kappa_{gly} = -0.74$, $\kappa_{ala} = -0.4$), while the most nearly prolate amino acids, leucine and glutamic acid, contain many more atoms (Figure 22). Thus, there is an offsetting balance to be considered in their detectability: the benefits of being (near) prolate versus the drawbacks of increasing number of atoms and structural size.

A.3. Structural Conformers

Without altering the overall bonding patterns (and thus changing the molecular make-up), there are often several ways for the atoms within a molecule to be arranged spatially. A single population of molecules can often be comprised of one or more different arrangements, or conformers, of the species. Because these conformers have distinct moments of inertia, they therefore have distinct rotational spectra. As a result, the more conformers that a population of molecules can exist in at a given temperature, the fewer molecules are available to undergo any given rotational transition.

The simplest case of conformers is perhaps that between cis- and trans- arrangements for a small molecule. Often, one conformer is substantially more stable with respect to the other, and there is little impact on the overall detectability of the species. A salient example is that of formic acid (HCOOH; Figure 23). Here, the trans conformer is greatly stabilized by a hydrogen-bonding interaction. As a result, while the lower-energy trans conformer was first detected in 1971 (Zuckerman et al. 1971), and is indeed quite common in regions with any degree of chemical complexity (Requena-Torres et al. 2006), the higher-energy cis conformer was only recently discovered and is only seen because of exceptional chemical and physical circumstances (Cuadrado et al. 2016).

For more complex molecules, such as amino acids, the number of conformers with similar energies is often greatly enhanced. The nine lowest-energy conformers of glutamic acid, for example, are shown in Figure 24 along with their relative energies; all are below 900 cm^{-1}. In this case, it is the spatial arrangement of the C(O)OH and NH_2 groups that differ between conformers. Indeed, dozens of additional higher-energy conformers, in which the relative arrangement changes

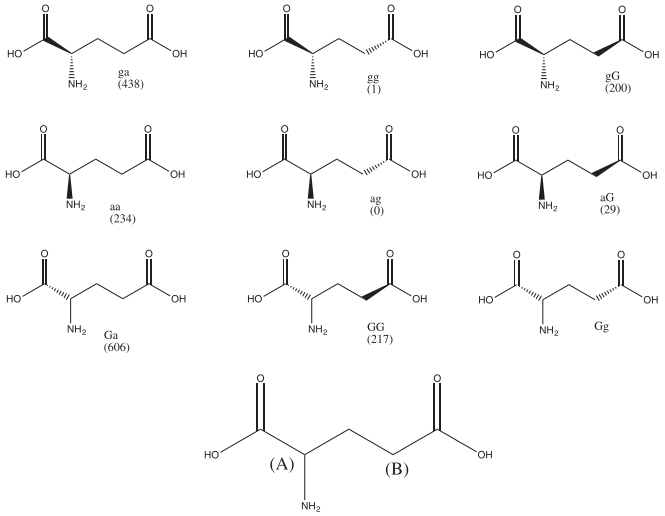

Figure 24. Nine lowest-energy conformers of glutamic acid. Bold angled lines indicate a bond which projects out of the plane of the page, while a dashed line indicates a bond into the plane. The conformers differ in the relative spatial location of the C(O)OH and NH_2 groups around the carbon atoms indicated by the (A) and (B) in the bottom (2D) structure. Where available, the zero-point corrected energies (in cm^{-1}) of the conformers are given, relative to the lowest energy (ag). This is figure is adapted from Figure 1 and Table S1 of Peña et al. (2012).

around other central points, including the hydroxyl-carbonyl hydrogen bonds, also exist.

From a practical standpoint, the additional conformer of formic acid has no impact on the detectability of the lower-energy trans species. There simply is not enough cis to reduce the overall levels of trans in a population in a significant way. On the other hand, an attempt to detect glutamic acid would be severely hindered by the existence of a number of low-energy conformers. Of these conformers, the ag, gg, and aG are the lowest in energy. When Peña et al. (2012) measured the microwave spectrum of a sample of glutamic acid in the gas phase, they observed all three conformers simultaneously. Instead of (practically) the entire population existing as the lowest-energy conformer, as in the case of formic acid, here the overall intensity of any one conformer's spectral signature was diminished, making it harder to detect than if only a single conformer were energetically favored.

A.4. Internal Motion

Considering a single conformer of a molecule, the complexity of the rotational spectrum can be further increased due to the internal structure of that molecule. In the case of formic acid, the molecule can interconvert between the two conformers by rotation about the C-OH bond. The barrier to this process is large ($4827 cm^{-1}$; Hocking 1976), meaning that it is rare for a full rotation about this bond to occur and this motion is unlikely to have a significant impact on the spectrum. For functional groups that can undergo internal motion and have only a modest barrier to overcome, however, additional degrees of complexity arise.

A.4.1. Rotation

Perhaps the most common form of internal motion that increases spectral complexity is that of internal rotation, specifically that of methyl ($–CH_3$) functional groups. A detailed review of the effects of internal rotation on spectra is given by

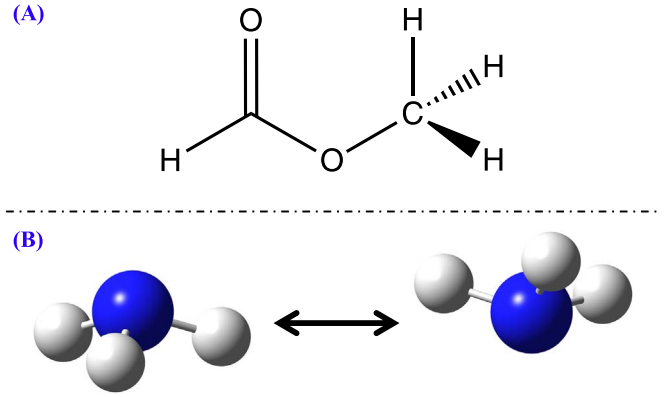

Figure 25. Examples of internal motions. (A) Structure of cis-methyl formate. As the methyl ($–CH_3$) group rotates about the C-O bond, the interaction potential between the hydrogen atoms and the oxygen atoms changes, affecting the coupling of the internal rotational angular momentum to that of the overall angular moment of the system, perturbing energy levels and increasing spectral complexity. (B) Representation of the umbrella-like inversion motion undergone by the NH_3 molecule, which perturbs the standard rotational energy levels and adds complexity to the rotational spectra.

Lin & Swalen (1959). In short, the rotational angular moment of the rotating (or pseudo-vibrating; i.e., torsion) sub-group within the molecule couples with the rotational angular moment of the molecule as a whole, perturbing the energy levels and resulting in new possible transitions.

As a brief example, the lower-energy cis conformer of methyl formate (CH_3OCHO) is shown in Figure 25(a). The methyl group is not locked into one orientation, and instead rotates around the C-O bond. As the hydrogen atoms move, their interaction with the carbonyl (C=O) and ester (C-O-C) oxygen atoms changes, hindering the rotation. As a result, every rotational energy level is split into three states: a pair of degenerate levels (denoted *E*) and a single non-degenerate state (donated *A*).[8] As a result, the spectrum becomes far more complex, and because there are now many more states accessible at the same temperature, the overall intensity of any given transition is substantially decreased. To make matters worse (or better), the degree of this splitting changes with frequency/energy. Some transitions will suffer from this decrease in intensity, but for others, the splitting will be far less than the line width and will be unobservable.

A.4.2. Inversion

A second common type of motion is inversion. The underlying principle is the same as that for internal rotation: the angular moment of internal functional groups moving within the system couples to the overall angular moment of the system and perturbs the energy levels. The most common example is seen in ammonia (NH_3), shown in Figure 25(b). In the case of NH_3, the entire molecule inverts in an umbrella motion. As with the internal rotation, this motion perturbs the standard rigid-rotor energy levels, increasing the number of states accessible, generating more transitions, and reducing individual spectral intensity. Townes (1946) and Townes & Schawlow (1975) provide excellent summaries of the laboratory and theoretical efforts to characterize this type of internal motion.

[8] The energy ordering and degree of splitting changes as a function of energy, barrier heights, and other factors beyond the scope of this discussion. See Lin & Swalen (1959) for a detailed review.

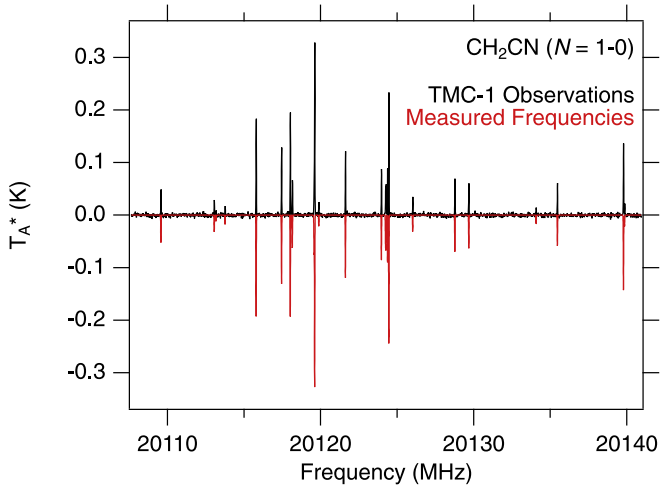

Figure 26. Observations of a single rotational transition ($N = 1$–0) of CH_2CN in TMC-1 from the Kaifu et al. (2004) survey in black, with the measured laboratory transitions overlaid in red. The split lines are the result of the coupling of both ^1H and ^{14}N hyperfine splitting of the transition.

A.5. Nuclear Hyperfine

A final common type of perturbation is the coupling of nuclear angular momentum (from atoms with non-zero nuclear angular moment) to the overall energy. This perturbation is often quite small; for example, the splitting from ^1H is rarely resolvable with even high-resolution instruments in the laboratory, much less in interstellar observations. ^{14}N hyperfine splitting, on the other hand, is routinely observed in the laboratory, and is often seen in interstellar observations in sources with sufficiently narrow line widths. Figure 26 shows an example of resolved hyperfine transitions from a single rotational transition CH_2CN in TMC-1 observations, showing both ^1H and ^{14}N splitting. The single rotational transition ($N = 1$–0) has been split into more than a dozen resolvable lines. The relative intensities of hyperfine-split transitions are well-known (Townes & Schawlow 1975), and combined with the structure, can provide unique fingerprints for identification and as probes of temperature and optical depth.

Column densities and spectral intensities. Given these sources of complexity in the spectrum, it is then useful to consider how the intensity of a spectral line actually changes as a result in a more quantitative way, and the influence of some telescope-specific parameters on the line as well. Given a detection of a molecular line from observations, a column density can be determined, or, alternatively, given an expected column density, a predicted observational intensity can be derived. A detailed examination of the radiative transfer processes behind these calculations is beyond the scope of this work; the interested reader is referred to the recent work of Condon & Ransom (2016) and Mangum & Shirley (2015). Here, only the widely used single-excitation model is described in detail. A discussion of the effects on detectability when this model breaks down follows.

A.6. The Single-excitation Model

The most common approach used to analyze observational data is described in detail in Goldsmith & Langer (1999), and is often referred to as the "rotation diagram" method or a "local thermodynamic equilibrium (LTE)" analysis. Both terms omit the key assumption made in the analysis, which is that the number of molecules in each molecular energy level is assumed to be described exactly by a Boltzmann distribution at a single, uniform excitation temperature, T_{ex}.

Table 11
Definition of Parameters in the Single-excitation Model Calculation of Column Density

Parameter	Definition	Units
N_T	Column density	cm^{-2}
T_{ex}	Excitation temperature	K
T_{bg}	Background temperature	K
k	Boltzmann's constant	$J\ K^{-1}$
h	Planck's constant	J s
Q	Partition Function at T_{ex}	
E_u	Upper state energy of the transition	K
ΔT_A	Peak observed intensity of the transition	K
ΔV	FWHM of the transition	$cm\ s^{-1}$
B	Beam filling factor	
S	Line strength	
μ^2	Square of transition dipole moment	$J\ cm^3$
η_B	Beam efficiency	

Hollis et al. (2004a) formalized the calculations used to determine column densities and excitation temperatures, and that formalism is adopted here for the purposes of this discussion. Equation (10) describes a calculation for molecules in emission or absorption, and the parameters used in this equation are given in Table 11. Detailed discussions of several of these parameters are given in Mangum & Shirley (2015):

$$N_T = \frac{1}{2}\frac{3k}{8\pi^3}\sqrt{\frac{\pi}{\ln 2}}\frac{Qe^{E_u/T_{ex}}\Delta T_A \Delta V}{B\nu S\mu^2\eta_B}\frac{1}{1-\frac{e^{h\nu/kT_{ex}}-1}{e^{h\nu/kT_{bg}}-1}}. \quad (10)$$

A key insight is provided by Equation (10) upon inspection of the $\left(1-\frac{e^{h\nu/kT_{ex}}-1}{e^{h\nu/kT_{bg}}-1}\right)$ term. In the case where $T_{ex} < T_{bg}$, this term becomes negative. As a negative value of N_T is unphysical, the value for ΔT_A must therefore be negative as well, indicating absorption.

A.7. Critical Density

When the number of molecules in each energy level is not well-described by a Boltzmann distribution, one of the most common causes is that the density of the gas in which the molecule resides has fallen below the density required to thermalize the population. The distribution of a population of molecules across energy states is a balance between radiative (emission or absorption) processes, and collisional (thermal) processes. Each transition of a given molecule has a characteristic rate (A_{ul}) that governs how quickly it undergoes spontaneous emission of photons, redistributing the population away from Boltzmann equilibrium. For a population of molecules to be in thermal equilibrium, collisions with other gas molecules must occur frequently enough to out-compete the radiative processes. In this case, T_{ex} becomes equal to the kinetic temperature (T_k) of the colliding gas, which is usually termed LTE conditions.

The density of gas required to ensure that these collisions dominate the distribution over radiative processes is the critical density (n_{cr}), given by Equation (11) (Tielens 2005) where A_{ul} is the Einstein A coefficient (s^{-1}) and γ_{ul} is the collisional rate coefficient ($cm^3\ s^{-1}$) for the transition from upper state u to

lower state l

$$n_{cr} = \frac{A_{ul}}{\gamma_{ul}}. \quad (11)$$

A_{ul} is directly related to the rate at which a given molecule in state u will spontaneously decay to state l and emit a photon. Transitions with large A_{ul} undergo emission rapidly. To maintain a population distribution described by the thermal temperature, a correspondingly higher density—that results in more frequent collisions—is therefore required. A generalized approach for multilevel systems with many transitions into and out of a given level can be written as Equation (12) (Tielens 2005):

$$n_{cr} = \frac{\Sigma_{l<u} A_{ul}}{\Sigma_{l\neq u} \gamma_{ul}}. \quad (12)$$

The rate at which these collisions occur is related to γ_{ul}, which is proportional to the cube of the average velocity of the molecules in the gas (v; governed by T_k), a cross-sectional area (σ) related to the size of each collision partner, and their rotational and vibrational excitation. These cross-sections are almost universally calculated theoretically, but are extraordinarily computationally expensive, especially with increasing molecular size (Faure et al. 2014).

In general, if the gas density exceeds n_{cr}, the relative populations of u and l will be described by a Boltzmann distribution at T_{ex} (which is nominally equal to T_k). Because n_{cr} is distinct for each transition, it is possible for only some of the energy levels of a molecule to be described by one T_{ex}, while the remaining energy levels are dominated by radiative processes and are not described by T_{ex}.

If all values of A_{ul} and γ_{ul} are known for a given molecule, then T_k and a column density can be modeled explicitly without the assumption of a single-excitation temperature in what is known as a radiative transfer calculation. The approximations described in Appendix A.6 are accurate in the limit that the density is much larger than n_{cr}, and a full radiative transfer calculation in such situations will return an equivalent value to that determined by Equation (10) and a single value for T_{ex} equal to T_k. A detailed review of radiative transfer calculations is given by van der Tak (2011).

A.8. Source and Beam Sizes

Often, the region of the sky from which molecular emission (or absorption) is seen is smaller than the telescope beam used for the observations. The result is a beam-diluted signal that reduces the intensity of the observed emission. Calculations that do not account for beam dilution would therefore underpredict the column density of a compact source. The beam filling correction factor, B, is given by Equation (13), where θ_s and θ_b are the circular Gaussian sizes of the source and the half-power telescope beam, respectively

$$B = \frac{\theta_s^2}{\theta_s^2 + \theta_b^2}. \quad (13)$$

By inspection, B approaches unity as the source size exceeds (fills) the beam size. Often, for single-dish observations where no reasonable a priori assumption can be made regarding the underlying source structure, the emission is assumed to "fill the beam," and no correction for beam dilution is performed.

A related issue, not explicitly accounted for in these calculations, is the loss of sensitivity in interferometric observations to extended emission as a function of increasing spatial resolution. The magnitude of this effect is often determined by comparing the total flux observed with a single-dish telescope beam that is assumed or known to contain all of the emission to that recovered by the interferometer. If the interferometric observations display significantly lower flux, meaning that it has been resolved out, a correction can be made to any column density calculations if the total column (and not just that of the compact sources resolved by the array) is desired.

Table 12
Approximate Line Density in Molecular Surveys of Sgr B2(N) at Different Frequencies

Source	Frequency	Line Density	
		Frequency Space	Velocity Space
PRIMOS	20 GHz	1 per 10 MHz	1 per 150 km s^{-1}
IRAM	100 GHz	1 per 10 MHz	1 per 30 km s^{-1}
NRAO 12 m	150 GHz	1 per 10 MHz	1 per 20 km s^{-1}
CSO	275 GHz	1 per 10 MHz	1 per 10 km s^{-1}

A.9. Background Continuum

The background continuum, T_{bg}, against which molecules absorb plays a crucial role in the overall intensity of the detected molecular signal. While the fractional absorption seen for a molecular transition is constant with column density, the absolute observed signal is of course dependent on the magnitude of the background being absorbed against. Thus, even a large population will present a small signal against a weak background, while, conversely, a very small population can be detected if T_{bg} is large. The background temperature also affects the intensity of emission lines, with the effect of reducing the overall ΔT_A that is observed.

A.10. Frequency-dependent Line Shapes

In interstellar observations, the width of a spectral line is defined, in the non-relativistic limit, in Equation (14), where ΔV is the velocity line width (km s^{-1}), $\Delta\nu$ is the width of the line in frequency space (MHz), ν_0 is the reference frequency (typically the central line frequency; MHz), and c is the speed of light (km s^{-1}):

$$\Delta V = \frac{\Delta\nu}{\nu_0} c. \quad (14)$$

The velocity width of a line is frequency-independent; it is a physical effect of the source.[9] Because ΔV is therefore constant, $\Delta\nu$ must increase with increasing ν_0. Thus, at higher frequencies, the lines are far broader in frequency space.

This has a somewhat subtle but profound effect on the ability to detect weak signals in sources with large degrees of molecular complexity. As a concrete example, we can consider the density of lines in observations of Sgr B2(N) taken at different frequencies from the centimeter through the submillimeter. These are tabulated in Table 12, and shown visually in Figure 27.[10]

[9] The uncertainty principle also dictates a quantum-mechanical width to every line, but in radioastronomical observations this is an immeasurably small contribution in almost all circumstances.

[10] References—PRIMOS: Neill et al. (2012); IRAM: Belloche et al. (2013), NRAO 12 m: Remijan et al. (2008b), CSO: McGuire et al. (2013b).

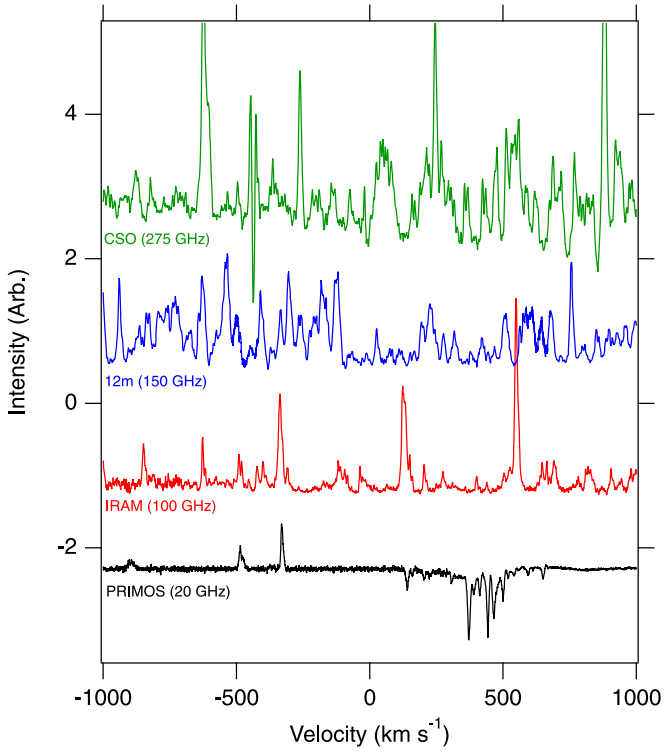

Figure 27. Comparison of observational data toward Sgr B2(N) at four different frequencies. The observations are plotted in velocity space, and the line widths are all quite similar (∼8–10 km s^{-1}).

Upon visual inspection, it is clear that in velocity space, the spectra are increasingly crowded at higher frequencies, even though the line density in frequency space remains the same. Indeed, at the highest frequencies, the spectra are nearly line-confusion-limited, a condition in which there is spectral line emission in every channel of the data. This issue sets in when the line density in velocity space becomes equal to the line width. Once a spectrum is line-confusion-limited, there is, to large extent, no additional information to be gained by deeper integration. All weaker lines from undetected molecules will be buried beneath the lines already visible, thus making it impractical to identify new, rare molecules.

It is important to note that the observations used here are just illustrative. They were taken with different facilities, having different beam sizes, and to different sensitivities. Still, the general trend does hold that lower frequency observations, while no less rich in molecular signals, have far more velocity space available to be filled with spectral lines. Indeed, of the observations shown here, those from PRIMOS at 20 GHz are the deepest and most sensitive (∼2 mK), but still have the lowest line density. Thus, even once line-confusion is reached in a source at millimeter and submillimeter frequencies, substantial discovery space often remains at centimeter wavelengths.

A.11. Partition Functions

The temperature-dependent partition function, $Q(T)$, for a molecule is a representation of the number of energy levels a population is spread out over. For astronomical purposes, $Q(T)$ is often comprised almost entirely of a rotational component, with small additional contributions from vibrational components (Equation (15))

$$Q = Q_{\rm v} \times Q_{\rm r}. \tag{15}$$

The rotational partition function, $Q_{\rm r}$, is often calculated according to a high-temperature approximation, given by Equation (16), where σ is a symmetry parameter, $T_{\rm ex}$ the excitation temperature (K), and A, B, and C, the rotational constants of the molecule (MHz), also as discussed earlier (c.f. Gordy & Cook 1984):

$$Q_{\rm r} = \left(\frac{5.34 \times 10^6}{\sigma}\right)\left(\frac{T_{\rm ex}^3}{ABC}\right)^{1/2}. \tag{16}$$

This approximation offers excellent values down to modestly low temperatures. Indeed, for most molecules, deviations from the explicitly calculated value do not reach 1% until $\leqslant$5 K. In cases where the temperature is low enough for this deviation to be significant, a direct summation of energy levels is required; this process is outlined in Gordy & Cook (1984). From inspection, it is also clear that larger, more complex molecules, with smaller rotational constants, will have a larger value of $Q_{\rm r}$. This is the same trend discussed earlier in a qualitative fashion. Finally, it is necessary to note that this approximation does not take into account many of the additional sources of complexity discussed earlier such as internal rotation and nuclear hyperfine splitting, which are not represented in the rotational constants A, B, and C. This can be addressed either through the addition of degeneracy terms, through explicit state counting, or a combination of both, as described in Gordy & Cook (1984).

The vibrational contribution, $Q_{\rm v}$, is given by Equation (17)

$$Q_{\rm v} = \prod_{i=1}^{3N-6} \frac{1}{1 - e^{-E_i/kT_{\rm ex}}}. \tag{17}$$

Here, the energies of each vibrational energy level E_i are considered. Only when $T_{\rm ex}$ is sufficiently high, and there are sufficiently low-lying vibrational states, does Q_v make any significant contribution. This correction factor accounts for the fact that the rotational energy level structure in an excited vibrational state is practically identical to that in the ground state. Thus, if some non-trivial population of molecules exist in a vibrationally excited state, those levels become accessible as well, spreading out intensity. Thus, the contribution to the total partition function Q from $Q_{\rm v}$ is multiplicative. Often the vibrational contribution is less than 1% up to at least 30–40 K, although it can be significant ($\geqslant$2) at warmer temperatures for some species. Strictly speaking, an electronic contribution Q_e may also be considered, but is almost never a factor in interstellar detections, at least with radio telescopes.

Generalized source types. Section 10 presented four generalized source types—SFRs, dark clouds, carbon stars, and LOS clouds—in which most detections have been made. The analysis there showed that the types of molecules that are detected for the first time in each of these environments tend to have distinct properties. Thus, the environment in which a molecular search is conducted can have a significant impact on the detectability from several standpoints. These include total abundance (related to chemistry and density), excitation temperature (density and kinetic temperature), line width and spectral crowding (turbulent versus quiescent regions), and source size (beam dilution). Below, five of the common types

of environments for these searches are described. While this is by no means an exhaustive list, it covers a large range in physical and chemical conditions, and provides a grounding in the factors that must be considered and can be applied to other situations.

A.12. Diffuse (LOS) Clouds

The first detections of interstellar molecules (CH, CH^+, and CN) were made in the LOS diffuse clouds that pervade the Galaxy (Swings & Rosenfeld 1937; McKellar 1940; Douglas & Herzberg 1941). While much of the molecular discovery quickly shifted to SFRs, dark clouds, and carbon stars, new detections in diffuse environments do still occur (see, e.g., the detection of SH by Neufeld et al. 2012).

These environments are characterized by low total number densities ($n_H \sim 10 - < 10^4$ cm^{-3}), cool, but not cold kinetic temperatures ($T_k < 100$ K), and enhanced radiation environments over those seen in "standard" dense molecular clouds (for a detailed review, see Snow & McCall 2006). The excitation temperature of most molecules observed in these clouds is extremely sub-thermal at T_{ex} ~3 K, with the population largely distributed over only the few lowest rotational energy levels. Most sources show moderately to extremely broad spectral absorption features (3–20 km s^{-1}; Corby et al. 2018). The width of the features tends to correspond to the density and compactness of the absorbing gas, with narrow features arising from denser, more compact sources.

The overall angular size of a distinct cloud can vary significantly with distance, but is typically assumed to be larger than the continuum against which it is observed, and is thus at least modestly extended (>10″). While the general assumption is that the gas is homogeneously distributed across the cloud, there is growing evidence that there may be significant substructure within each complex (Corby et al. 2018). This can lead to regions of increased density, and decreased temperature and radiation effects.

These physical conditions put constraints on the type and extent of complex chemistry that can occur in these regions. The harsh radiation environment largely prevents a build up of the icy dust grain layers thought to be needed to make many complex species, although there is some recent evidence showing surprising chemical complexity (Thiel et al. 2017), and the overall low number density results in difficulties achieving detectable abundances of molecules. Many of the new species detected in these environments are small, simpler precursor molecules that have often reacted away to form more complex molecules in other, more evolved sources.

A.13. Dark Clouds

The prototypical dark cloud is TMC-1, a largely homogeneous, extended (>60″), cold (T_{kin} ~10 – 20 K), and modestly dense ($n_H \sim 10^4$ cm^{-3}) source (Bell et al. 1998; Hincelin et al. 2011; Liszt & Ziurys 2012) with extremely narrow line widths (~0.3 km s^{-1}; McGuire et al. 2017a). The higher density compared to diffuse clouds (with correspondingly high extinction) shields the source, and allows the formation of ices on the surfaces of dust grains. While saturated COMs may evolve on these surfaces, the cold kinetic temperatures and quiescent environment tend to force these species to remain on the surface. As a result, the (detectable) gas-phase inventory tends to be dominated by complex, unsaturated organic molecules formed by gas-phase reactions, typically long-chain carbon molecules like the cyanopolyynes (HC_nN; n = 3, 5, 7, 9). As discussed in Appendix A.1, these larger molecules will tend to have more transitions at lower frequencies. At the temperatures in these sources, the Boltzmann peak will tend to fall at low frequencies as well, and has a favorable effect on the otherwise very large partition function (Appendix A.11). Thus, these regions tend to see a particularly pronounced number of detections of large, unsaturated molecules at frequencies below ~100 GHz. Because of the narrow velocity widths, line blending is rarely an issue.

A.14. Star-forming Regions

Upon gravitational collapse, dense molecular clouds begin to form molecular cores: compact, warm ($T_{kin} > 100$ K), and dense ($n_H \sim 10^5$–10^8 cm^{-3}) sources, often associated with a nascent star. In these regions, as the icy surfaces of the dust grains are heated, or are subjected to shocks, the complex molecular inventories are liberated into the gas phase and become detectable with radio astronomy. As was shown in Section 10, these molecules tend to be more saturated than those seen in dark clouds. Furthermore, the molecules formed on these surfaces tend to be highly reactive, and can then interact with the previously (largely) isolated gas-phase inventory from the dense cloud stage, depleting those abundances. The more complex physical environment, including transient events such as shocks and longer-term interactions from protostellar outflows, inject additional energy into the system, driving chemistry not otherwise possible under cooler, more quiescent conditions (Burkhardt et al. 2016).

The higher densities tend to thermalize the excitation temperatures, pushing the distributions toward LTE. Single-dish observations of these cores typically fail to resolve a single sub-source, resulting in modestly broad line widths (5–15 km s^{-1}; see, e.g., Widicus Weaver et al. 2017). Interferometric observations in these regions, however, can often isolate individual cores, significantly narrowing the line widths to a few km s^{-1} (Belloche et al. 2016). The large abundances and warm temperatures often result in spectra rapidly approaching (or having reached) line confusion in the millimeter and submillimeter regimes with modern facilities, both single-dish and interferometric.

A.15. Evolved (Carbon) Stars

While complex chemistry in the ISM is dominated by carbon, a number of exotic—by interstellar standards—species are also seen in evolved star sources, the definition of which is expanded here to include oxygen-rich stars. Indeed, every detected molecule with six or more atoms contains a carbon atom; the largest molecule detected without a carbon atom is SiH_4, which was first detected (perhaps ironically) in the evolved carbon-rich star IRC+10216 (Goldhaber & Betz 1984). The intense physical environments of sources like IRC+10216 and the hypergiant VY Canis Majoris inject heavier atoms like Si, as well as Mg, Fe, Ti, and Al into the gas phase, where they can be detected as components of molecules such as SiH_4, MgCN, FeCN, TiO_2, and AlOH (Ziurys et al. 1995; Tenenbaum & Ziurys 2010; Zack et al. 2011; Kamiński et al. 2013). While the circumstellar envelope around the stars themselves is compact, molecular

Table 13
Attributes of HC_5S and Their Effects on Detectability

HC_5S …	Effects
… is prolate	Most ISM molecules are prolate or near-prolate—high symmetry reduces Q, generally increasing line intensity
… is highly unsaturated	Highly unsaturated molecules tend to be first detected in carbon stars and dark clouds
… has two added sources of spectral complexity (Λ-doubling and resolvable ^{1}H splitting)	Q will be increased and the line intensities decreased if the splitting is resolved in observations
… has a rotational constant of ∼876 MHz	The primary rotational transitions will occur at low frequency (cm-wavelengths)
… has no low-lying structural conformers	Nearly all the population will be in the ground-state conformer - no decrease in its line intensities

emission is often seen in an extended distribution around the star itself (Cernicharo et al. 2013a). The physical conditions change as a function of distance from the star, often in a measurable manner, providing the opportunity to study, for example, dust evolutionary processes within the ISM using a single source (Cernicharo et al. 2011). Line confusion is rarely an issue in these sources.

Bringing it all together. With these tools in hand, and the trends and statistics discussed in Section 10, it is possible to make some informed guesses about the likely environments, facilities, and frequency ranges needed to detect a potential interstellar molecule. The thought process for two such example cases, HC_5S and *n*-propanol ($CH_3CH_2CH_2OH$), is outlined below. These discussions presume that the chemistry and elemental abundances in the ISM are favorable enough to produce at least some abundance of a species.

A.16. Searching for HC_5S

HC_5O (Section 3.164) was recently detected in the ISM in observations of TMC-1 at centimer-wavelengths with the GBT. Having often similar bonding characteristics with oxygen and being isovalent, it's logical to assume the S-substituted versions of O-containing compounds may be good interstellar candidates (e.g., CH_3OH/CH_3SH, C_3O/C_3S, SiO/SiS). The rotational spectrum of HC_5S is known (Gordon et al. 2002). Table 13 below lists a few key considerations for the molecule, and the corresponding effects on its likely detectability.

Given the highly unsaturated and C-rich nature of HC_5S, it is reasonable to expect that a carbon star or dark cloud are the most likely places for a detection (Section 10.4). The molecule is to zeroth-order a linear rotor, and so will have a relatively simple spectrum. The Λ-doubling splitting is a few MHz and the ^{1}H splitting ∼0.5 MHz for the lowest of its centimeter-wave transitions. The ^{1}H splitting quickly collapses, while the Λ-doubling splitting remains. These splittings translate to as little as 1 km s^{-1} (^{1}H) to as much as 250 km s^{-1} (Λ-doubling) across the centimeter-wave region (where the small B constant dictates most transitions will fall). In a carbon star source such as IRC+10216, line widths >10 km s^{-1} are routine, and thus only the Λ-doubling is likely to be resolved; the ^{1}H contribution (and reduction in line intensity) could be ignored. In a dark cloud, where line widths can be as little as 0.1 km s^{-1}, both splittings are in play. Molecules detected in carbon stars tend to be modestly warm (>50 K), increasing Q and decreasing line intensities by a factor of ∼6 over molecules at the temperatures typical of dark clouds (5–15 K).

Carbon star search. For a detection experiment toward a carbon star, the broader line widths, and accompanying unresolved hyperfine structure, may slightly offset the increased value of Q. The small B value likely necessitates a centimeter-wave observation. Molecules in these sources are seen both in extended emission in the expanding envelope and surrounding gas, and in compact emission near the star (Cernicharo et al. 2013a), thus a combined search with both an interferometer and a single-dish facility may be required.

Dark cloud search. For a detection experiment toward a dark cloud, the very narrow line widths will likely resolve much of the hyperfine structure, reducing the overall intensity. The decreased value of Q at low temperatures may help offset this, but nevertheless a high sensitivity will likely be required in narrow spectral channels and high resolution, indicating long integration times. At these even lower temperatures, observations in the centimeter-wave are more or less mandatory. Molecules in these sources tend to be quite extended, and thus interferometers will resolve out most signal, requiring a single-dish facility to observe.

Verdict? A search in either a carbon star or a dark cloud would seem logical, given the unsaturated nature of the molecule. Insight from a chemical model as to an approximate abundance may help to break the tie. Any search will need to be done at cm-wavelengths, and given that both source types likely require a single-dish measurement, that would seem a logical place to start.

A.17. Searching for $CH_3CH_2CH_2OH$

The detections of methanol (CH_3OH; Section 3.135) and ethanol (CH_3CH_2OH; Section 3.178), along with their large abundances, makes the next largest fully saturated alcohol, propanol ($CH_3CH_2CH_2OH$) a logical target, and it has indeed been recently searched for without success (Müller et al. 2016). The rotational spectrum of $CH_3CH_2CH_2OH$ is known (Kisiel et al. 2010). Table 14 below lists a few key considerations for the molecule, and the corresponding effects on its likely detectability.

The fully saturated nature of the molecule suggests SFRs and LOS clouds are the most likely sources for detection, but the size of the molecule strongly favors SFRs (Section 10.4). The line widths in these sources are modest depending on whether single-dish or array observations are used (∼1–5 km s^{-1}), but these are far broader than the expected internal rotor splitting, so this should not greatly affect the observations. The temperature in these sources, however, is often quite warm (80–300 K). This can non-trivially populate both the low-lying vibrational states of the lowest energy conformer, but also populate the other conformers of the molecule as well, all with cumulative decreases in the population of the lowest conformer

Table 14
Attributes of $CH_3CH_2CH_2OH$ and Their Effects on Detectability

$CH_3CH_2CH_2OH$ …	Effects
… is nearly prolate ($\kappa = -0.84$)	Most ISM molecules are prolate or near-prolate—high symmetry reduces Q, generally increasing line intensity
… is fully saturated	Fully saturated molecules are most commonly observed in SFRs and LOS clouds
… is large (12 atoms, 60 amu)	Large molecules are rarely found in LOS clouds, and have large partition functions
… has an internal methyl rotor	Q will be increased and the line intensities decreased if the splitting is resolved in observations
… has modest rotational constants (5–10 GHz)	The primary rotational transitions will occur in the mm- and lower sub-mm wavelength ranges
… has five structural conformers	Some population may be spread out into these other conformers, reducing the overall intensity of the main conformer's lines
… has low-lying vibrational states	The contribution of these states to Q is likely to be non-trivial

in its ground vibrational state. At these temperatures, the strongest transitions will fall around 200 GHz, and will extend into the submillimeter.

Verdict? Given the expected low line intensity due to the large partition function and the existence of multiple low-lying vibrational states and conformers, individual lines are expected to be quite weak. At (sub)millimeter-wavelengths, single-dish spectra of SFRs are often line-confusion-limited, making the identification of weak features challenging. The compact nature of these sources also causes single-dish observations to suffer from beam dilution effects. Interferometric observations are likely better suited to these observations, as they generally result in narrower line widths that permit the observation of weaker lines before line-confusion sets in. Choosing a target SFR that is on the cooler side would help push the population toward the ground vibrational state and lowest-energy conformer.

Appendix B
Python 3 Script

As supplemental information, a Python 3 script containing nearly all of the data presented here is available. The file hosted by the Journal is a snapshot of the script at time of submission. A live version is accessible at https://github.com/bmcguir2/astromolecule_census. The preamble of the script contains a substantial block of text outlining the capabilities, restrictions, and cautions for use. Here, a few simple possible use cases are outlined.

The code is intended for use in an interactive Python 3 environment. It has been tested in IPython 6.1.0 using Python 3.6.3. It may work in other Python environments as well, potentially with some minor customization. It is unlikely to readily work in Python 2.7, and is in fact hard-coded to exit if it detects Python 2.7 in use.

The entirety of the information content of the script is contained in the `Molecule` and `Source` custom classes. The `Molecule` class has 53 non-trivial attributes, while the `Source` class has 6. Not all attributes are required, and many are not currently in use, but are in place for future development. The default value for most is `None`.

Many utility functions are included with the script. Depending on when in development they were written, several functions may do the same thing as part of their execution in several different ways. Some are still in development, may not be fully implemented, or may need additional manipulation of their output before it is useful for its intended purpose. Users are strongly encouraged to read a function carefully before using, or to write their own.

The `summary(y)` function returns nearly the entire database's worth of information for a `Molecule` or `Source` `y`. For example, issuing

≫ `summary(CO)`

produces the output shown in Figure 28 for the databases entry for carbon monoxide (CO). Similarly, for a source like IRC+10216, issuing

≫ `summary(IRC10216)`

produces the output shown in Figure 29.

The script contains hard-coded python lists that contain all molecules and all sources, with variable names of `full_list` and `source_tag_list`, respectively. These can be iterated over to find molecules or sources that satisfy a desired set of conditions. For example, to find all molecules containing sulfur that were first detected in Sgr B2, the loop below could be used.

```
for x in full_list:
 if x.S > 0 and ''Sgr B2'' in x.sources:
  print(x.formula)
```

```
--------------------
carbon monoxide (CO)
--------------------

Atoms:  2
Mass:   28 amu
Year Detected:  1970
Source(s):      Orion
Telescope(s) Used:      NRAO 36-ft
Attributes:     Neutral

Also Detected In:       Ices, Protoplanetary Disks, External Galaxies, Exoplanetary Atmospheres

Sources of External Galaxy Detections:  M82, NGC 253

Isotopologues Also Detected in Protoplanetary Disks:    13CO, C18O, C17O

Detection Reference(s)
[1] Wilson et al. 1970 ApJ 161, L43

Laboratory Reference(s)
[1] Cord et al. 1968 Microwave Spectral Tables V5

Ice Reference(s)
[Det] Soifer et al. 1979 ApJ 232, L53
[Lab] Mantz et al. 1975 JMS 57, 155

Protoplanetary Disks Reference(s)
[CO] Beckwith et al. 1986 ApJ 309, 755
[13CO] Sargent & Beckwith 1987 ApJ 323, 294
[C18O] Dutrey et al. 1994 A&A 286, 149
[C17O] Smith et al. 2009 ApJ 701, 163; Guilloteau et al. 2013 A&A 549, A92

External Galaxies Reference(s)
[CO] Rickard et al. 1975 ApJ 199, L75

Exoplanetary Atmospheres Reference(s)
[CO] Madhusudhan et al. 2011 Nature 469, 64; Barman et al. 2011 ApJ 733, 65; Lanotte et al. 2014 A&A 572, A73; Barman et al. 2015 ApJ 804, 61
```

Figure 28. Results of issuing the command `summary(CO)`.

```
---------
IRC+10216
---------

RA (J2000):     09:47:57.406
DEC (J2000):    +13:16:43.56

Generalized Type:       Carbon Star

Number of Detections:   51

Simbad URL:     http://simbad.u-strasbg.fr/simbad/sim-id?Ident=IRC%2B10216

------------------------------
Molecules Detected in IRC+10216
------------------------------
CS, SiS, NaCl, AlCl, KCl, AlF, SiC, CP, SiN, CN-, SiC2, C2S, C3, MgNC, NaC
N, MgCN, SiCN, AlNC, SiNC, HCP, CCP, KCN, FeCN, CCN, SiCSi, C2H2, C3N, l-C
3H, C3S, HC2N, SiC3, C3N-, PH3, HMgNC, C4H, SiH4, C5, SiC4, C4H-, C2H4, C5
H, H2C4, C5S, HC4N, C5N-, SiH3CN, C6H-, C7H, CH3SiH3, C8H, C8H-
```

Figure 29. Results of issuing the command `summary(IRC10216)`.

ORCID iDs

Brett A. McGuire https://orcid.org/0000-0003-1254-4817

References

Adams, W. S. 1941, ApJ, 93, 11
Agúndez, M., Cernicharo, J., De Vicente, P., et al. 2015a, A&A, 579, L10
Agúndez, M., Cernicharo, J., Decin, L., Encrenaz, P., & Teyssier, D. 2014a, ApJL, 790, L27
Agúndez, M., Cernicharo, J., & Guélin, M. 2007, ApJL, 662, L91
Agúndez, M., Cernicharo, J., Guélin, M., et al. 2010, A&A, 517, L2
Agúndez, M., Cernicharo, J., & Guélin, M. 2014b, A&A, 570, A45
Agúndez, M., Cernicharo, J., & Guélin, M. 2015b, A&A, 577, L5
Agúndez, M., Cernicharo, J., Pardo, J. R., Guélin, M., & Phillips, T. G. 2008, A&A, 485, L33
Agúndez, M., Marcelino, N., & Cernicharo, J. 2018a, ApJL, 861, 0
Agúndez, M., Marcelino, N., Cernicharo, J., & Tafalla, M. 2018b, A&A, 611, L1
Ahrens, V., Lewen, F., & Takano, S. 2002, ZNatA, 57, 669
Aladro, R., Martín, S., Riquelme, D., et al. 2015, A&A, 579, A101
Alexander, A. J., Kroto, H. W., Maier, M., & Walton, D. R. M. 1978, JMoSp, 70, 84
Alexander, A. J., Kroto, H. W., & Walton, D. R. M. 1976, JMoSp, 62, 175
Allen, M. D., Ziurys, L. M., & Brown, J. M. 1996, CPL, 257, 130
Aller, L. H. 1966, PNAS, 55, 671
Altman, R. S., Crofton, M. W., & Oka, T. 1984, JChPh, 80, 3911
Amano, T. 2008, JChPh, 129, 244305
Amano, T., Amano, T., & Warner, H. E. 1991, JMoSp, 146, 519
Amano, T., Saito, S., Hirota, E., & Morino, Y. 1969, JMoSp, 32, 97
Amano, T., & Scappini, F. 1991, JChPh, 95, 2280
Anderson, J. K., Halfen, D. T., & Ziurys, L. M. 2015, JMoSp, 307, 1
Anderson, J. K., & Ziurys, L. M. 2014, ApJL, 795, L1
Anderson, M. A., Steimle, T. C., & Ziurys, L. M. 1994, ApJL, 429, L41
Apponi, A. J., Barclay, W. L. J., & Ziurys, L. M. 1993, ApJL, 414, L129
Apponi, A. J., McCarthy, M. C., Gottlieb, C. A., & Thaddeus, P. 1999a, ApJL, 516, L103
Apponi, A. J., McCarthy, M. C., Gottlieb, C. A., & Thaddeus, P. 1999b, JChPh, 111, 3911
Apponi, A. J., McCarthy, M. C., Gottlieb, C. A., & Thaddeus, P. 2000, ApJL, 536, L55
Araki, M., Furuya, T., & Saito, S. 2001, JMoSp, 210, 132
Arié, E., & Johns, J. W. C. 1992, JMoSp, 155, 195
Artur de la Villarmois, E., Kristensen, L. E., Jørgensen, J. K., et al. 2018, A&A, 614, A26
Avery, L. W., Broten, N. W., MacLeod, J. M., Oka, T., & Kroto, H. W. 1976, ApJL, 205, L173
Bailleux, S., Bogey, M., Demuynck, C., Liu, Y., & Walters, A. 2002, JMoSp, 216, 465
Baird, K. M., & Bredohl, H. 1971, ApJL, 169, L83
Baldacci, A., Ghersetti, S., & Rao, K. N. 1973, JMoSp, 48, 600
Ball, J. A., Gottlieb, C. A., Lilley, A. E., & Radford, H. E. 1970, ApJL, 162, L203
Barlow, M. J., Swinyard, B. M., Owen, P. J., et al. 2013, Sci, 342, 1343
Barman, T. S., Konopacky, Q. M., Macintosh, B., & Marois, C. 2015, ApJ, 804, 1
Barman, T. S., Macintosh, B., Konopacky, Q. M., & Marois, C. 2011, ApJ, 733, 65
Beckwith, S., Sargent, A. I., Scoville, N. Z., et al. 1986, ApJ, 309, 755
Beers, Y., & Howard, C. J. 1975, JChPh, 63, 4212
Bekooy, J. P., Verhoeve, P., Meerts, W. L., & Dymanus, A. 1985, JChPh, 82, 3868
Bell, M. B., Avery, L. W., & Feldman, P. A. 1993, ApJL, 417, L37
Bell, M. B., Feldman, P. A., Travers, M. J., et al. 1997, ApJL, 483, L61
Bell, M. B., Watson, J. K. G., Feldman, P. A., & Travers, M. J. 1998, ApJ, 508, 286
Bellet, J., Deldalle, A., Samson, C., Stenbeckeliers, G., & Wertheimer, R. 1971a, JMoSt, 9, 65
Bellet, J., Samson, C., Steenbeckliers, G., & Wertheimer, R. 1971b, JMoSt, 9, 49
Belloche, A., Garrod, R. T., Müller, H. S. P., et al. 2009, A&A, 499, 215
Belloche, A., Garrod, R. T., Müller, H. S. P., & Menten, K. M. 2014, Sci, 345, 1584
Belloche, A., Menten, K. M., Comito, C., et al. 2008, A&A, 482, 179
Belloche, A., Meshcheryakov, A. A., Garrod, R. T., et al. 2017, A&A, 601, A49
Belloche, A., Müller, H. S. P., Garrod, R. T., & Menten, K. M. 2016, A&A, 587, A91
Belloche, A., Müller, H. S. P., Menten, K. M., Schilke, P., & Comito, C. 2013, A&A, 559, A47
Benson, R. C., Flygare, W. H., Oda, M., & Breslow, R. 1973, JAChS, 95, 2772
Benz, A. O., Bruderer, S., van Dishoeck, E. F., et al. 2010, A&A, 521, L35
Bergin, E. A., Cleeves, L. I., Gorti, U., et al. 2013, Natur, 493, 644
Bergman, P., Parise, B., Liseau, R., et al. 2011, A&A, 531, L8
Bernard-Salas, J., Peeters, E., Sloan, G. C., et al. 2006, ApJL, 652, L29
Bernath, P. F. 2005, Spectra of Atoms and Molecules (2nd ed.; New York: Oxford Univ. Press)
Bernath, P. F., Hinkle, K. H., & Keady, J. J. 1989, Sci, 244, 562
Berné, O., Mulas, G., & Joblin, C. 2013, A&A, 550, L4
Betz, A. L. 1981, ApJL, 244, L103
Birk, M., Winnewisser, M., & Cohen, E. A. 1989, JMoSp, 136, 402
Bizzocchi, L., Thorwirth, S., Müller, H. S. P., Lewen, F., & Winnewisser, G. 2001, JMoSp, 205, 110
Blackman, G. L., Brown, R. D., Godfrey, P. D., & Gunn, H. I. 1976, Natur, 261, 395
Blake, G. A., Keene, J., & Phillips, T. G. 1985, ApJ, 295, 501
Blake, G. A., Sutton, E. C., Masson, C. R., et al. 1984, ApJ, 286, 586
Blake, G. A., van Dishoeck, E. F., & Sargent, A. I. 1992, ApJL, 391, L99
Blom, C. E., Grassi, G., & Bauder, A. 1984, JAChS, 106, 7427
Blukis, U., Kasai, P. H., & Myers, R. J. 1963, JChPh, 38, 2753
Bogey, M., Demuynck, C., Denis, M., & Destombes, J. L. 1985a, A&A, 148, L11
Bogey, M., Demuynck, C., & Destombes, J. L. 1984, A&A, 138, L11
Bogey, M., Demuynck, C., & Destombes, J. L. 1985b, JChPh, 83, 3703
Bogey, M., Demuynck, C., Destombes, J. L., & Vallee, Y. 1995, JMoSp, 172, 344
Bogey, M., Destombes, J. L., Vallee, Y., & Ripoll, J. L. 1988, CPL, 146, 227
Bogey, M., Dubus, H., & Guillemin, J. C. 1990, JMoSp, 143, 180
Boogert, A. C. A., Gerakines, P. A., & Whittet, D. C. B. 2015, ARA&A, 53, 541
Botschwina, P., & Oswald, R. 2008, JChPh, 129, 044305
Bouchy, A., Demaison, J., Roussy, G., & Barriol, J. 1973, JMoSt, 18, 211
Brazier, C. R., & Brown, J. M. 1983, JChPh, 78, 1608
Brewster, M. A., Apponi, A. J., Xin, J., & Ziurys, L. M. 1999, CPL, 310, 411
Brogan, C. L., Pérez, L. M., Hunter, T. R., et al. 2015, ApJL, 808, 1
Broten, N. W., MacLeod, J. M., Avery, L. W., et al. 1984, ApJL, 276, L25
Broten, N. W., MacLeod, J. M., Oka, T., et al. 1976, ApJL, 209, L143
Broten, N. W., Oka, T., Avery, L. W., MacLeod, J. M., & Kroto, H. W. 1978, ApJL, 223, L105
Brown, F. X., Saito, S., & Yamamoto, S. 1990, JMoSp, 143, 203
Brown, J. M., Curl, R. F., & Evenson, K. M. 1985a, ApJ, 292, 188
Brown, J. M., & Müller, H. S. P. 2009, JMoSp, 255, 68
Brown, R. D., Crofts, J. G., Gardner, F. F., et al. 1975a, ApJL, 197, L29
Brown, R. D., Eastwood, F. W., Elmes, P. S., & Godfrey, P. D. 1983, JAChS, 105, 6496
Brown, R. D., Godfrey, P. D., Cragg, D. M., et al. 1985b, ApJ, 297, 302
Brown, R. D., Godfrey, P. D., & Storey, J. 1975b, JMoSp, 58, 445
Brünken, S., Belloche, A., Martín, S., Verheyen, L., & Menten, K. M. 2010, A&A, 516, A109
Brünken, S., Gottlieb, C. A., McCarthy, M. C., & Thaddeus, P. 2009a, ApJ, 697, 880
Brünken, S., Gupta, H., Gottlieb, C. A., McCarthy, M. C., & Thaddeus, P. 2007, ApJL, 664, L43
Brünken, S., Kluge, L., Stoffels, A., Asvany, O., & Schlemmer, S. 2014, ApJL, 783, L4
Brünken, S., Müller, H. S. P., Menten, K. M., McCarthy, M. C., & Thaddeus, P. 2008, ApJ, 676, 1367
Brünken, S., Yu, Z., Gottlieb, C. A., McCarthy, M. C., & Thaddeus, P. 2009b, ApJ, 706, 1588
Buhl, D., & Snyder, L. E. 1970, Natur, 228, 267
Buhl, D., & Snyder, L. E. 1973, in Molecules in the Galactic Environment, ed. M. A. Gordon & L. E. Snyder (New York: Wiley), 187
Buhl, D., Snyder, L. E., & Edrich, J. 1972, ApJ, 177, 625
Burkhardt, A. M., Dollhopf, N. M., Corby, J. F., et al. 2016, ApJ, 827, 1
Burkholder, J. B., Howard, C. J., & McKellar, A. R. W. 1988, JMoSp, 127, 415
Butcher, S. S., & Wilson, E. B., Jr. 1964, JChPh, 40, 1671
Cabezas, C., Cernicharo, J., Alonso, J. L., et al. 2013, ApJ, 775, 133
Cameron, A. G. W. 1973, SSRv, 15, 121
Cami, J., Bernard-Salas, J., Peeters, E., & Malek, S. E. 2010, Sci, 329, 1180
Campbell, E. K., Holz, M., Gerlich, D., & Maier, J. P. 2015, Natur, 523, 322
Campbell, E. K., Holz, M., Maier, J. P., et al. 2016, ApJ, 822, 17

Carr, J. S., & Najita, J. R. 2008, Sci, 319, 1504
Carr, J. S., Tokunaga, A. T., & Najita, J. 2004, ApJ, 603, 213
Carrington, A., & Ramsay, D. A. 1982, PhyS, 25, 272
Carroll, P. B., McGuire, B. A., Blake, G. A., et al. 2015, ApJ, 799, 15
Carruthers, G. R., & Carruthers, G. R. 1970, ApJL, 161, L81
Cazzoli, G., & Puzzarini, C. 2006, JMoSp, 239, 64
Ceccarelli, C., Dominik, C., Caux, E., Lefloch, B., & Caselli, P. 2005, ApJL, 631, L81
Ceccarelli, C., Dominik, C., Lefloch, B., Caselli, P., & Caux, E. 2004, ApJL, 607, L51
Cernicharo, J., Agúndez, M., Kahane, C., et al. 2011, A&A, 529, L3
Cernicharo, J., Agúndez, M., Velilla Prieto, L., et al. 2017, A&A, 606, L5
Cernicharo, J., Bailleux, S., Alekseev, E., et al. 2014, ApJ, 795, 40
Cernicharo, J., Cernicharo, J., Guélin, M., & Guelin, M. 1987a, A&A, 183, L10
Cernicharo, J., Daniel, F., Castro-Carrizo, A., et al. 2013a, ApJL, 778, L25
Cernicharo, J., Goicoechea, J. R., & Caux, E. 2000, ApJL, 534, L199
Cernicharo, J., Gottlieb, C. A., Guélin, M., et al. 1991a, ApJL, 368, L39
Cernicharo, J., Gottlieb, C. A., Guélin, M., et al. 1991b, ApJL, 368, L43
Cernicharo, J., Gottlieb, C. A., Guélin, M., Thaddeus, P., & Vrtilek, J. M. 1989, ApJL, 341, L25
Cernicharo, J., & Guélin, M. 1996, A&A, 309, L27
Cernicharo, J., Guélin, M., Agúndez, M., et al. 2007, A&A, 467, L37
Cernicharo, J., Guélin, M., Agúndez, M., McCarthy, M. C., & Thaddeus, P. 2008, ApJL, 688, L83
Cernicharo, J., Guélin, M., Menten, K. M., & Walmsley, C. M. 1987b, A&A, 181, L1
Cernicharo, J., Guélin, M., & Pardo, J. R. 2004, ApJL, 615, L145
Cernicharo, J., Guélin, M., & Walmsley, C. M. 1987c, A&A, 172, L5
Cernicharo, J., Heras, A. M., Tielens, A. G. G. M., et al. 2001, ApJL, 546, L123
Cernicharo, J., Kahane, C., Gomez-Gonzales, J., & Guelin, M. 1986a, A&A, 167, L5
Cernicharo, J., Kahane, C., Gómez-González, J., & Guélin, M. 1986b, A&A, 164, L1
Cernicharo, J., Kahane, C., Guélin, M., & Gómez-González, J. 1988, A&A, 189, L1
Cernicharo, J., Kahane, C., Guélin, M., & Hein, H. 1987d, A&A, 181, L9
Cernicharo, J., Kisiel, Z., Tercero, B., et al. 2016, A&A, 587, L4
Cernicharo, J., Lefloch, B., Agúndez, M., et al. 2018, ApJL, 853, L22
Cernicharo, J., Liu, X. W., González-Alfonso, E., et al. 1997, ApJL, 483, L65
Cernicharo, J., Marcelino, N., Roueff, E., et al. 2012, ApJL, 759, L43
Cernicharo, J., McCarthy, M. C., Gottlieb, C. A., et al. 2015, ApJL, 806, L3
Cernicharo, J., Tercero, B., Fuente, A., et al. 2013b, ApJL, 771, L10
Champion, J. P., Hilico, J. C., Wenger, C., & Brown, L. R. 1989, JMoSp, 133, 256
Chapillon, E., Dutrey, A., Guilloteau, S., et al. 2012, ApJ, 756, 58
Charbonneau, D., Brown, T. M., Noyes, R. W., & Gilliland, R. L. 2002, ApJ, 568, 377
Charnley, S. B., Ehrenfreund, P., & Kuan, Y.-J. 2001, AcSpA, 57, 685
Charo, A., & De Lucia, F. C. 1982, JMoSp, 94, 426
Charo, A., Herbst, E., de Lucia, F. C., & Sastry, K. V. L. N. 1981, ApJL, 244, L111
Chen, W., Grabow, J. U., Travers, M. J., et al. 1998, JMoSp, 192, 1
Cheung, A. C., Rank, D. M., Townes, C. H., Thornton, D. D., & Welch, W. J. 1968, PhRvL, 21, 1701
Cheung, A. C., Rank, D. M., Townes, C. H., Thornton, D. D., & Welch, W. J. 1969, Natur, 221, 626
Chomiak, D., Taleb-Bendiab, A., Civis, S., & Amano, T. 1994, CaJPh, 72, 1078
Christen, D., Coudert, L. H., Suenram, R. D., & Lovas, F. J. 1995, JMoSp, 172, 57
Churchwell, E., & Winnewisser, G. 1975, A&A, 45, 229
Churchwell, E., Witzel, A., Huchtmeier, W., et al. 1977, A&A, 54, 969
Cleeton, C. E., & Williams, N. H. 1934, PhRv, 45, 234
Cochran, E. L., Adrian, F. J., & Bowers, V. A. 1964, JChPh, 40, 213
Combes, F., Gerin, M., Wootten, A., et al. 1987, A&A, 180, L13
Condon, J. J., & Ransom, S. J. 2016, Essential Radio Astronomy (Princeton, NJ: Princeton Univ. Press) 2016
Cooke, I. R., Fayolle, E. C., & Öberg, K. I. 2016, ApJ, 832, 5
Corby, J. F., McGuire, B. A., Herbst, E., & Remijan, A. J. 2018, A&A, 610, A10
Cord, M. S., Lojko, M. S., & Petersen, J. D. 1968, Microwave spectral tables (Washington, DC: Superintendent of Documents)
Cordiner, M. A., Charnley, S. B., Kisiel, Z., McGuire, B. A., & Kuan, Y.-J. 2017, ApJ, 850, 187
Cuadrado, S., Goicoechea, J. R., Roncero, O., et al. 2016, A&A, 596, L1
Cummins, S. E., Linke, R. A., & Thaddeus, P. 1986, ApJS, 60, 819
Cunningham, M. R., Jones, P. A., Godfrey, P. D., et al. 2007, MNRAS, 376, 1201
Cupp, R. E., Kempf, R. A., & Gallagher, J. J. 1968, PhRv, 171, 60
Decin, L., Danilovich, T., Gobrecht, D., et al. 2018, ApJ, 855, 113
De Luca, M., Gupta, H., Neufeld, D., et al. 2012, ApJL, 751, L37
De Lucia, F. C., Helminger, P., & Gordy, W. 1971, PhRvA, 3, 1849
Delucia, F., & Gordy, W. 1969, PhRv, 187, 58
Demaison, J., Boucher, D., BURIE, J., & Dubrulle, A. 1984, ZNatA, 39, 560
Deming, D., Wilkins, A., McCullough, P., et al. 2013, ApJ, 774, 95
de Zafra, R. L. 1971, ApJ, 170, 165
D'Hendecourt, L. B., & Allamandola, L. J. 1986, A&AS, 64, 453
D'Hendecourt, L. B., & Jourdain de Muizon, M. 1989, A&A, 223, L5
Dickens, J. E., Irvine, W. M., Nummelin, A., et al. 2001a, AcSpA, 57, 643
Dickens, J. E., Irvine, W. M., Nummelin, A., et al. 2001b, AcSpA, 57, 643
Dickens, J. E., Irvine, W. M., Ohishi, M., et al. 1997, ApJ, 489, 753
Dickinson, D. F. 1972, ApL, 12, 235
Dixon, R. N. 1959, CaJPh, 37, 1171
Dixon, T. A., & Woods, R. C. 1975, PhRvL, 34, 61
Dixon, T. A., & Woods, R. C. 1977, JChPh, 67, 3956
Domenech, J. L., Cueto, M., Herrero, V. J., et al. 2013, ApJL, 771, L11
Douglas, A. E., & Herzberg, G. 1941, ApJ, 94, 381
Drouin, B. J., Yu, S., Miller, C. E., et al. 2010, JQSRT, 111, 1167
Duley, W. W., & Hu, A. 2012, ApJL, 745, L11
Dunham, T. J. 1937, PASP, 49, 26
Dutrey, A., Guilloteau, S., & Guélin, M. 1997, A&A, 317, L55
Dutrey, A., Guilloteau, S., & Simon, M. 1994, A&A, 286, 149
Dutrey, A., Henning, T., Guilloteau, S., et al. 2007, A&A, 464, 615
Ehrenfreund, P., Boogert, A. C. A., Gerakines, P. A., Tielens, A. G. G. M., & van Dishoeck, E. F. 1997, A&A, 328, 649
Ehrenstein, G., Townes, C. H., & Stevenson, M. J. 1959, PhRvL, 3, 40
Endo, Y., & Hirota, E. 1987, JChPh, 86, 4319
Endo, Y., & Mizushima, M. 1982, JaJAP, 21, L379
Endo, Y., Saito, S., & Hirota, E. 1984, JChPh, 81, 122
Erickson, N. R., Snell, R. L., Loren, R. B., Mundy, L., & Plambeck, R. L. 1981, ApJL, 245, L83
Fabian, J. 1996, PhRvB, 53, 13864
Faure, A., Remijan, A. J., Szalewicz, K., & Wiesenfeld, L. 2014, ApJ, 783, 72
Favre, C., Fedele, D., Semenov, D., et al. 2018, ApJL, 862, L2
Fayolle, E. C., Öberg, K. I., Jørgensen, J. K., et al. 2017, NatAs, 1, 703
Fedoseev, G., Cuppen, H. M., Ioppolo, S., Lamberts, T., & Linnartz, H. 2015, MNRAS, 448, 1288
Feuchtgruber, H., Helmich, F. P., van Dishoeck, E. F., & Wright, C. M. 2000, ApJL, 535, L111
Flory, M. A., & Ziurys, L. M. 2011, JChPh, 135, 184303
Fortenberry, R. C., Huang, X., Crawford, T. D., & Lee, T. J. 2013, ApJ, 772, 39
Fortman, S. M., McMillan, J. P., Neese, C. F., et al. 2012, JMoSp, 280, 11
Fourikis, N., Sinclair, M. W., Robinson, B. J., Godfrey, P. D., & Brown, R. D. 1974a, AuJPh, 27, 425
Fourikis, N., Takagi, K., & Morimoto, M. 1974b, ApJL, 191, L139
Frerking, M. A., Linke, R. A., & Thaddeus, P. 1979, ApJL, 234, L143
Friberg, P., Hjalmarson, Å., Guélin, M., & Irvine, W. M. 1980, ApJL, 241, L99
Friesen, R. K., Medeiros, L., Schnee, S., et al. 2013, MNRAS, 436, 1513
Fuchs, G. W., Fuchs, U., Giesen, T. F., & Wyrowski, F. 2005, A&A, 444, 521
Fuchs, U., Winnewisser, G., Groner, P., De Lucia, F. C., & Herbst, E. 2003, ApJS, 144, 277
Fuente, A., Cernicharo, J., Agúndez, M., et al. 2010, A&A, 524, A19
Fuente, A., García-Burillo, S., Gerin, M., et al. 2006, ApJL, 641, L105
Fuente, A., Goicoechea, J. R., Pety, J., et al. 2017, ApJL, 851, L49
Furuya, R. S., Walmsley, C. M., Nakanishi, K., Schilke, P., & Bachiller, R. 2003, A&A, 409, L21
Gallagher, J. J., & Johnson, C. M. 1956, PhRv, 103, 1727
García-Burillo, S., Martin-Pintado, J., Fuente, A., Usero, A., & Neri, R. 2002, ApJL, 575, L55
Gardner, F. F., & Whiteoak, J. B. 1974, Natur, 247, 526
Gardner, F. F., & Winnewisser, G. 1975, ApJL, 195, L127
Garrod, R. T., Weaver, S. L. W., & Herbst, E. 2008, ApJ, 682, 283
Gausset, L., Herzberg, G., Lagerqvist, A., & Rosen, B. 1965, ApJ, 142, 45
Geballe, T. R., Goto, M., Usuda, T., Oka, T., & McCall, B. J. 2006, ApJ, 644, 907
Geballe, T. R., & Oka, T. 1996, Natur, 384, 334
Gerin, M., De Luca, M., Black, J., et al. 2010, A&A, 518, L110
Gerry, M. C. L., Stroh, F., & Winnewisser, M. 1990, JMoSp, 140, 147
Gerry, M. C. L., & Winnewisser, G. 1973, JMoSp, 48, 1

Gibb, E. L., & Horne, D. 2013, ApJL, 776, L28
Gillett, F. C., & Forrest, W. J. 1973, ApJ, 179, 483
Godfrey, P. D., Brown, R. D., Robinson, B. J., & Sinclair, M. W. 1973, ApL, 13, 119
Golden, S., Wentink, T., Hillger, R., & Strandberg, M. W. 1948, PhRv, 73, 92
Goldhaber, D. M., & Betz, A. L. 1984, ApJL, 279, L55
Goldsmith, P. F., Krotkov, R., Snell, R. L., Brown, R. D., & Godfrey, P. 1983, ApJ, 274, 184
Goldsmith, P. F., & Langer, W. D. 1999, ApJ, 517, 209
Goldsmith, P. F., Li, D., Bergin, E. A., et al. 2002, ApJ, 576, 814
Goldsmith, P. F., Liseau, R., Bell, T. A., et al. 2011, ApJ, 737, 96
González-Alfonso, E., Fischer, J., Bruderer, S., et al. 2013, A&A, 550, A25
González-Alfonso, E., Smith, H. A., Fischer, J., & Cernicharo, J. 2004, ApJ, 613, 247
Gordon, V. D., McCarthy, M. C., Apponi, A. J., & Thaddeus, P. 2001, ApJS, 134, 311
Gordon, V. D., McCarthy, M. C., Apponi, A. J., & Thaddeus, P. 2002, ApJS, 138, 297
Gordy, W., & Cook, R. L. 1984, Microwave Molecular Spectra (3rd ed.; New York: Wiley)
Goss, W. M. 1966, ApJ, 145, 707
Gottlieb, C. A. 1973, in Molecules in the Galactic Environment, ed. M. A. Gordon & L. E. Snyder (New York: John Wiley and Sons), 181
Gottlieb, C. A., Apponi, A. J., McCarthy, M. C., Thaddeus, P., & Linnartz, H. 2000, JChPh, 113, 1910
Gottlieb, C. A., & Ball, J. A. 1973, ApJL, 184, L59
Gottlieb, C. A., Ball, J. A., Gottlieb, E. W., Lada, C. J., & Penfield, H. 1975, ApJL, 200, L147
Gottlieb, C. A., Gottlieb, E. W., & Thaddeus, P. 1986, A&A, 164, L5
Gottlieb, C. A., Gottlieb, E. W., Thaddeus, P., & Kawamura, H. 1983, ApJ, 275, 916
Gottlieb, C. A., Vrtilek, J. M., Gottlieb, E. W., Thaddeus, P., & Hjalmarson, Å. 1985, ApJL, 294, L55
Gottlieb, C. A., Vrtilek, J. M., & Thaddeus, P. 1989, ApJL, 343, L29
Graham, W. R. M., Dismuke, K. I., & Weltner, W., Jr. 1974, JChPh, 60, 3817
Gratier, P., Pety, J., Guzmán, V., et al. 2013, A&A, 557, A101
Green, S., A, J., Montgomery, J., & Thaddeus, P. 1974, ApJL, 193, L89
Green, S., Schor, H., Siegbahn, P., & Thaddeus, P. 1976, CP, 17, 479
Grim, R. J. A., Baas, F., Geballe, T. R., Greenberg, J. M., & Schutte, W. 1991, A&A, 243, 473
Gudeman, C. S., Haese, N. N., Piltch, N. D., & Woods, R. C. 1981, ApJL, 246, L47
Gudeman, C. S., & Woods, R. C. 1982, PhRvL, 48, 1344
Guélin, M., & Cernicharo, J. 1991, A&A, 244, L21
Guélin, M., Cernicharo, J., Kahane, C., & Gomez-Gonzales, J. 1986, A&A, 157, L17
Guélin, M., Cernicharo, J., Paubert, G., & Turner, B. E. 1990, A&A, 230, L9
Guélin, M., Cernicharo, J., Travers, M. J., et al. 1997, A&A, 317, L1
Guélin, M., Green, S., & Thaddeus, P. 1978, ApJL, 224, L27
Guélin, M., Muller, S., Cernicharo, J., et al. 2000, A&A, 363, L9
Guélin, M., Muller, S., Cernicharo, J., McCarthy, M. C., & Thaddeus, P. 2004, A&A, 426, L49
Guélin, M., Neininger, N., & Cernicharo, J. 1998, A&A, 335, L1
Guélin, M., & Thaddeus, P. 1977, ApJL, 212, L81
Guillemin, J. C., Wlodarczak, G., López, J. C., & Demaison, J. 1990, JMoSp, 140, 190
Guilloteau, S., Di Folco, E., Dutrey, A., et al. 2013, A&A, 549, A92
Guilloteau, S., Dutrey, A., Wakelam, V., et al. 2012, A&A, 548, A70
Guilloteau, S., Piétu, V., Dutrey, A., & Guélin, M. 2006, A&A, 448, L5
Gunther-Mohr, G. R., White, R. L., Schawlow, A. L., Good, W. E., & Coles, D. K. 1954, PhRv, 94, 1184
Gupta, H., Brünken, S., Tamassia, F., et al. 2007, ApJL, 655, L57
Gupta, H., Drouin, B. J., & Pearson, J. C. 2012, ApJL, 751, L38
Gupta, H., Gottlieb, C. A., Lattanzi, V., Pearson, J. C., & McCarthy, M. C. 2013, ApJL, 778, L1
Guzmán, V. V., Öberg, K. I., Loomis, R., & Qi, C. 2015, ApJ, 814, 53
Haas, S., Winnewisser, G., Yamada, K. M. T., Matsumura, K., & Kawaguchi, K. 1994, JMoSp, 167, 176
Habara, H., & Yamamoto, S. 2000, JChPh, 112, 10905
Habara, H., Yamamoto, S., & Amano, T. 2002, JChPh, 116, 9232
Halfen, D. T., Clouthier, D. J., & Ziurys, L. M. 2008, ApJL, 677, L101
Halfen, D. T., Ilyushin, V. V., & Ziurys, L. M. 2015, ApJL, 812, 1
Halfen, D. T., Ziurys, L. M., Brünken, S., et al. 2009, ApJL, 702, L124
Hayashi, M., & Kuwada, K. 1975, JMoSt, 28, 147
Haynes, K., Mandell, A. M., Madhusudhan, N., Deming, D., & Knutson, H. 2015, ApJ, 806, 146
Heath, G. A., Thomas, L. F., Sherrard, E. I., & Sheridan, J. 1955, Discussions of the Faraday Society, 19, 38
Heikkilä, A., Johansson, L. E. B., & Olofsson, H. 1999, A&A, 344, 817
Heise, H. M., Lutz, H., & Dreizler, H. 1974, ZNatA, 29, 1345
Helminger, P., Bowman, W. C., & De Lucia, F. C. 1981, JMoSp, 85, 120
Henkel, C., & Bally, J. 1985, A&A, 150, L25
Henkel, C., Jacq, T., Mauersberger, R., Menten, K. M., & Steppe, H. 1987, A&A, 188, L1
Henkel, C., Mauersberger, R., & Schilke, P. 1988, A&A, 201, L23
Henning, T., Semenov, D., Guilloteau, S., et al. 2010, ApJ, 714, 1511
Herbst, E., & van Dishoeck, E. F. 2009, ARA&A, 47, 427
Hily-Blant, P., Magalhaes, V., Kastner, J., et al. 2017, A&A, 603, L6
Hincelin, U., Wakelam, V., Hersant, F., et al. 2011, A&A, 530, A61
Hinkle, K. W., Keady, J. J., & Bernath, P. F. 1988, Sci, 241, 1319
Hirose, C. 1974, ApJL, 189, L145
Hocking, W. H. 1976, ZNatA, 31, 1113
Hoeft, J. 1965, Zeitschrift für Naturforschung A, A20, 1327
Hogerheijde, M. R., Bergin, E. A., Brinch, C., et al. 2011, Sci, 334, 338
Hollis, J. M., Churchwell, E. B., Herbst, E., & de Lucia, F. C. 1986, Natur, 322, 524
Hollis, J. M., Jewell, P. R., & Lovas, F. J. 1989, ApJ, 346, 794
Hollis, J. M., Jewell, P. R., & Lovas, F. J. 1995, ApJ, 438, 259
Hollis, J. M., Jewell, P. R., Lovas, F. J., & Remijan, A. 2004a, ApJL, 613, L45
Hollis, J. M., Jewell, P. R., Lovas, F. J., Remijan, A., & Møllendal, H. 2004b, ApJL, 610, L21
Hollis, J. M., Lovas, F. J., & Jewell, P. R. 2000, ApJL, 540, L107
Hollis, J. M., Lovas, F. J., Jewell, P. R., & Coudert, L. H. 2002, ApJL, 571, L59
Hollis, J. M., Lovas, F. J., Remijan, A. J., et al. 2006a, ApJL, 643, L25
Hollis, J. M., Remijan, A. J., Jewell, P. R., & Lovas, F. J. 2006b, ApJ, 642, 933
Hollis, J. M., Snyder, L. E., Blake, D. H., et al. 1981, ApJ, 251, 541
Hollis, J. M., Snyder, L. E., Ziurys, L. M., & McGonagle, D. 1991, in ASP Conf. Ser. 16, Atoms, Ions and Molecules: New Results in Spectral Line Astrophysics (San Francisco, CA: ASP), 407
Hovde, D. C., & Saykally, R. J. 1987, JChPh, 87, 4332
Huang, J., & Öberg, K. I. 2015, ApJL, 809, L26
Huang, X., Fortenberry, R. C., & Lee, T. J. 2013, ApJL, 768, L25
Iida, M., Ohshima, Y., & Endo, Y. 1991, ApJL, 371, L45
Ikuta, S. 1997, JChPh, 106, 4536
Ilyushin, V. V., Alekseev, E. A., Dyubko, S. F., Kleiner, I., & Hougen, J. T. 2004, JMoSp, 227, 115
Ilyushin, V. V., Alekseev, E. A., Dyubko, S. F., Motiyenko, R. A., & Lovas, F. J. 2005, JMoSp, 231, 15
Irvine, W. M., Brown, R. D., Cragg, D. M., et al. 1988a, ApJL, 335, L89
Irvine, W. M., Friberg, P., Hjalmarson, Å., et al. 1988b, ApJL, 334, L107
Irvine, W. M., & Pollack, J. B. 1968, Icar, 8, 324
Jabs, W., Winnewisser, M., Belov, S., Klaus, T., & Winnewisser, G. 1997, CP, 225, 77
Jefferts, K. B., Penzias, A. A., & Wilson, R. W. 1970, ApJL, 161, L87
Jefferts, K. B., Penzias, A. A., Wilson, R. W., & Solomon, P. M. 1971, ApJL, 168, L111
Jenkins, F. A., & Wooldridge, D. E. 1938, PhRv, 53, 137
Jevons, W. 1932, Report on Band-spectra of Diatomic Molecules (London: Physical Society)
Johansson, L. E. B. 1991, in IAU Symp. 146, Dynamics of Galaxies and Their Molecular Cloud Distributions, ed. F. Combes & F. Casoli (Dordrecht: Kluwer), 1
Johns, J. W. C., Stone, J. M. R., & Winnewisser, G. 1972, JMoSp, 42, 523
Johnson, D. R., & Lovas, F. J. 1972, CPL, 15, 65
Johnson, D. R., Lovas, F. J., Gottlieb, C. A., et al. 1977, ApJ, 218, 370
Johnson, D. R., & Powell, F. X. 1970, Sci, 169, 679
Johnson, D. R., Suenram, R. D., & Lafferty, W. J. 1976, ApJ, 208, 245
Johnson, H. R., & Strandberg, M. W. P. 1952, JChPh, 20, 687
Jones, P. A., Cunningham, M. R., Godfrey, P. D., & Cragg, D. M. 2007, MNRAS, 374, 579
Kaifu, N., Morimoto, M., Nagane, K., et al. 1974, ApJL, 191, L135
Kaifu, N., Ohishi, M., Kawaguchi, K., et al. 2004, PASJ, 56, 69
Kaifu, N., Suzuki, H., Ohishi, M., et al. 1987, ApJL, 317, L111
Kamiński, T., Gottlieb, C. A., Menten, K. M., et al. 2013, A&A, 551, 113
Kania, P., Hermanns, M., Brünken, S., Müller, H. S. P., & Giesen, T. F. 2011, JMoSp, 268, 173
Kasai, P. H., & Myers, R. J. 1959, JChPh, 30, 1096
Kasai, Y., Obi, K., Ohshima, Y., et al. 1993, ApJL, 410, L45
Kasai, Y., Sumiyoshi, Y., Endo, Y., & Kawaguchi, K. 1997, ApJL, 477, L65
Kasten, W., & Dreizler, H. 1986, ZNatA, 41, 1173
Kastner, J. H., Zuckerman, B., Weintraub, D. A., & Forveille, T. 1997, Sci, 277, 67

Kaushik, V. K. 1977, CPL, 49, 89
Kawaguchi, K., Kagi, E., Hirano, T., Takano, S., & Saito, S. 1993, ApJL, 406, L39
Kawaguchi, K., Kasai, Y., Ishikawa, S.-I., et al. 1994, ApJL, 420, L95
Kawaguchi, K., Kasai, Y., & Ishikawa, S. I. 1995, PASJ, 47, 853
Kawaguchi, K., Ohishi, M., Ishikawa, S.-I., & Kaifu, N. 1992a, ApJL, 386, L51
Kawaguchi, K., Saito, S., & Hirota, E. 1983, JChPh, 79, 629
Kawaguchi, K., Saito, S., & Hirota, E. 1985, MolPh, 55, 341
Kawaguchi, K., Takano, S., Ohishi, M., et al. 1992b, ApJL, 396, L49
Kern, B., Strelnikov, D., Weis, P., Böttcher, A., & Kappes, M. M. 2013, JPCA, 117, 8251
Kessler, M., Ring, H., Trambarulo, R., & Gordy, W. 1950, PhRv, 79, 54
Kewley, R., Sastry, K. V. L. N., & Winnewisser, M. 1963, JMoSp, 10, 418
Kilb, R. W. 1955, JChPh, 23, 1736
Kilb, R. W., Lin, C. C., & Wilson, E. B., Jr. 1957, JChPh, 26, 1695
Killian, T. C., Gottlieb, C. A., Gottlieb, E. W., Vrtilek, J. M., & Thaddeus, P. 1990, ApJL, 365, L89
King, W. C., & Gordy, W. 1954, PhRv, 93, 407
Kirby, C., Kroto, H. W., & Walton, D. R. M. 1980, JMoSp, 83, 261
Kirchhoff, W. H. 1972, JMoSp, 41, 333
Kisiel, Z., Dorosh, O., Maeda, A., et al. 2010, PCCP, 12, 8329
Klaus, T., Takano, S., & Winnewisser, G. 1997, A&A, 322, L1
Klemperer, W. 1970, Natur, 227, 1230
Klisch, E., Klaus, T., Belov, S. P., et al. 1996, ApJ, 473, 1118
Knauth, D. C., Andersson, B. G., McCandliss, S. R., & Moos, H. W. 2004, Natur, 429, 636
Knez, C., Lacy, J. H., Evans, N. J., van Dishoeck, E. F., & Richter, M. J. 2009, ApJ, 696, 471
Kolesniková, L., Daly, A. M., Alonso, J. L., Tercero, B., & Cernicharo, J. 2013, JMoSp, 289, 13
Kolesniková, L., Tercero, B., Cernicharo, J., et al. 2014, ApJL, 784, L7
Kreidberg, L., Bean, J. L., Désert, J.-M., et al. 2014, ApJL, 793, L27
Kreidberg, L., Line, M. R., Bean, J. L., et al. 2015, ApJ, 814, 66
Kretschmer, U., Consalvo, D., Knaack, A., et al. 1996, MolPh, 87, 1159
Kroto, H. W., Kirby, C., Walton, D. R. M., et al. 1977, BAAS, 9, 303
Kroto, H. W., Kirby, C., Walton, D. R. M., et al. 1978, ApJL, 219, L133
Krueger, M., Dreizler, H., Preugschat, D., & Lentz, D. 2010, ChemInform, 23, 1644
Kuan, Y.-J., Charnley, S. B., Huang, H.-C., Tseng, W.-L., & Kisiel, Z. 2003, ApJ, 593, 848
Kuiper, T. B. H., Kakar, R. K., Kuiper, E. N. R., & Zuckerman, B. 1975, ApJL, 200, L151
Kuiper, T. B. H., Kuiper, E. N. R., Dickinson, D. F., Turner, B. E., & Zuckerman, B. 1984, ApJ, 276, 211
Kukolich, S. G. 1965, PhRv, 138, A1322
Kukolich, S. G. 1967, PhRv, 156, 83
Kukolich, S. G. 1972, JChPh, 57, 869
Kwok, S., & Zhang, Y. 2013, ApJ, 771, 5
Lacy, J. H., Carr, J. S., J, N., et al. 1991, ApJ, 376, 556
Lacy, J. H., Faraji, H., Sandford, S. A., & Allamandola, L. J. 1998, ApJL, 501, L105
Lahuis, F., van Dishoeck, E. F., Boogert, A. C. A., et al. 2006, ApJL, 636, L145
Lambeau, C., Fayt, A., Duncan, J. L., & Nakagawa, T. 1980, JMoSp, 81, 227
Langer, W. D., Velusamy, T., Kuiper, T. B. H., et al. 1997, ApJL, 480, L63
Lanotte, A. A., Gillon, M., Demory, B. O., et al. 2014, A&A, 572, A73
Larsson, B., Liseau, R., Pagani, L., et al. 2007, A&A, 466, 999
Latter, W. B., Walker, C. K., & Maloney, P. R. 1993, ApJL, 419, L97
Laurie, V. W. 1959, JChPh, 31, 1500
Lee, J.-Y., Marti, K., Severinghaus, J. P., et al. 2006, GeCoA, 70, 4507
Lee, S. K., & Amano, T. 1987, ApJL, 323, L145
Lees, R. M., & Mohammadi, M. A. 1980, CaJPh, 58, 1640
Lide, D. R. 1962, JMoSp, 8, 142
Lin, C. C., & Swalen, J. D. 1959, RvMP, 31, 841
Lindenmayer, J., Magg, U., & Jones, H. 1988, JMoSp, 128, 172
Linke, R. A., Frerking, M. A., & Thaddeus, P. 1979, ApJL, 234, L139
Linnartz, H., Ioppolo, S., & Fedoseev, G. 2015, IRPC, 34, 205
Lis, D. C., Pearson, J. C., Neufeld, D. A., et al. 2010, A&A, 521, L9
Liszt, H. S. 1978, ApJ, 219, 454
Liszt, H. S., & Turner, B. E. 1978, ApJL, 224, L73
Liszt, H. S., & Ziurys, L. M. 2012, ApJ, 747, 55
Little, L. T., Macdonald, G. H., Riley, P. W., & Matheson, D. N. 1978, MNRAS, 183, 45P
Liu, D.-J., & Oka, T. 1985, PhRvL, 54, 1787
Lockwood, A. C., Johnson, J. A., Bender, C. F., et al. 2014, ApJL, 783, L29
Lofthus, A., & Krupenie, P. H. 1977, JPCRD, 6, 113
Loomis, R. A., Öberg, K. I., Andrews, S. M., et al. 2018, AJ, 155, 182
Loomis, R. A., Shingledecker, C. N., Langston, G., et al. 2016, MNRAS, 463, 4175
Loomis, R. A., Zaleski, D. P., Steber, A. L., et al. 2013, ApJL, 765, L9
Loren, R. B., Mundy, L. G., & Wootten, A. 1984, ApJL, 286, L23
Lovas, F. J. 1978, JPCRD, 7, 1445
Lovas, F. J., Hollis, J. M., Remijan, A. J., & Jewell, P. R. 2006a, ApJL, 645, L137
Lovas, F. J., Kawashima, Y., Grabow, J. U., et al. 1995, ApJL, 455, L201
Lovas, F. J., Remijan, A. J., Hollis, J. M., Jewell, P. R., & Snyder, L. E. 2006b, ApJL, 637, L37
Lovas, F. J., Suenram, R. D., & Evenson, K. M. 1983, ApJL, 267, L131
Lovas, F. J., & Tiemann, E. 1974, JPCRD, 3, 609
MacLeod, J. M., Avery, L. W., & Broten, N. W. 1984, ApJL, 282, L89
Mäder, H., Heise, H. M., & Dreizler, H. 1974, ZNatA, 29, 164
Madhusudhan, N., Agúndez, M., Moses, J. I., & Hu, Y. 2016, SSRv, 205, 285
Madhusudhan, N., Harrington, J., Stevenson, K. B., et al. 2011, Natur, 469, 64
Magain, P., & Gillet, D. 1987, A&A, 184, L5
Mandell, A. M., Mumma, M. J., Blake, G. A., et al. 2008, ApJL, 681, L25
Mangum, J. G., & Shirley, Y. L. 2015, PASP, 127, 266
Mantz, A. W., Maillard, J. P., Roh, W. B., & Narahari Rao, K. 1975, JMoSp, 57, 155
Marcelino, N., Agúndez, M., Cernicharo, J., Roueff, E., & Tafalla, M. 2018, A&A, 612, L10
Marcelino, N., Cernicharo, J., Agúndez, M., et al. 2007, ApJL, 665, L127
Marcelino, N., Cernicharo, J., Tercero, B., & Roueff, E. 2009, ApJL, 690, L27
Marstokk, K. M., & Møllendal, H. 1973, JMoSt, 16, 259
Martin, D. W., McDaniel, E. W., & Meeks, M. L. 1961, ApJ, 134, 1012
Martin, M. C., Koller, D., & Mihaly, L. 1993, PhRvB, 47, 14607
Martin, R. N., & Ho, P. T. P. 1979, A&A, 74, L7
Martín, S., Mauersberger, R., Martin-Pintado, J., García-Burillo, S., & Henkel, C. 2003, A&A, 411, L465
Martín, S., Mauersberger, R., Pintado, J. M., Henkel, C., & Burillo, S. G. 2006, ApJS, 164, 450
Matsuura, M., Zijlstra, A. A., van Loon, J. T., et al. 2002, ApJL, 580, L133
Matthews, H. E., Irvine, W. M., Friberg, P., Brown, R. D., & Godfrey, P. D. 1984, Natur, 310, 125
Matthews, H. E., & Sears, T. J. 1983, ApJ, 272, 149
Mauersberger, R., & Henkel, C. 1991, A&A, 245, 457
Mauersberger, R., Henkel, C., & Chin, Y. N. 1995, A&A, 294, 23
Mauersberger, R., Henkel, C., & Sage, L. J. 1990, A&A, 236, 63
Mauersberger, R., Henkel, C., Walmsley, C. M., Sage, L. J., & Wiklind, T. 1991, A&A, 247, 307
McCall, B. J., & Griffin, R. E. 2012, RSPSA, 469, 20120604
McCarthy, M. C. 1997, Sci, 275, 518
McCarthy, M. C., Apponi, A. J., & Thaddeus, P. 1999, JChPh, 110, 10645
McCarthy, M. C., Baraban, J. H., Changala, P. B., et al. 2015, The Journal of Physical Chemistry Letters, 6, 2107
McCarthy, M. C., Gottlieb, C. A., Gupta, H., & Thaddeus, P. 2006, ApJL, 652, L141
McCarthy, M. C., Levine, E. S., Apponi, A. J., & Thaddeus, P. 2000, JMoSp, 203, 75
McCarthy, M. C., Travers, M. J., Kovacs, A., Gottlieb, C. A., & Thaddeus, P. 1996, A&A, 309, L31
McGuire, B. A., Burkhardt, A. M., Kalenskii, S. V., et al. 2018, Sci, 359, 202
McGuire, B. A., Burkhardt, A. M., Shingledecker, C. N., et al. 2017a, ApJL, 843, L28
McGuire, B. A., Carroll, P. B., Gratier, P., et al. 2014, ApJ, 783, 36
McGuire, B. A., Carroll, P. B., Loomis, R. A., et al. 2013a, ApJ, 774, 56
McGuire, B. A., Carroll, P. B., Loomis, R. A., et al. 2016, Sci, 352, 1449
McGuire, B. A., Carroll, P. B., & Remijan, A. J. 2013b, arXiv:1306.0927
McGuire, B. A., Loomis, R. A., Charness, C. M., et al. 2012, ApJL, 758, L33
McGuire, B. A., Shingledecker, C. N., Willis, E. R., et al. 2017b, ApJL, 851, L46
McKellar, A. 1940, PASP, 52, 187
Medvedev, I. R., De Lucia, F. C., & Herbst, E. 2009, ApJS, 181, 433
Meerts, W. L., & Ozier, I. 1982, JMoSp, 94, 38
Mehringer, D. M., Snyder, L. E., Miao, Y., & Lovas, F. J. 1997, ApJL, 480, L71
Menten, K. M., Wyrowski, F., Belloche, A., et al. 2011, A&A, 525, A77
Meyer, D. M., & Roth, K. C. 1991, ApJL, 376, L49
Michalopoulos, D. L., Geusic, M. E., Langridge Smith, P. R. R., & Smalley, R. E. 1984, JChPh, 80, 3556
Millen, D. J., Topping, G., & Lide, D. R. 1962, JMoSp, 8, 153
Mockler, R. C., & Bird, G. R. 1955, PhRv, 98, 1837
Mohamed, S., McCarthy, M. C., Cooksy, A. L., Hinton, C., & Thaddeus, P. 2005, JChPh, 123, 234301

Moïses, A., Boucher, D., Burie, J., Demaison, J., & Dubrulle, A. 1982, JMoSp, 92, 497
Momose, T., Endo, Y., Hirota, E., & Shida, T. 1988, JChPh, 88, 5338
Monje, R. R., Lis, D. C., Roueff, E., et al. 2013, ApJ, 767, 81
Monje, R. R., Phillips, T. G., Peng, R., et al. 2011, ApJL, 742, L21
Morino, I., & Kawaguchi, K. 1995, JMoSp, 170, 172
Morris, M., Gilmore, W., Palmer, P., Turner, B. E., & Zuckerman, B. 1975, ApJL, 199, L47
Motiyenko, R., Margules, L., Despois, D., & Guillemin, J.-C. 2018, PCCP, 20, 5509
Müller, H. S. P. 2013, JQSRT, 130, 335
Müller, H. S. P., Belloche, A., Xu, L.-H., et al. 2016, A&A, 587, A92
Müller, H. S. P., Coutens, A., Walters, A., Grabow, J.-U., & Schlemmer, S. 2011, JMoSp, 267, 100
Müller, H. S. P., Muller, S., Schilke, P., et al. 2015, A&A, 582, L4
Muller, S., Beelen, A., Black, J. H., et al. 2013, A&A, 551, A109
Muller, S., Beelen, A., Guélin, M., et al. 2011, A&A, 535, A103
Muller, S., Black, J. H., Guélin, M., et al. 2014a, A&A, 566, L6
Muller, S., Combes, F., Guélin, M., et al. 2014b, A&A, 566, A112
Muller, S., Kawaguchi, K., Black, J. H., & Amano, T. 2016, A&A, 589, L5
Muller, S., Müller, H. S. P., Black, J. H., et al. 2017, A&A, 606, A109
Murakami, A., Kawaguchi, K., & Saito, S. 1987, PASJ, 39, 189
Mürtz, P., Zink, L. R., Evenson, K. M., & Brown, J. M. 1998, JChPh, 109, 9744
Namiki, K.-i., Saito, S., Robinson, J. S., & Steimle, T. C. 1998, JMoSp, 191, 176
Neill, J. L., Bergin, E. A., Lis, D. C., et al. 2014, ApJ, 789, 8
Neill, J. L., Muckle, M. T., Zaleski, D. P., et al. 2012, ApJ, 755, 153
Nemes, L., Ram, R. S., Bernath, P. F., et al. 1994, CPL, 218, 295
Neufeld, D. A., Falgarone, E., Gerin, M., et al. 2012, A&A, 542, L6
Neufeld, D. A., Schilke, P., Menten, K. M., et al. 2006, A&A, 454, L37
Neufeld, D. A., Zmuidzinas, J., Schilke, P., & Phillips, T. G. 1997, ApJL, 488, L141
Nguyen-Q-Rieu, H. C., Jackson, J. M., & Mauersberger, R. 1991, A&A, 241, L33
Nolt, I. G., Radostitz, J. V., Dilonardo, G., et al. 1987, JMoSp, 125, 274
Nugroho, S. K., Kawahara, H., Masuda, K., et al. 2017, AJ, 154, 221
Öberg, K. I., Guzmán, V. V., Furuya, K., et al. 2015, Natur, 520, 198
Öberg, K. I., Murray-Clay, R., & Bergin, E. A. 2011, ApJL, 743, L16
Ohashi, N., Kawabe, R., Ishiguro, M., & Hayashi, M. 1991, AJ, 102, 2054
Ohishi, M., Ishikawa, S.-I., Amano, T., et al. 1996, ApJL, 471, L61
Ohishi, M., Kaifu, N., Kawaguchi, K., et al. 1989, ApJL, 345, L83
Ohishi, M., McGonagle, D., Irvine, W. M., Yamamoto, S., & Saito, S. 1994, ApJL, 427, L51
Ohishi, M., Suzuki, H., Ishikawa, S.-I., et al. 1991, ApJL, 380, L39
Ohishi, M., Yamamoto, S., Saito, S., et al. 1988, ApJ, 329, 511
Ohshima, Y., & Endo, Y. 1993, JMoSp, 159, 458
Oka, T. 1980, PhRvL, 45, 531
Ossenkopf, V., Müller, H. S. P., Muller, H., et al. 2010, A&A, 518, L111
Palumbo, M. E., Geballe, T. R., & Tielens, A. G. G. M. 1997, ApJ, 479, 839
Palumbo, M. E., Tielens, A. G. G. M., & Tokunaga, A. T. 1995, ApJ, 449, 674
Parise, B., Bergman, P., & Du, F. 2012, A&A, 541, L11
Paso, R., Kauppinen, J., & Anttila, R. 1980, JMoSp, 79, 236
Pauzat, F., Ellinger, Y., & McLean, A. D. 1991, ApJL, 369, L13
Pearson, J. C., Gottlieb, C. A., Woodward, D. R., & Thaddeus, P. 1988, A&A, 189, L13
Pearson, J. C., Sastry, K. V. L. N., Herbst, E., & De Lucia, F. C. 1997, ApJ, 480, 420
Pearson, J. C., Sastry, K. V. L. N., Herbst, E., & DELUCIA, F. C. 1994, JMoSp, 166, 120
Peña, I., Sanz, M. E., López, J. C., & Alonso, J. L. 2012, JAChS, 134, 2305
Penzias, A. A., Solomon, P. M., Wilson, R. W., & Jefferts, K. B. 1971, ApJL, 168, L53
Petkie, D. T., Goyette, T. M., Holton, J. J., DELUCIA, F. C., & HELMINGER, P. 1995, JMoSp, 171, 145
Petuchowski, S. J., & Bennett, C. L. 1992, ApJ, 391, 137
Pety, J., Gratier, P., Guzmán, V., et al. 2012, A&A, 548, A68
Phillips, J. G. 1948, ApJ, 107, 389
Phuong, N. T., Chapillon, E., Majumdar, L., et al. 2018, A&A, 616, L5
Plummer, G. M., Anderson, T., Herbst, E., & De Lucia, F. C. 1986, JChPh, 84, 2427
Plummer, G. M., Herbst, E., & De Lucia, F. C. 1985, JChPh, 83, 1428
Poletto, G., & Rigutti, M. 1965, Il Nuovo Cimento (1955-1965), 39, 519
Priem, D., Cosléou, J., Demaison, J., et al. 1998, JMoSp, 191, 183
Pulliam, R. L., Savage, C., Agúndez, M., et al. 2010, ApJL, 725, L181
Qi, C., Kessler, J. E., Koerner, D. W., Sargent, A. I., & Blake, G. A. 2003, ApJ, 597, 986
Qi, C., Öberg, K. I., Wilner, D. J., & Rosenfeld, K. A. 2013, ApJL, 765, L14
Qi, C., Wilner, D. J., Aikawa, Y., Blake, G. A., & Hogerheijde, M. R. 2008, ApJ, 681, 1396
Qiu, J., Wang, J., Shi, Y., et al. 2018, A&A, 613, A3
Rangwala, N., Maloney, P. R., Glenn, J., et al. 2011, ApJ, 743, 94
Ray, B. S. 1932, ZPhy, 78, 74
Raymonda, J. W. 1970, JChPh, 52, 3458
Reichle, H. G., Jr, & Young, C. 1972, CaJPh, 50, 2662
Remijan, A. J., Hollis, J. M., Lovas, F. J., et al. 2007, ApJL, 664, L47
Remijan, A. J., Hollis, J. M., Lovas, F. J., et al. 2008a, ApJL, 675, L85
Remijan, A. J., Hollis, J. M., Lovas, F. J., Plusquellic, D. F., & Jewell, P. R. 2005, ApJ, 632, 333
Remijan, A. J., Hollis, J. M., Snyder, L. E., Jewell, P. R., & Lovas, F. J. 2006, ApJL, 643, L37
Remijan, A. J., Leigh, D. P., Markwick-Kemper, A. J., & Turner, B. E. 2008b, arXiv:0802.2273
Remijan, A. J., Snyder, L. E., McGuire, B. A., et al. 2014, ApJ, 783, 77
Requena-Torres, M. A., Martin-Pintado, J., Rodríguez-Franco, A., et al. 2006, A&A, 455, 971
Ribeiro, F. D. A., Almeida, G. C., Garcia-Basabe, Y., et al. 2015, PCCP, 17, 27473
Rickard, L. J., Palmer, P., Morris, M., Turner, B. E., & Zuckerman, B. 1975, ApJL, 199, L75
Rickard, L. J., Turner, B. E., Palmer, P., Morris, M., & Zuckerman, B. 1977, ApJ, 214, 390
Ridgway, S. T., Hall, D. N. B., Kleinmann, S. G., Weinberger, D. A., & Wojslaw, R. S. 1976, Natur, 264, 345
Ring, H., Edwards, H., Kessler, M., & Gordy, W. 1947, PhRv, 72, 1262
Rivilla, V. M., Beltrán, M. T., Cesaroni, R., et al. 2017, A&A, 598, A59
Robinson, J. S., Apponi, A. J., & Ziurys, L. M. 1997, CPL, 278, 1
Rodler, M. 1985, JMoSp, 114, 23
Rodler, M., Brown, R. D., Godfrey, P. D., & Kleibömer, B. 1986, JMoSp, 118, 267
Rodler, M., Brown, R. D., Godfrey, P. D., & Tack, L. M. 1984, CPL, 110, 447
Rubin, R. H., Swenson, G. W. J., Benson, R. C., Tigelaar, H. L., & Flygare, W. H. 1971, ApJL, 169, L39
Rydbeck, O. E. H., Ellder, J., & Irvine, W. M. 1973, Natur, 246, 466
Sage, L. J., & Ziurys, L. M. 1995, ApJ, 447, 625
Saito, S. 1972, ApJL, 178, L95
Saito, S. 1977, JMoSp, 65, 229
Saito, S., & Amano, T. 1970, JMoSp, 34, 383
Saito, S., Endo, Y., & Hirota, E. 1983, JChPh, 78, 6447
Saito, S., Endo, Y., & Hirota, E. 1984, JChPh, 80, 1427
Saito, S., Kawaguchi, K., Yamamoto, S., et al. 1987, ApJL, 317, L115
Saito, S., & Takagi, K. 1973, JMoSp, 47, 99
Saito, S., Yamamoto, S., Irvine, W. M., et al. 1988, ApJL, 334, L113
Saito, S., Yamamoto, S., Kawaguchi, K., et al. 1989, ApJ, 341, 1114
Salinas, V. N., Hogerheijde, M. R., Bergin, E. A., et al. 2016, A&A, 591, A122
Salyk, C., Pontoppidan, K. M., Blake, G. A., et al. 2008, ApJL, 676, L49
Sargent, A. I., & Beckwith, S. 1987, ApJ, 323, 294
Sastry, K. V. L. N., HELMINGER, P., Charo, A., Herbst, E., & de Lucia, F. C. 1981a, ApJL, 251, L119
Sastry, K. V. L. N., Helminger, P., Herbst, E., & de Lucia, F. C. 1981b, ApJL, 250, L91
Sastry, K. V. L. N., Helminger, P., Plummer, G. M., Herbst, E., & de Lucia, F. C. 1984, ApJS, 55, 563
Saykally, R. J., Dixon, T. A., Anderson, T. G., Szanto, P. G., & Woods, R. C. 1976, ApJL, 205, L101
Schilke, P., Benford, D. J., Hunter, T. R., Lis, D. C., & Phillips, T. G. 2001, ApJS, 132, 281
Schlawin, E., Greene, T. P., Line, M., Fortney, J. J., & Rieke, M. 2018, AJ, 156, 0
Schutte, W. A., Boogert, A. C. A., Tielens, A. G. G. M., et al. 1999, A&A, 343, 966
Schutte, W. A., & Greenberg, J. M. 1997, A&A, 317, L43
Schwahn, G., Schieder, R., Bester, M., & Winnewisser, G. 1986, JMoSp, 116, 263
Scoville, N. Z., & Solomon, P. M. 1978, ApJL, 220, L103
Seaquist, E. R., & Bell, M. B. 1986, ApJL, 303, L67
Sedaghati, E., Boffin, H. M. J., MacDonald, R. J., et al. 2017, Natur, 549, 238
Sewiło, M., Indebetouw, R., Charnley, S. B., et al. 2018, ApJL, 853, L19
Shigenari, T. 1967, JPSJ, 23, 404
Shklovskii, I. S. 1953, DoSSR, 92, 25
Sinclair, M. W., Fourikis, N., Ribes, J. C., et al. 1973, AuJPh, 26, 85
Smith, R. L., Pontoppidan, K. M., Young, E. D., Morris, M. R., & van Dishoeck, E. F. 2009, ApJ, 701, 163

Snow, T. P., & McCall, B. J. 2006, ARA&A, 44, 367
Snyder, L., Lovas, F., Hollis, J., et al. 2005, ApJ, 619, 914
Snyder, L. E., & Buhl, D. 1971, ApJL, 163, L47
Snyder, L. E., & Buhl, D. 1972a, NYASA, 194, 17
Snyder, L. E., & Buhl, D. 1972b, ApJ, 177, 619
Snyder, L. E., Buhl, D., Schwartz, P. R., et al. 1974, ApJL, 191, L79
Snyder, L. E., Buhl, D., Zuckerman, B., & Palmer, P. 1969, PhRvL, 22, 679
Snyder, L. E., Hollis, J. M., Jewell, P. R., Lovas, F. J., & Remijan, A. 2006, ApJ, 647, 412
Snyder, L. E., Hollis, J. M., Ulich, B. L., et al. 1975, ApJL, 198, L81
Snyder, L. E., Hollis, J. M., & Ulich, B. L. 1976, ApJL, 208, L91
Snyder, L. E., Kuan, Y.-J., Ziurys, L. M., & Hollis, J. M. 1993, ApJL, 403, L17
Soifer, B. T., Puetter, R. C., Russell, R. W., et al. 1979, ApJL, 232, L53
Solomon, P. M., Jefferts, K. B., Penzias, A. A., & Wilson, R. W. 1971, ApJL, 168, L107
Sousa-Silva, C., Yurchenko, S. N., & Tennyson, J. 2013, JMoSp, 288, 28
Souter, C. E., & Wood, J. L. 1970, JChPh, 52, 674
Souza, S. P., & Lutz, B. L. 1977, ApJL, 216, L49
Stark, A. A., & Wolff, R. S. 1979, ApJ, 229, 118
Stark, G., Huber, K. P., Yoshino, K., et al. 2000, ApJ, 531, 321
Steenbeckeliers, G. 1968, Ann. Soc. Sic. Brux., 82, 331
Stevenson, K. B., Harrington, J., Nymeyer, S., et al. 2010, Natur, 464, 1161
Strahan, S. E., Mueller, R. P., & Saykally, R. J. 1986, JChPh, 85, 1252
Stratmann, R. E., Scuseria, G. E., & Frisch, M. J. 1998, JRSp, 29, 483
Stull, V. R., Wyatt, P. J., & Plass, G. N. 1962, JChPh, 37, 1442
Suenram, R. D., Golubiatnikov, G. Y., Leonov, I. I., et al. 2001, JMoSp, 208, 188
Suenram, R. D., & Lovas, F. J. 1980, JAChS, 102, 7180
Suenram, R. D., Lovas, F. J., & Matsumura, K. 1989, ApJL, 342, L103
Sutton, E. C., Blake, G. A., Masson, C. R., & Phillips, T. G. 1985, ApJS, 58, 341
Suzuki, H., Ohishi, M., Kaifu, N., Ishikawa, S.-I., & Kasuga, T. 1986, PASJ, 38, 911
Swain, M. R., Vasisht, G., & Tinetti, G. 2008, Natur, 452, 329
Swings, P., & Rosenfeld, L. 1937, ApJ, 86, 483
Tabor, W. J. 1957, JChPh, 27, 974
Takagi, K., & Kojima, T. 1973, ApJL, 181, L91
Takano, M., Sasada, Y., & Satoh, T. 1968, JMoSp, 26, 157
Tang, J., Sumiyoshi, Y., & Endo, Y. 1999, CPL, 315, 69
Tanimoto, M., Klaus, T., Müller, H. S. P., & Winnewisser, G. 2000, JMoSp, 199, 73
Tenenbaum, E. D., Woolf, N. J., & Ziurys, L. M. 2007, ApJL, 666, L29
Tenenbaum, E. D., & Ziurys, L. M. 2008, ApJL, 680, L121
Tenenbaum, E. D., & Ziurys, L. M. 2009, ApJL, 694, L59
Tenenbaum, E. D., & Ziurys, L. M. 2010, ApJL, 712, L93
Tercero, B., Cernicharo, J., López, A., et al. 2015, A&A, 582, L1
Tercero, B., Kleiner, I., Cernicharo, J., et al. 2013, ApJL, 770, L13
Tercero, B., Margulès, L., Carvajal, M., et al. 2012, A&A, 538, A119
Thaddeus, P., Cummins, S. E., & Linke, R. A. 1984, ApJL, 283, L45
Thaddeus, P., Gottlieb, C. A., Hjalmarson, Å., et al. 1985a, ApJL, 294, L49
Thaddeus, P., Gottlieb, C. A., Gupta, H., et al. 2008, ApJ, 677, 1132
Thaddeus, P., Guélin, M., & Linke, R. A. 1981, ApJL, 246, L41
Thaddeus, P., Kutner, M. L., Penzias, A. A., Wilson, R. W., & Jefferts, K. B. 1972, ApJL, 176, L73
Thaddeus, P., & Turner, B. E. 1975, ApJL, 201, L25
Thaddeus, P., Vrtilek, J. M., & Gottlieb, C. A. 1985b, ApJL, 299, L63
Thi, W. F., Menard, F., Meeus, G., et al. 2011, A&A, 530, L2
Thi, W.-F., van Dishoeck, E. F., Blake, G. A., van Zadelhoff, G.-J., & Hogerheijde, M. R. 1999, ApJL, 521, L63
Thiel, V., Belloche, A., Menten, K. M., Garrod, R. T., & Müller, H. S. P. 2017, A&A, 605, L6
Thompson, R. I., Lebofsky, M. J., & Rieke, G. H. 1978, ApJL, 222, L49
Thomson, R., & Dalby, F. W. 1968, CaJPh, 46, 2815
Thorwirth, S., Müller, H. S. P., & Winnewisser, G. 2000, JMoSp, 199, 116
Tielens, A. G. G. M. 2005, The Physics and Chemistry of the Interstellar Medium (Cambridge, MA: Cambridge Univ. Press)
Tielens, A. G. G. M. 2008, ARA&A, 46, 289
Tinetti, G., Vidal-Madjar, A., Liang, M.-C., et al. 2007, Natur, 448, 169
Törring, T. 1968, ZNatA, 23, 777
Törring, T., Bekooy, J. P., Meerts, W. L., et al. 1980, JChPh, 73, 4875
Townes, C. H. 1946, PhRv, 70, 665
Townes, C. H., & Schawlow, A. L. 1975, Microwave Spectroscopy (New York: Dover)
Trambarulo, R., & Gordy, W. 1950, JChPh, 18, 1613
Travers, M. J., McCarthy, M. C., Gottlieb, C. A., & Thaddeus, P. 1996a, ApJL, 465, L77
Travers, M. J., McCarthy, M. C., Kalmus, P., Gottlieb, C. A., & Thaddeus, P. 1996b, ApJL, 469, L65
Tucker, K. D., Kutner, M. L., & Thaddeus, P. 1974, ApJL, 193, L115
Tudorie, M., Kleiner, I., Hougen, J. T., et al. 2011, JMoSp, 269, 211
Turner, B. E. 1971, ApJL, 163, L35
Turner, B. E. 1974, ApJL, 193, L83
Turner, B. E. 1977, ApJL, 213, L75
Turner, B. E. 1989, ApJS, 70, 539
Turner, B. E. 1992a, ApJL, 396, L107
Turner, B. E. 1992b, ApJL, 388, L35
Turner, B. E., & Apponi, A. J. 2001, ApJL, 561, L207
Turner, B. E., & Bally, J. 1987, ApJL, 321, L75
Turner, B. E., Liszt, H. S., Kaifu, N., & Kisliakov, A. G. 1975, ApJL, 201, L149
Turner, B. E., Steimle, T. C., & Meerts, L. 1994, ApJL, 426, L97
Tyler, J. K., & Sheridan, J. 1963, Transactions of the Faraday Society, 59, 2661
Tyler, J. K., Sheridan, J., & Costain, C. C. 1972, JMoSp, 43, 248
Ulich, B. L., Hollis, J. M., & Snyder, L. E. 1977, ApJL, 217, L105
Usero, A., García-Burillo, S., Fuente, A., Martin-Pintado, J., & Rodríguez -Fernández, N. J. 2004, A&A, 419, 897
Vacherand, J. M., Van Eijck, B. P., Burie, J., & Demaison, J. 1986, JMoSp, 118, 355
Vala, M., Chandrasekhar, T. M., Szczepanski, J., Van Zee, R., & Weltner, W., Jr. 1989, JChPh, 90, 595
van Broekhuizen, F. A., Pontoppidan, K. M., Fraser, H. J., & van Dishoeck, E. F. 2005, A&A, 441, 249
van der Tak, F. 2011, in IAU Symp 240, The Molecular Universe (Cambridge: Cambridge Univ. Press), 449
van der Tak, F. F. S., Aalto, S., & Meijerink, R. 2007, A&A, 477, L5
van der Werf, P. P., Isaak, K. G., Meijerink, R., et al. 2010, A&A, 518, L42
van Dishoeck, E. F., Helmich, F. P., de Graauw, T., et al. 1996, A&A, 315, L349
van Dishoeck, E. F., Jansen, D. J., Schilke, P., & Phillips, T. G. 1993, ApJL, 416, L83
van Dishoeck, E. F., Thi, W. F., & van Zadelhoff, G. J. 2003, A&A, 400, L1
van Vaals, J. J., Meerts, W. L., & Dymanus, A. 1984, CP, 86, 147
van Zadelhoff, G. J., van Dishoeck, E. F., Thi, W. F., & Blake, G. A. 2001, A&A, 377, 566
von Czarnowski, A., & Meiwes-Broer, K. H. 1995, CPL, 246, 321
Vrtilek, J. M., Gottlieb, C. A., & Thaddeus, P. 1987, ApJ, 314, 716
Vrtilek, J. M., Thaddeus, P., Gottlieb, C. A., Gottlieb, E. W., & Killian, T. C. 1990, ApJL, 364, L53
Wagener, V., Winnewisser, M., & Bellini, M. 1995, JMoSp, 170, 323
Walker, G. A. H., Bohlender, D. A., Maier, J. P., & Campbell, E. K. 2015, ApJL, 812, L8
Walmsley, C. M., Bachiller, R., Pineau des Forêts, G., & Schilke, P. 2002, ApJL, 566, L109
Walmsley, C. M., Jewell, P. R., Snyder, L. E., & Winnewisser, G. 1984, A&A, 134, L11
Walsh, C., Loomis, R. A., Öberg, K. I., et al. 2016, ApJL, 823, L10
Walsh, C., Millar, T. J., Nomura, H., et al. 2014, A&A, 563, A33
Walsh, C., Vissapragada, S., & McGee, H. 2017, arXiv:1710.01219
Weinreb, S., Barrett, A. H., Meeks, M. L., & Henry, J. C. 1963, Natur, 200, 829
Weiß, A., Requena-Torres, M. A., Güsten, R., et al. 2010, A&A, 521, L1
Weliachew, L. 1971, ApJL, 167, L47
Welty, D. E., Howk, J. C., Lehner, N., & Black, J. H. 2012, MNRAS, 428, 1107
Whiteoak, J. B., Gardner, F. F., & Hoglund, B. 1980, MNRAS, 190, 17P
Widicus Weaver, S. L., Laas, J. C., Zou, L., et al. 2017, ApJS, 232, 3
Willacy, K. 2003, ApJL, 600, L87
Wilson, R. W., Jefferts, K. B., & Penzias, A. A. 1970, ApJL, 161, L43
Wilson, R. W., Penzias, A. A., Jefferts, K. B., Kutner, M., & Thaddeus, P. 1971, ApJL, 167, L97
Wilson, S., & Green, S. 1977, ApJL, 212, L87
Winnewisser, G. 1973, JMoSp, 46, 16
Winnewisser, G., & Churchwell, E. 1975, ApJL, 200, L33
Winnewisser, G., & Walmsley, C. M. 1978, A&A, 70, L37
Winnewisser, M., Sastry, K. V. L. N., Cook, R. L., & Gordy, W. 1964, JChPh, 41, 1687
Winnewisser, M., Seibert, J. W. G., & Yamada, K. M. T. 1992, JMoSp, 153, 635
Winnewisser, M., & Winnewisser, B. P. 1971, ZNatA, 26, 128
Winnewisser, M., Winnewisser, G., Honda, T., & Hirota, E. 1975, ZNatA, 30, 1001

Wlodarczak, G., Boucher, D., Bocquet, R., & Demaison, J. 1986, JMoSp, 116, 251
Wlodarczak, G., & Demaison, J. 1988, A&A, 192, 313
Wlodarczak, G., Demaison, J., Heineking, N., & Császár, A. G. 1994, JMoSp, 167, 239
Wohlfart, K., Schnell, M., Grabow, J.-U., & Küpper, J. 2008, JMoSp, 247, 119
Wong, M., Ozier, I., & Meerts, W. L. 1983, JMoSp, 102, 89
Woods, R. C., Dixon, T. A., Saykally, R. J., & Szanto, P. G. 1975, PhRvL, 35, 1269
Woods, R. C., Gudeman, C. S., Dickman, R. L., et al. 1983, ApJ, 270, 583
Woon, D. E. 2002, ApJ, 569, 541
Wootten, A., Boulanger, F., Bogey, M., et al. 1986, A&A, 166, L15
Wootten, A., Turner, B. E., Mangum, J. G., et al. 1991, ApJL, 380, L79
Wyrowski, F., Menten, K. M., Güsten, R., & Belloche, A. 2010, A&A, 518, A26
Wyse, F. C., Gordy, W., & Pearson, E. F. 1970, JChPh, 52, 3887
Wyse, F. C., Manson, E. L., & Gordy, W. 1972, JChPh, 57, 1106
Yamada, C., Cohen, E. A., Fujitake, M., & Hirota, E. 1990, JChPh, 92, 2146
Yamada, C., Hirota, E., & Kawaguchi, K. 1981, JChPh, 75, 5256
Yamada, C., Saito, S., Kanamori, H., & Hirota, E. 1985, ApJL, 290, L65
Yamamoto, S., & Saito, S. 1992, JChPh, 96, 4157
Yamamoto, S., Saito, S., Kawaguchi, K., et al. 1987a, ApJL, 317, L119
Yamamoto, S., Saito, S., Ohishi, M., et al. 1987b, ApJL, 322, L55
Zack, L. N., Halfen, D. T., & Ziurys, L. M. 2011, ApJL, 733, L36
Zaleski, D. P., Seifert, N. A., Steber, A. L., et al. 2013, ApJL, 765, L10
Ziurys, L. M. 1987, ApJL, 321, L81
Ziurys, L. M., & Apponi, A. J. 1995, ApJL, 455, L73
Ziurys, L. M., Apponi, A. J., Guélin, M., & Cernicharo, J. 1995, ApJL, 445, L47
Ziurys, L. M., Apponi, A. J., Hollis, J. M., & Snyder, L. E. 1994a, ApJL, 436, L181
Ziurys, L. M., Apponi, A. J., & Phillips, T. G. 1994b, ApJ, 433, 729
Ziurys, L. M., Hollis, J. M., & Snyder, L. E. 1994c, ApJ, 430, 706
Ziurys, L. M., Savage, C., Highberger, J. L., et al. 2002, ApJL, 564, L45
Ziurys, L. M., & Turner, B. E. 1986, ApJL, 302, L31
Zuckerman, B., Ball, J. A., & Gottlieb, C. A. 1971, ApJL, 163, L41
Zuckerman, B., Morris, M., Palmer, P., & Turner, B. E. 1972, ApJL, 173, L125
Zuckerman, B., Turner, B. E., Johnson, D. R., et al. 1975, ApJL, 196, L99